2020

Creation and Analysis of an Enhanced RASCAL-LVC Framework Capable of Simulating Ionizing Radiation Damage to Emergency Responders During a Nuclear Power Plant Disaster: A Case Study in Unmanned Aerial Vehicle Electronic System Survivability

Buder Shageer
University of Central Florida

CREATION AND ANALYSIS OF AN ENHANCED RASCAL-LVC FRAMEWORK CAPABLE OF SIMULATING IONIZING RADIATION DAMAGE TO EMERGENCY RESPONDERS DURING A NUCLEAR POWER PLANT DISASTER: A CASE STUDY IN UNMANNED AERIAL VEHICLE ELECTRONIC SYSTEM SURVIVABILITY

by

BUDER M. SHAGEER
B.S. University of Illinois, Champaign Urbana, 2011
M.S. University of Central Florida, 2013

A dissertation submitted in partial fulfillment of the requirements
for the degree of Doctor of Philosophy
in the Department of Industrial Engineering and Management Systems
in the College of Engineering and Computer Science
at the University of Central Florida
Orlando, Florida

Spring Term
2020

Major Advisor: Michael D. Proctor

ABSTRACT

This study developed and analyzed the use of a live virtual constructive (LVC) framework capable of simulating ionizing radiation damage to Unmanned Aerial Vehicles (UAV) during a nuclear power plant disaster. UAV response promises greater safety to humans over helicopters as well as provides longer survivability in the presence of irradiated environments. However, electronics in unmanned systems are subject to radiation damage and over time eventual failure. A LVC simulation framework may offer an independent and low-cost assessment of equipment life expectancy. Knowing life expectancy of equipment for operational scenarios is critical for emergency management planners. This research creates an enhanced RASCAL-LVC simulation framework by modeling and simulating NPP disaster radiation release based on the NRC RASCAL simulation and radioactive cloud dispersion in STAGE. The resulting framework enables analysis of length of operational survivability of UAV electronics for three illustrative missions. The three scenarios examined are: (1) an In-And-Out Mission that simulates Parts Delivery, Surveillance, or passenger pickup/delivery; (2) a Fukushima-like Spent Fuel Pool water replenishment mission with radiation hot spot; and (3) an exploratory Chernobyl-magnitude Reactor Fire-extinguishing Mission with an open reactor radiation hot spot. More generally, the enhanced RASCAL-LVC framework is capable of: (1) supporting human-in-the-loop training and mission rehearsal; (2) design and analysis of a broad spectrum of NPP disaster scenarios and mission responses; (3) analysis of various response vehicles within mission-scenario combinations; and (4) system engineering support to each system's life cycle.

EXTENDED ABSTRACT

Emergency Nuclear Power Plant (NPP) disasters potentially have widespread and even global consequences that may be mitigated by rapid and effective response. A nuclear disaster may arise through a Chernobyl-like human accident, a Fukushima-like chain-of-events arising from an act of nature, an act of terror, or, of more recent concern, a cyber-attack. Slow and often ineffective response at Fukushima revealed to the world the need for improved: (1) nuclear infrastructure resilience; (2) nuclear disaster planning; (3) capabilities of response equipment, and (4) crisis management processes. One improved capability of response equipment may be unmanned vehicles. In particular, Unmanned Aerial Vehicle (UAV) response promises greater safety to humans over manned alternatives like helicopters as well as provide longer survivability in the presence of irradiated environments. Longer survivability of the response equipment promises longer periods of equipment performance for assigned mission. None the less, electronics in unmanned systems are subject to radiation damage and over time eventual failure. A live virtual constructive (LVC) simulation framework may offer an independent and low-cost assessment of equipment life expectancy for various operational missions conducted in the presence of ionizing radiation. Knowing life expectancy of equipment for operational scenarios is critical for emergency management planners. Building on the (Davis, Proctor et al. 2016) Systems-Of-Systems Conceptual Model and integrated LVC simulation framework, this research creates an enhanced RASCAL-LVC simulation framework by modeling and simulating NPP disaster radiation release based on the Nuclear Regulatory Commission's RASCAL simulation and radioactive cloud dispersion in Stage based on meteorological data. The resulting framework enables analysis of length of operational survivability of UAV electronics for three illustrative missions within the context of different NPP disaster irradiation scenarios. Using factors identified in the (Davis 2017) screening experiment, the three scenarios examined are: (1) an In-And-Out Mission that simulates Parts Delivery, Surveillance, or passenger pickup/delivery; (2) a Fukushima-like Spent Fuel Pool water replenishment mission with radiation hot spot; and (3) an exploratory Chernobyl-magnitude Reactor Fire-extinguishing Mission with an open reactor radiation hot spot. More generally, the enhanced RASCAL-LVC framework in capable of: (1) supporting human-in-the-loop training and mission rehearsal; (2) design and analysis of a broad spectrum of NPP disaster scenarios and mission responses; (3) analysis of various response vehicles within mission-scenario combinations; and (4) system engineering support to each system's life cycle.

ACKNOWLEDGMENTS

My gratitude goes to my Advisor/Leader/Professor Dr. Michael Proctor who guided me through my graduate-school experience. His enthusiasm for modeling and simulation and ability to remember deadlines always kept me engaged in my research! I couldn't have envisioned a more wonderful person to assist me in this process and I'm reminded on a regular basis of it.

My appreciation also extends to my laboratory colleagues, Matthew Davis, Eric Lucas, Lance Schreiber, Jonathan Coad, Jared Clark and Lamar Harrell who were all wonderful to work with and kept the lab an enjoyable place to be even on those long days. I would also like to extend my appreciation for Ricardo Scuotto, Waldemar Karwowski, and Liz Stalvey, in the IEMS Department.

Lastly, I am forever indebted to my family, and most importantly my parents, who have instilled their wisdom upon me and pushed me to reach this point. For without them I would not have an acknowledgment section to thank anyone.

TABLE OF CONTENTS

LIST OF FIGURES

LIST OF TABLES

CHAPTER ONE: INTRODUCTION

Introduction

After the Fukushima Nuclear Power Plant (NPP) disaster, one may wonder, what is the risk, breadth and depth of a future NPP disaster? What can we do to prepare for and then act to mitigate the next disaster when it occurs?

Nuclear power accounts for more than 10% of the world's energy consumption (NEI 2016), with 30 countries worldwide operating 444 nuclear reactors and over 60 new plants under construction (NEI 2016). Domestically, the United States contains 135 nuclear power plants (100 commercial, 35 research), making up over 25% of the world's nuclear reactors (NRC 2015)

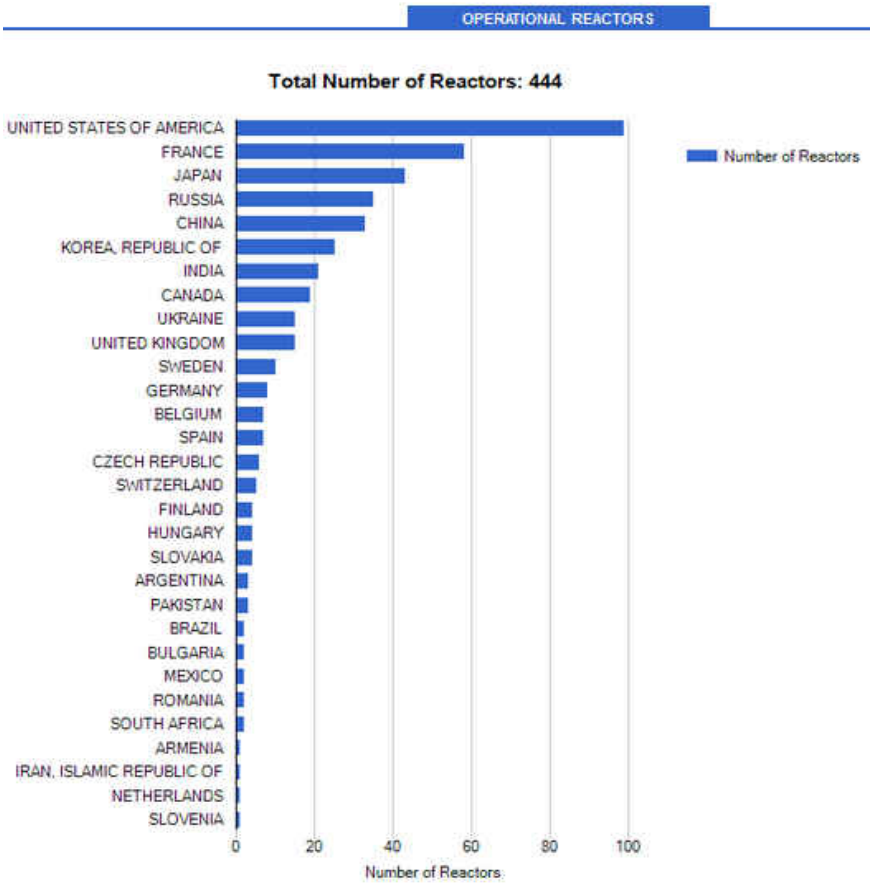

Figure 1 – Total Number of Reactors Worldwide (IAEA 2016)

Although nuclear energy is safe to produce, the outcomes of nuclear power plant (NPP) disasters can be catastrophic (Miller 2011, OPA 2013, OPA 2013, NRC 2014, NRC 2014). NPPs are vulnerable to accidents (OPA 2013, OPA 2013), cascading events associated with natural events such as floods, earthquakes, tsunamis, hurricanes (Huh and Haldar 2011), terrorist attack or sabotage (Sokolski 2016), or even a power outage from a Stuxnet-like cyber-attack (Shea 2004, Langner 2011). The most infamous NPP disasters are Three Mile Island, Chernobyl, and most recently Fukushima Dai-ichi (TEPCO 2013).

The Three Mile Island incident occurred in 1979, setting the precedent for many Nuclear Regulatory Commission (NRC) regulations and changing the safety oversight of the nuclear industry (OPA 2013). Three Mile Island resulted in a severe core meltdown but began as a loss-of-coolant accident. The situation escalated due to a combination of personnel error, design deficiencies, and component failures. Response teams used helicopters to sample the radioactivity in the atmosphere following the disaster to determine the health risk to the surrounding community. Although the radioactive release was minimal, the outcomes of a core meltdown have the potential to be very hazardous. This incident brought about drastic changes in emergency response planning, reactor operator training, human factors engineering, and radiation protection (OPA 2013).

On April 26 1986, a sudden surge of power during a reactor systems test destroyed one of the reactor units at the Soviet Union Chernobyl NPP (OPA 2013). The accident, explosion, and subsequent fire aerially released massive amounts of radioactive material into the environment that spread not only across the eastern part of the Soviet Union but into other parts of Europe. Part of a huge response to contain the disaster, military helicopters enabled soldiers and other emergency response personnel to directly pour sand and boron into the reactor. Sand stopped the fire and retarded additional aerial release of radioactive material while boron retarded the nuclear reactions. Beginning May 20, 1986, the Soviets designed a sarcophagus with cooling slab under the reactor to prevent the hot nuclear fuel from burning through the foundations and to contain the estimated 200 tons of radioactive corium, 30 tons of contaminated dust, and 16 tons of uranium and plutonium. Construction was completed in

November 1986 (NRC 2014, CCI 2016). With only a 30-year life, the sarcophagus is being further entombed with a New Safe Confinement with a minimum of 100-year life. Construction started in late 2010 and was scheduled to be completed in 2017 (Wendle 2016), however limiting radiation exposure to the crew, construction delays and finance shortages led to another 2 years of work. It was unveiled to the public in July 2019, and weeks after its unveiling, experts revealed “the sarcophagus had a very high probability of collapse”, leading to the current deconstruction efforts (Bendix 2019), which further exposes construction crews to radiation, and risks collapse onto a radioactive disaster site potentially contaminating Chernobyl and Russia all over again. Disaster cleanup and sarcophagus construction efforts exposed thousands of workers to elevated levels of radiation (OPA 2013). Response equipment included remote-controlled bulldozers and robot-carts that could detect radioactivity and carry hot debris. Valery Legasov (first deputy director of the Kurchatov Institute of Atomic Energy in Moscow) said, in 1987: "But we learned that robots are not the great remedy for everything. Where there was very high radiation, the robot ceased to be a robot—the electronics quit working." (Edwards 1987)

The Fukushima Dai-ichi nuclear power plant meltdown began on March 11, 2011. An earthquake off the coast of Japan led to a cascading chain-of-events that resulted in the nuclear disaster. First the earthquake downed electrical power lines to the plant. The plant switched to backup generators for electric power. Shortly after the switch to backup generators a tsunami overcame the seawall and flooded the generators that were located in lower levels of the NPP (TEPCO 2013). With no generator or grid power, reactor and Spent Fuel Pool (SFP)

cooling systems shut down. Next fuel rods began to overheat creating superheated steam. The zirconium cladding on the rods began to crack, exposing the radioactive material while also producing volatile hydrogen gas (TEPCO 2013). In order to reduce this increasing pressure, emergency relief valves opened moving the gases into suppression pools which leaked out into the various containment buildings. The buildup of these gases combined with oxygen, eventually ignited like a dirty bomb, blew off the roof and walls of several containment buildings, and released radiation into the atmosphere (TEPCO 2013). Due to the venting system and design of the power plant, the core meltdowns in Units 1-3 caused the explosions in reactor buildings 1, 3, and 4 (Foundation 2012). With subsequent fires, radiation release and scattered loose debris, emergency personnel were unable to reach the containment buildings (TEPCO 2013). Unit 4 did not have an operating reactor however hydrogen gas from Unit 3's reactor venting into the building caused an explosion, damaging the containment building's structure and compromising the SFP located in that building (TEPCO 2013).

As background, a SFP is where used fuel assemblies are stored to cool until they are ready for dry-cask storage. During the cooling period the fuel assemblies constantly give off decay heat (WNA 2012). In Figure 2, the SFP is next to the primary containment vessel (PCV) that houses the reactor pressure vessel allowing for the transfer of fuel to and from the reactor which occurs underwater.

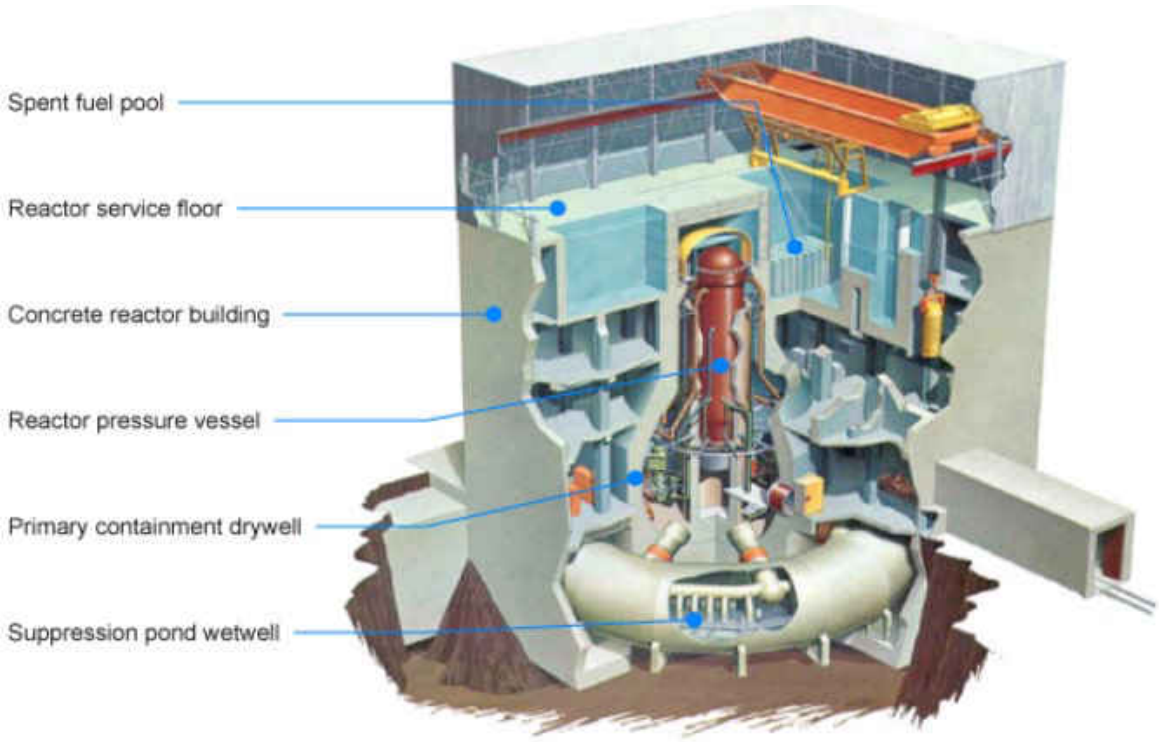

Figure 2 - Reactor Containment Building BWR (WNA 2012)

The water in the SFP serves a dual purpose. Water acts as a heat sink for the decay heat and provides a medium for the radiation, given off by the fuel assemblies, to be absorbed. If water-height and temperature in the SFP are not maintained at an adequate level the potential for large amounts of radiation release exists.

During the Fukushima disaster with multiple reactors undergoing partial core meltdowns, the unit 4 SFP was not initially of primary concern. However, overheating of the unit 4 SFP was potentially more catastrophic than a reactor core meltdown due to the large number of assemblies, 1,535 of the 1590 SFP capacity, involved (WNA, 2012). Unit 4 was in the process of large-scale construction, so all of the fuel assemblies from the reactor pressure vessel were transferred to the pool further increasing the amount of decay heat given off by

Unit 4's SFP. Table 1 below shows the decay heat coming from Unit 4's SFP before the power loss (March 11) is far greater than any of the other SFPs.

Table 1 - SFP Inventories and Estimated Total Decay Heat

Spent-Fuel Pool	Stored Fuel (Number of Bundles)[a]	Capacity Number of Bundles	Decay Heat (MWt)	
			March 11	June 11
Unit 1	392 (100)	900	0.18	0.16
Unit 2	615 (28)	1240	0.62	0.52
Unit 3	556 (52)	1220	0.54	0.46
Unit 4	1535 (204)	1590	2.26	1.58
Unit 5	994 (48)	1590	1.00	0.76
Unit 6	940 (64)	1770	0.87	0.73
Common	6375 (0)	6840	1.13	1.12

(ANS 2011)

As the progressing threat of an overheating SFP became imminent (TEPCO, 2013), lack of functioning instruments coupled with high radiation levels preventing access forced emergency personnel to make assumptions about the condition of the SFP (ANS 2011). Although there is speculation about the cause of the hydrogen explosion in Unit 4 that damaged the containment structure, it is certain that without coolant the water temperature would rise. On March 16 2011, manned helicopters from Japan's Defense Forces (Ministry of Defense 2011) emptied buckets of slung-load water on the SFP but safety of the aircrew limited their ability to get close enough to be effective. Deployed water cannons did not prove to be effective either and eventually a cement delivery vehicle with an articulating boom provided

cooling water. The cement delivery vehicle had to be shipped halfway across the world to Japan (NRC 2012).

Due to the global consequences of potential future nuclear disasters (Deverell 2012), Fukushima demonstrated the insufficiency of and need for improved: infrastructure resilience (Kerigan-Kyro 2012), disaster response planning (NAAIC 2012), capabilities of responding equipment and systems, and crisis management processes. For NPPs across the world, chain of event disasters received new attention. As an example, fire department assets reached the Fukushima NPP by road. But in a chain of event disaster, road access to an NPP is not always possible due to debris blocking or naturally eroding roads and bridges. For NPPs located on barrier reefs consequences may be even more devastating than seen at Fukushima. For example, 2012 Superstorm Sandy not only clogged roads with debris and sand but swallowed roads (AP 2012). 2009 Hurricane Bill swept away a shore road in Nova Scotia (News 2009). 2016 Hurricane Matthew washed away a segment of the Florida highway (WTHR 2016). Furthermore, category 2 Hurricane Frances threatened the St Lucie Florida Power and Light (FPL) nuclear power plant discharge canal with breaching due to the toe erosion of the confinement berm and erosion of the intake canal (R83) interior side slopes (Protection 2004).

(NRC 2010) recognized specific earthquake-related prolonged station blackouts and chain of event threats to numerous NPPs including storm surge threats to Gulf and East Coast NPPs including the NPP at St Lucie, FL (Prasad, Hibler et al. 2011). "There are many nuclear plants on the Atlantic Coast or on rivers that may be affected by a tidal bore resulting from a

tsunami. These include St. Lucie, Turkey Point, Brunswick, Oyster Creek, Millstone, Pilgrim, Seabrook, Calvert Cliffs, Salem/Hope Creek, and Surry (NRC 2011)."

With so many NPP's located in storm surge prone areas, theoretically, what might a reliable and safe emergency response look like had the St Lucie NPP, as an example, been hit with a category 4 hurricane with the scale and effects that Hurricane Katrina devastated New Orleans?

In facing unprecedented situations, emergency responders develop novel solutions to help avoid further catastrophe (Johnson 2006, OPA 2013, TEPCO 2013). The use of helicopters has been a common tool to develop these solutions. However manned crews in each of three incidents shown in Figures 3, 4, & 5 put responders at a heightened safety risk due to radiation exposure and operations in close proximity to a nuclear disaster site. In Chernobyl, helicopter crews endured plumes of radioactive super-heated gas and constant radiation exposure during their efforts (Johnson 2006, OPA 2013). One crew tragically crashed into crane cables near the reactor, falling to their death (Pripyat 2006). These examples provide insight into the potential benefits that helicopters lend in nuclear disaster response, but also the risk that their respective crew faces.

Figure 3 - Fukushima (Fukushima 2011)

Figure 4 – Chernobyl (Chernobyl 2012)

Figure 5 - Three Mile Island (Sun 2014)

If requested, (JTF-CS 2015) tasks the United States military to support civilian agencies responding to nuclear disasters with manpower and resources that may include unmanned systems. Unmanned systems provide many advantages over manned systems especially in radioactive, high heat environments.

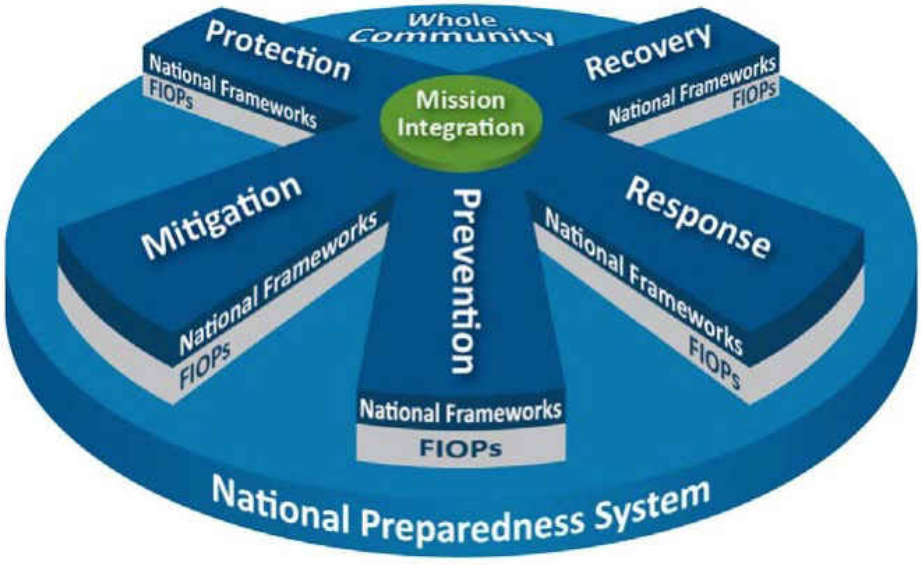

Figure 6 - Five Phases of National Preparedness System (FEMA 2014)

Unmanned systems offer assistance in response and recovery including: clearing debris (e.g. Chernobyl), surveillance and monitoring (e.g. Three Mile Island), and heavy lift tasks (e.g. Chernobyl and Fukushima) (Guizzo 2011, Foundation 2012, OPA 2013, OPA 2013). The use of Unmanned Aerial Systems (UASs)/Unmanned Aerial Vehicles (UAVs) is traditionally for missions, too risky for pilots, that are considered "dull, dirty and dangerous" (Blyenburgh 2000) making nuclear disaster response a possible candidate. In order to ensure effective integration of these unmanned systems in accordance with the five phases of the National Preparedness System as seen in Figure 6, the unmanned systems must be designed to operate in high radiation environments as well as emergency responders must be familiar with their use and properly trained in their operation.

The U.S. military uses UAVs for ISR (intelligence, surveillance, and reconnaissance) operations such as the MQ-9 in Figure 7, and lift operations, such as the K-MAX shown in Figure 8. The Fire Scout unmanned system in Figure 9, designed by Northrop Grumman, can perform both slung-load and ISR missions. The K-MAX and Fire Scout are possible replacements to manned aircrafts used in Fukushima's water replenishment efforts (DailyMail 2011). Fukushima responders deployed unmanned systems to support nuclear disaster response on more than just an aerial front. Unmanned ground and maritime systems provided further benefits in catastrophe relief efforts (Campbell, Abu-Tair et al. 2014, Hsu 2014, Sharma, Sutton et al. 2014, Svec, Thakur et al. 2014, Oikawa 2015).

Figure 7 - MQ-9 UAV (Force 2007)

Figure 8 - K-MAX UAV (Martin 2015)

Figure 9 – MQ-8C Fire Scout

Additionally, UAVs now perform civilian and industry tasks once accomplished by manned helicopters (Saggiani and Teodorani 2004, Farradyne 2005, UTM 2007, Bernard, Kondak et al. 2008, McGonigle, Aiuppa et al. 2008, Alexis, Nikolakopoulos et al. 2009, Marconi, Melchiorri et al. 2012, Mase 2013). These tasks include survey, inspection, and assessment of facilities such as performed by small rotary UAV's with photogrammetric surveying technology. IATEC Plant Solutions developed and deployed a new surveying technology capable of replacing their current survey methods: Scan (high Precision, high Cost) and Direct Inspection (difficult to access, human risk) (Pix4D 2016). Figure 10 provides the drone surveying method on the left along with the reconstruction scene on the right. The drone was capable of successfully reconstructing 750,000 square meters within 3 days.

Figure 10 – Drone Photogrammetric Survey Technology (Pix4D 2016)

Modeling and simulation (M & S) offers a wide range of benefits to the nuclear emergency and disaster preparedness community (INNG 2015) allowing researchers to explore concepts, develop response equipment/systems, and conduct mission rehearsal and management as well as operator training. M & S is already widely used in emergency management exercises (Van Niekerk, Coetzee et al. 2015) and nuclear plant safety training. Simulation-based acquisition (Zittel 2001, Proctor, Posey-Macalintal et al. 2003) and system design and engineering (Brantley, McFadden et al. 2002) enable safe and cost effective exploration of the implementation of these unmanned systems for nuclear disaster response, mitigation, and recovery (Davis, Proctor et al. 2016). M & S is also used to design radiation shields for operational missions such as Tel Aviv-based StemRad did when creating the AstroRad Radiation Shield to protect astronauts from deadly solar particles (Lewis and Harash 2017). However, as discussed further below, there is a gap in expectations for and operational assessment of the levels of tolerance to radiation that may be needed for unmanned system electronics during a nuclear disaster response (Proctor, Shageer et al. 2015).

Given the likely use of a UAV's in a future NPP chain-of-events disaster, Chapter 2 and 3 will address the question, what modeling and simulation tools exist that may enable an assessment of various response scenarios and the length of UAV survivability within irradiated environments?

Chapter Summary and Dissertation Overview

Chapter 1 provides the motivation behind the study of unmanned aerial vehicles operating in an irradiated environment. The brief overview revealed the potential threats (e.g. loss of coolant due to power outage, containment structure fracture due to earthquake, denial of access and other damages due to storm surge, etcetera) that accident, natural chain of events, terrorist attack or sabotage, or cyber-attack pose to NPS. A review of the Chernobyl and Fukushima power plant disasters revealed the breadth and depth of widespread radiation dispersion and threat to humans that a reactor meltdown or spent fuel pool cooling failure pose. Unlike Chernobyl where loss of human life was an accepted part of the helicopter portion of emergency response, helicopter operations at Fukushima proved largely ineffective due to operational constraints arising from radiation and other dangers to human operators. Review of the unmanned systems implemented at Chernobyl and Fukushima revealed not only the susceptibility of their electronics to radiation but over-optimistic robot creators about their survivability in irradiated environments. Thus, the literature appears to lack identification of expectations for electronic survivability of UAV suitable for reactor or SFP water replenishment or other heavy lift missions in irradiated environments common to a NPP or other nuclear disaster response.

In contextualizing the prior general research questions, the following technical literature review for this dissertation is divided into Chapter two and Chapter three. Chapter two discusses radiation and the various nuclear models and simulations capable of simulating a nuclear disaster scenario similar to that at Fukushima and Chernobyl. Chapter three discusses and investigates Systems-of-Systems conceptual modeling (Davis, Proctor et al. 2016) and scenario instantiation onto a distributed, Live Virtual and Constructive (LVC) simulation framework as a generalized research approach for nuclear disaster modeling. The focus of consideration of the framework is its ability or inability to identify radiation tolerance levels that are needed by electronics systems of unmanned systems to survive various operational scenarios. To that end, this research seeks to perform proof of principle research by expanding a LVC simulation framework into a RASCAL-LVC simulation framework that is both low cost, reliable, and independent of the nuclear industry or even governments. The RASCAL-LVC simulation framework enables operational assessment of UAV electronic survivability in irradiated environments. To illustrate the RASCAL-LVC usability for assessing UAV electronic survivability, three response missions are considered. A repetitive In-and-Out Mission (e.g. delivery of parts), a Fukushima-like SFP Cooling Mission (e.g. dumping water into an overheating SFP), and a Chernobyl-like Reactor Extinguishing Mission (e.g. dumping sand and boron into a breached reactor). Chapter Four proposes a generalized methodology to determine the efficacy of unmanned systems by creating a RASCAL-LVC simulation framework and implementing UAVs in irradiated environments for disaster mitigation. Experimental design is based on the emergency response efforts at Fukushima and Chernobyl (most catastrophic

disasters) and the experimental design findings by (Davis 2017), as a context for factor selection. The experimental runs focus on efforts of responders to replenish cooling water to the SFP at the Fukushima NPP Unit 4 but use rotary UAVs based on STAGE flight models to deliver water/parts/boron instead of the ineffective manned helicopter seen at Fukushima. NRC's RASCAL dispersion model program calculates and provides radiation contamination zones in a time-dependent dose fashion. Proof of principle goals include: (1) incorporating RASCAL radiation clouds into live, virtual, and constructive simulation; (2) providing a RASCAL-LVC simulation platform and methodology for operational evaluation of various unmanned systems (aerial, ground and maritime) in irradiated environments; (3) conducting a RASCAL_LVC simulation of and collecting data from three NPP disaster, operational scenarios;(4) identification of lessons learned on the approach, identification of additional research gaps, and recommendation of future research. Chapter five provides the data and analysis of the research case study. Chapter six includes the conclusion as well as recommendations for future research.

CHAPTER TWO: LITERATURE REVIEW

Literature Review of Radiation and its Impact on Humans and Electronics

When one considers UAV survivability when responding to a NPP disaster, one may ask, what radiation must one consider and what level is considered dangerous?

Radiation is energy that emits from a source and is produced in the form of waves and particles (Nordion 2016, WNA 2016). There are two types of radiation: non-ionizing and ionizing. Non-ionizing radiation is found at the long-wavelength end of the electromagnetic spectrum and includes: radio waves, microwaves, visible light, ultraviolet light and infrared light (Nordion 2016). Non-Ionizing radiation only has enough energy to excite atoms, like water molecules exhibiting movement when heated by microwaves. Non-ionizing radiation is still harmful "and can pose a considerable health risk to potentially exposed workers if not properly controlled." (Labor 2016) For example, Microwave radiation (MW) and Radiofrequency (RF) radiation "at high enough intensities both will damage tissue through heating" (Labor 2016). Ionizing radiation has a higher frequency and shorter wavelength than non-ionizing radiation. Ionizing radiation travels in the form of electromagnetic waves (gamma or X-rays) or particles (neutrons, beta or alpha). Ionizing radiation has more energy than non-ionizing, enough energy to cause a chemical change by breaking the chemical bond that occurs in molecules and atoms thereby causing neutral atoms to become electrically charged (Ionized) (Britannica 2016, Mirion Technologies 2016). Ionizing radiation is more dangerous than non-ionizing radiation because ionizing radiation is able to change the makeup of atoms in cells, like DNA molecules in humans

(Mirion Technologies 2016). The diagram of the electromagnetic spectrum in Figure 11 provides some examples of both forms of radiation.

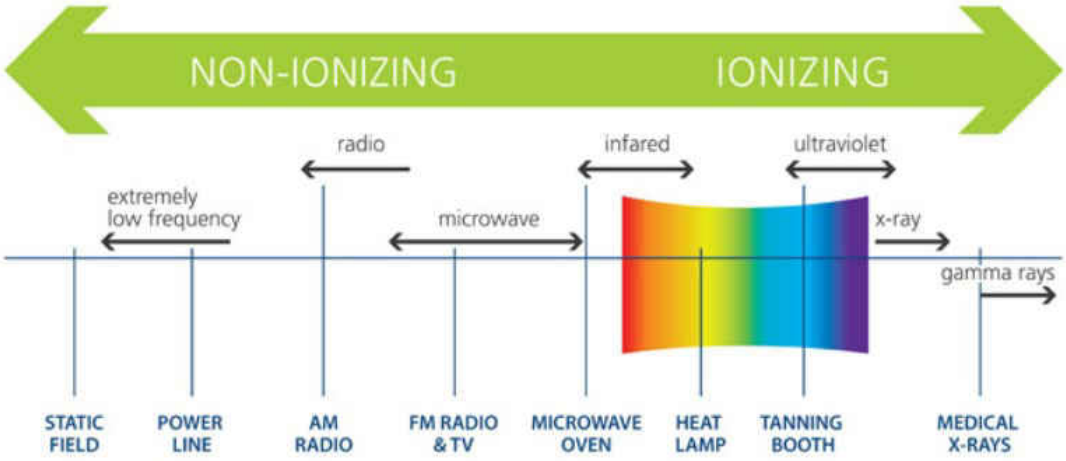

Figure 11 – Electromagnetic Spectrum (Nordion 2016)

The sun emits radiation continuously and hence levels of ionizing radiation may be measured on the earth with greater levels of Gamma radiation at higher altitudes than at lower altitudes. Figure 12 indicates the level of terrestrial gamma ray exposure at 1m above the ground due to the sun.

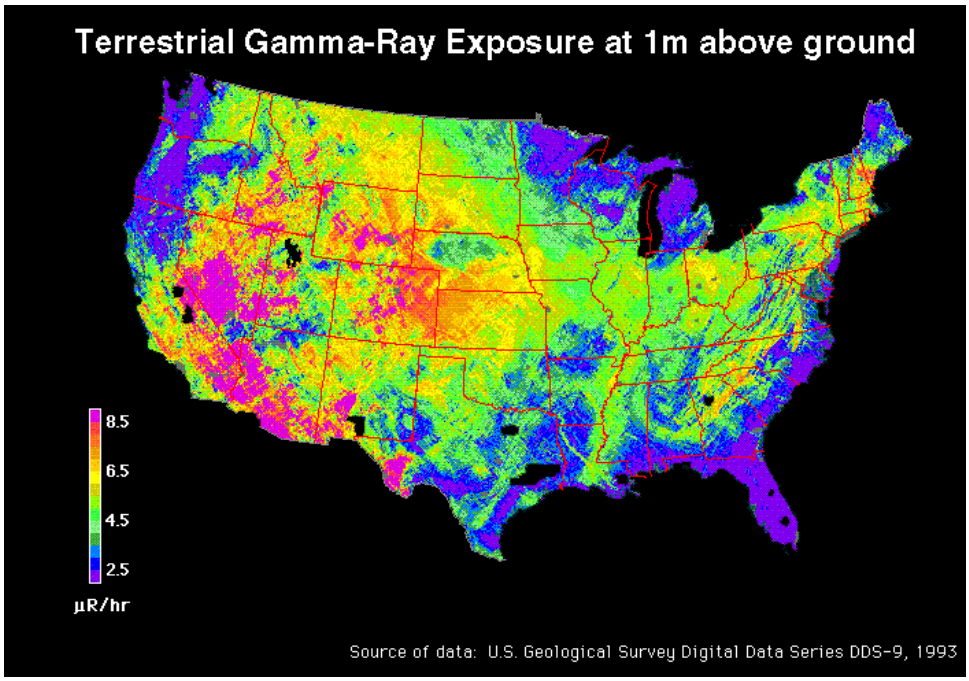

Figure 12 – USGS U.S. Gamma Ray Exposure Map (µrems/hr) (Systems 2016)

Radiation is found in food, televisions and certain medical tests (Systems 2016). Ionizing radiation has many medical uses but over-exposure can cause burns, radiation sickness, cancer and genetic damage (Mirion Technologies 2016). The dosage of ionizing radiation of one roentgen of gamma-ray exposure is defined as roentgen equivalent man (rem). In terms of international definitions, an SI unit of dose equivalent is Sieverts (Sv) where one Sv equals an effective dose of a joule of energy per kilogram of recipient mass. Conversion from sievert to rem is 1.0 Sv = 100 rem. Typical amounts of ionizing radiation may be absorbed from various sources shown in Figure 13. Various health impacts of radiation are described in mrem in Figure 14.

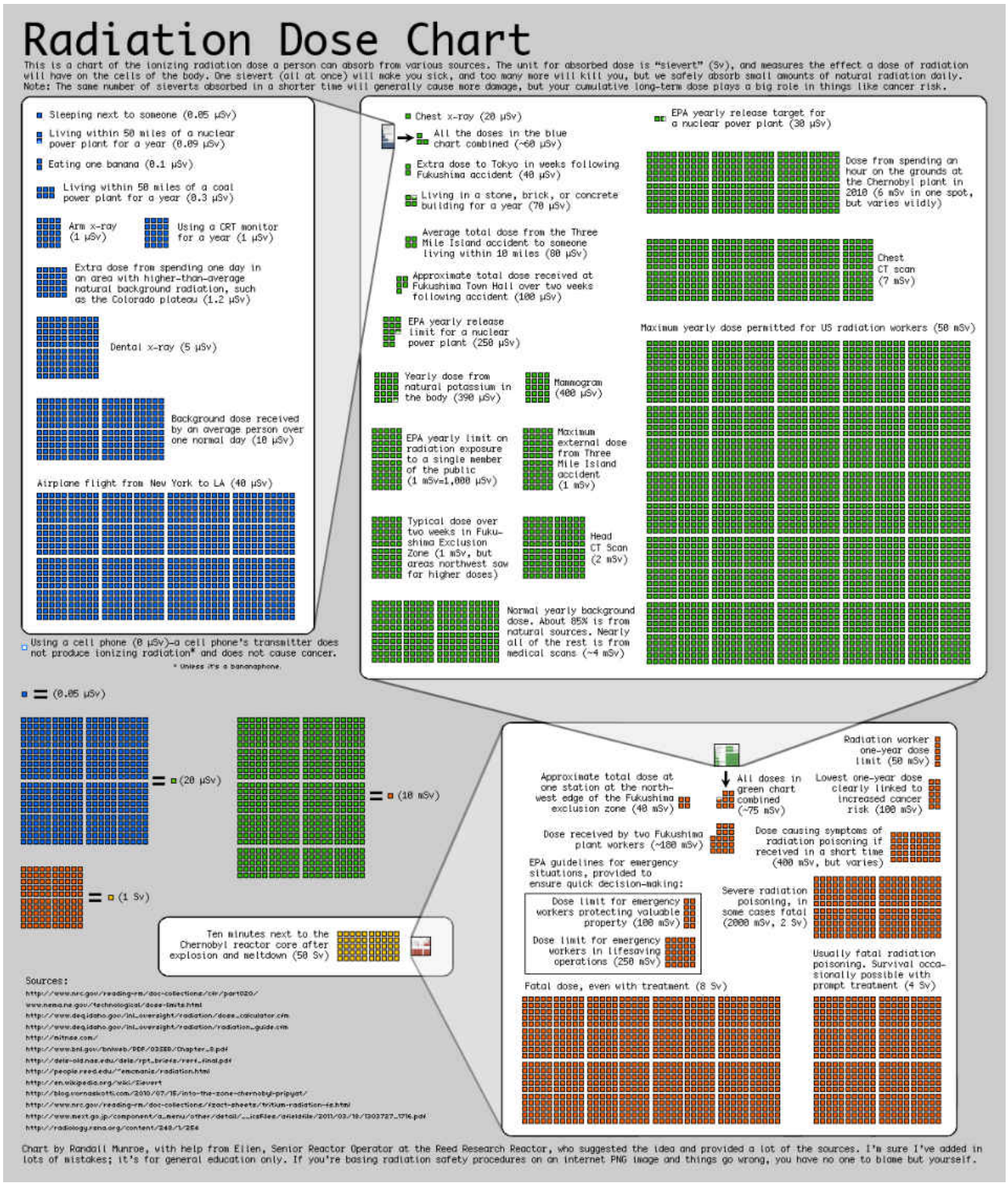

Figure 13 – Radiation Dose Chart (Lee 2011)

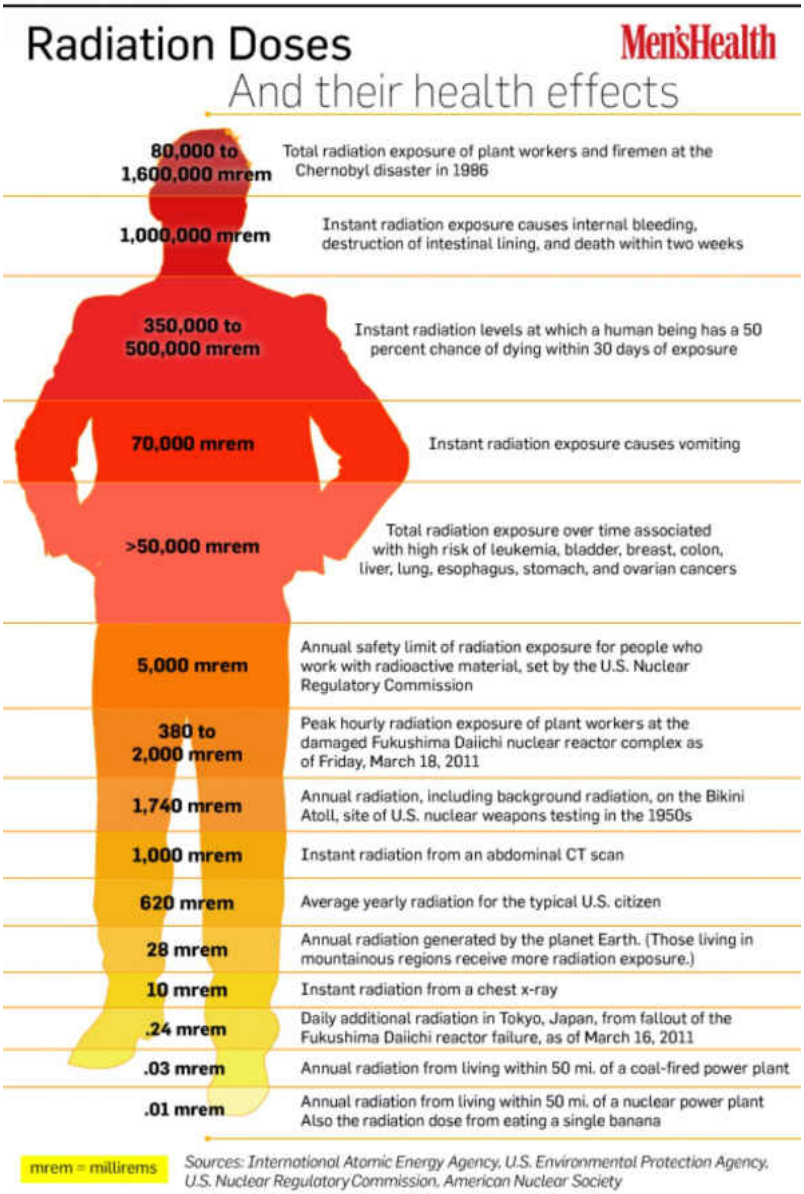

Figure 14 - Effects of Radiation (MensHealth 2011)

Ionizing radiation is produced in the following forms: Alpha particles, Beta particles, Neutron particles, and Gamma and X-Ray waves. Each form of ionizing radiation has a different penetrating capability and health effect. Alpha particles' penetrating power is limited but can cause serious cell damage if ingested with food or inhaled (Mirion Technologies 2016, WNA

2016). Beta particles have a slightly greater penetrating power and pose a minimal external health risk but like alpha particles can cause serious damage if inhaled or ingested. Gamma waves have a much greater penetrating power and can travel much further through air than alpha and beta particles. Gamma waves lose about half their energy for every 500 feet. Gamma waves can be stopped by a thick enough material such as lead or iron (Mirion Technologies 2016). X-ray waves are similar to gamma ray waves and are not present in nuclear power plant environments but they provide static images of teeth and bones for dental and medical purposes (NRC 2016). Neutron particles have the greatest penetrating power. Neutron particles consist of a free neutron that is able to travel hundreds or even thousands of meters in the air unless stopped by a hydrogen-rich material (Water or Concrete) (Mirion Technologies 2016, NRC 2016). Stable atoms that absorb neutron particles become unstable or radioactive. Neutron particles are the only type of radiation that turns other materials radioactive (NRC 2016). The process of "neutron activation" produces many of the radiation sources used in the medical, academic and industrial fields (NRC 2016). The penetrating power of the different types of ionizing radiation is illustrated in the diagram below:

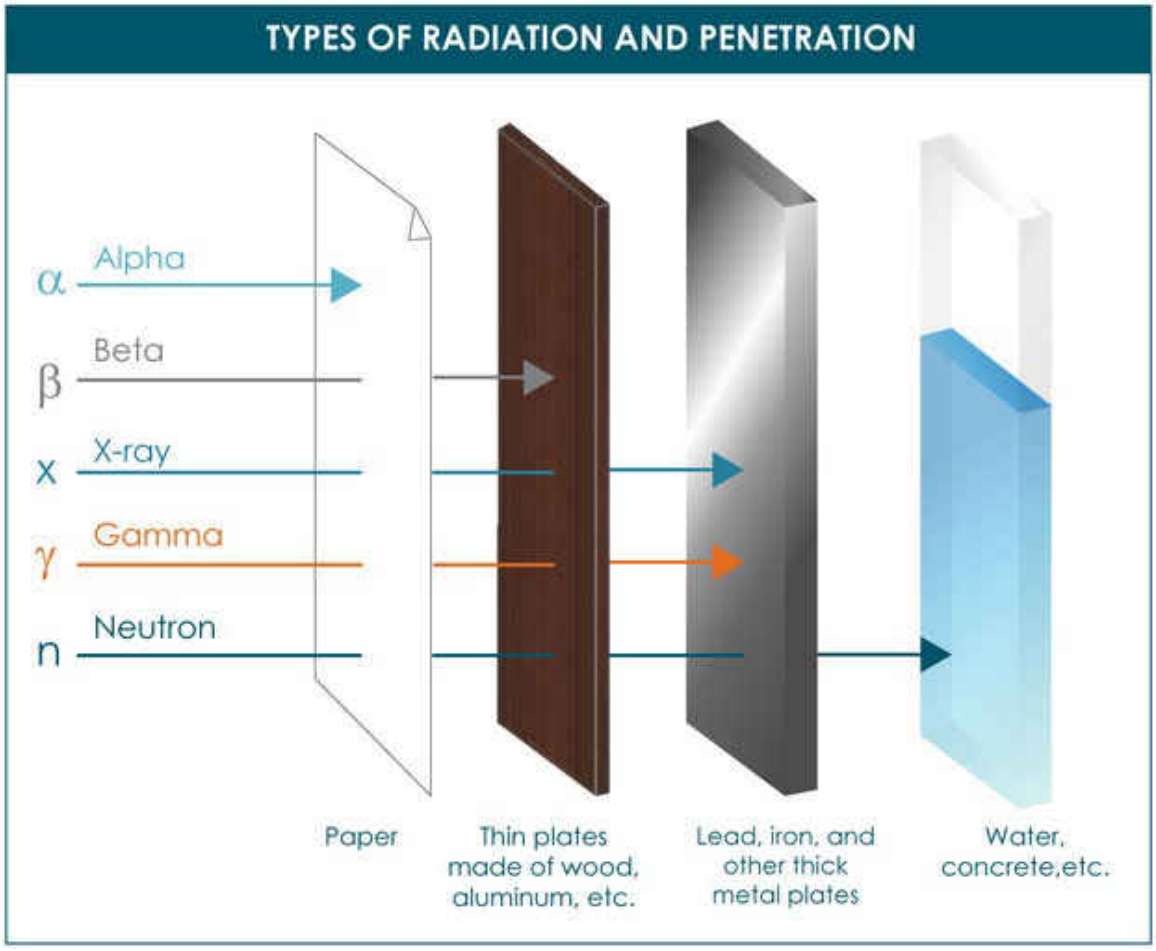

Figure 15 – Forms of Ionizing Radiation (Mirion Technologies 2016)

When a nuclear reactor is operating at full power for a long period of time there is a considerable build-up of gamma rays from the fission products. The amount of fission products present in the fuel elements depends on how long and at what power level the reactor operates at before shut-down. Neutron radiation is also present even after long-term shutdown, in the form of Photoneutrons (Power 2016).

Radioactive

An atom is radioactive if it is unstable due to excess energy or mass. In the pursuit of stability, atoms emit excess energy in the form of ionizing radiation (Commission 2012, Mirion Technologies 2016). A substance/material is radioactive if it is made up of or contains a large quantity of radioactive materials. A radioactive isotope, also called radioisotope, radionuclide, or radioactive nuclide, may be any chemical element whose nuclei are unstable and dissipate excess energy by spontaneously emitting radiation in the form of alpha, beta, and gamma rays (Britannica 2016). Every chemical element has one or more radioactive isotopes. For example, hydrogen, the lightest element, has three forms with mass numbers 1, 2, and 3 (Britannica 2016). Only hydrogen-3 (tritium), however, is a radioactive isotope, the other two forms being stable. More than 1,000 radioactive isotopes of the various elements are known. Approximately 50 of these are found in nature; the rest are produced artificially as the direct products of nuclear reactions or indirectly as the radioactive descendants of these products (Britannica 2016). Humans naturally contain Potassium, Carbon-14, and other radionuclides. This makes a human radioactive to the tune of around 40 mrem a year. Other people are also radioactive, so one gets slight doses from being around others as well (Systems 2016).

Nuclear fallout is another source of radiation. The KODAK film company first recognized radiation contamination from nuclear testing fallout, because their film was being destroyed by the strawboard used to separate film. Specifically, due to the straw mill's placement along a river, the material to make the strawboard was being contaminated by radioactive particles contained in rainwater carried by wind from above ground A-bomb testing (Blitz, 2016). KODAK

recognized that after a period of time following an above ground nuclear explosion, radioactivity disappeared.

Over time as the number of unstable atoms decrease the material becomes less radioactive. Reduction in radioactivity is measured in terms of a "half-life". A half-life of radioactive substances can vary greatly from a few seconds to 441 trillion years in the case of Iridium-115 (Mirion Technologies 2016). If a substance has a half-life of 10 days, then after 10 days, 50% of the radioactivity remains. After 10 more days only 25% of the original radioactivity remains.

The radioactive isotopes released in the nuclear accident at Fukushima and their respective half-lives are listed in Table 2. Figure 16 graphs preliminary data measuring radioactive releases by Isotope from the Fukushima incident.

Table 2 – Radioactive Isotopes released in Fukushima

Radioactive Isotope	Half-Life
Cesium-137	30 Years
Cesium-134	2 Years
Iodine-131	8.02 Days
Iodine-132	2.3 Hours
Iodine-133	20.8 Hours
Tellurium-132	3.2 Days

(American 2014, Physics 2016)

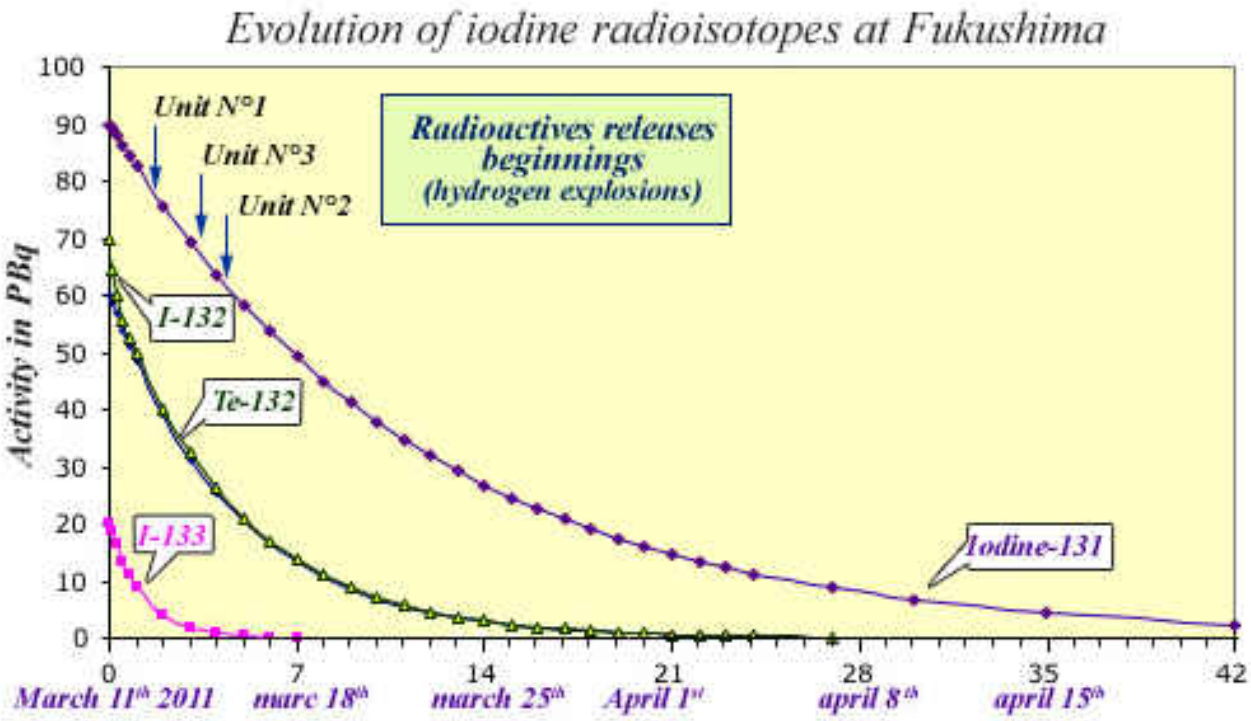

Figure 16 – Evolution of iodine radioisotopes at Fukushima (Physics 2016)

Measuring Radiation Exposure

Measurement confusion is partly attributed to the difference between the international system (SI) and customary units (U.S.). However, the various ways in which radiation is represented and measured, can also pose confusion. Radiation measurements include: Rads vs Gray; Roentgens vs Coulombs per Kg; Sieverts vs Rems; Curies vs Becquerels; Electronvolts vs Joules (Palmer 2011). Rads (U.S.) or Gray (SI) measures radiation entering a person or object. Roentgens (U.S.) or Coulombs per kilogram (SI) measures radiation floating through the air. Sieverts (SI) and Rem (U.S.) provide a measure of the harm caused by radiation in a sample of tissue/material. Curies (U.S.) or Becquerels (SI) measures rate of radiation emission from a

source. Electronvolts (Ev) or Joules(J) measures of the energy rather than emission rate (Palmer 2011). Because different types of radiation affect the body and materials differently (e.g. alpha and beta particles vs gamma rays), types of radiation and sensitivity of tissue/material should be taken into account when converting from radiation absorption to measures of effective dose (Palmer 2011). To view it simply: 1 rad of absorbed dose gives the object 1 rem of effective dose.

Radiation Contamination and Exposure Health Affects

Contamination occurs when a radioisotope (gas, liquid, or solid) releases into the environment and is then ingested, inhaled, or deposited on a surface. If an individual or device is contaminated, then a reading will be present on a radiation survey monitor. Radiation Exposure occurs when an individual or material absorbs penetrating ionizing radiation from an external source. Exposure stops when a person leaves the area of the source. APPENDIX L provides examples of each.

The effect of radiation on humans varies depending on intensity and duration of exposure. The negative health effects can range from nausea, to cancer, and lastly death. A single dose of around 450 rems (450,000 mR) is considered to produce death in 50% of the cases (Systems 2016). The chart below provides a variety of doses, and their respective effects.

Dose	Effect
0.05 Sv to 0.2 Sv (5 rem to 20 rem)	No symptoms.
0.2 Sv to 0.5 Sv (20 rem to 50 rem)	No noticeable symptoms. Red blood cell count decreases temporarily.
0.5 Sv to 1 Sv (50 rem to 100 rem)	Mild radiation sickness with headache and increased risk of infection due to disruption of immunity cells. Temporary male sterility is possible.
1 Sv to 2 Sv (100 rem to 200 rem)	Light radiation poisoning, 10 % fatality after 30 d (LD 10/30). Typical symptoms include mild to moderate nausea, with occasional vomiting. The immune system is depressed, with convalescence extended and increased risk of infection. Temporary male sterility is common.
2 Sv to 3 Sv (200 rem to 300 rem)	Severe radiation poisoning, 35 % fatality after 30 d (LD 35/30). Nausea is common, with risk of vomiting. There is a massive loss of leukocytes, increasing the risk of infection. Permanent female sterility is possible. Convalescence takes 1 mo to several months.
3 Sv to 4 Sv (300 rem to 400 rem)	Severe radiation poisoning, 50 % fatality after 30 d (LD 50/30). Other symptoms are similar to the 2–3 Sv dose, with uncontrollable bleeding in the mouth, under the skin, and in the kidneys.
4 Sv to 6 Sv (400 rem to 600 rem)	Acute radiation poisoning, 60 % fatality after 30 d (LD 60/30). Fatality increases from 60 % at 4.5 Sv to 90 % at 6 Sv. Female sterility is common at this point. Convalescence takes several months to 1 yr. The primary causes of death (in general 2 wk to 12 wk after irradiation) are infections and internal bleeding.
6 Sv to 10 Sv (600 rem to 1000 rem)	Acute radiation poisoning, 100 % fatality after 14 d (LD 100/14). Survival depends on intense medical care. Bone marrow is nearly or completely destroyed, requiring a bone marrow transplantation. Gastric and intestinal tissue are severely damaged. Death is from infection or internal bleeding. Recovery would take several years and probably would never be complete.
10 Sv to 50 Sv (1000 rem to 5000 rem)	Acute radiation poisoning, 100 % fatality after 7 d (LD 100/7). Spontaneous symptoms occur after 5 min to 30 min. After powerful fatigue and immediate nausea, there is a period of several days of comparable well-being, after which cell death occurs in the gastric and intestinal tissue, causing massive diarrhea, intestinal bleeding, and loss of water. Death is preceded by delirium and coma. Death is inevitable; the only treatment that can be offered is pain therapy.
50 Sv to 80 Sv (5000 rem to 8000 rem)	Immediate disorientation and coma in seconds or minutes. Death occurs after a few hours by total collapse of nervous system.
> 80 Sv (>8000 rem)	Immediate death.

Figure 17 – Health Effects of Radiation Exposure (Training 2007)

Radioactive Impacts from NPP disasters

Three Mile Island – nuclear power reactor

Scientific studies found no evidence of any harm resulting from radiation exposure and in 1996, 2,100 lawsuits claiming adverse health effects from the accident were dismissed for lack of evidence.

Chernobyl – nuclear power reactor

In the Chernobyl NPP radiological emergency firefighters were dosed with hot spot radiation as high as 17,540 Rads/hr (Sanchez 2016), as recorded above Chernobyl during the disaster. After the disaster in 1986 around 24,000 people living within 15 km of the plant received an average of 45 Rads before they were evacuated. During the response, 134 workers and firemen were severely exposed to nuclear radiation and 28 died as a result of acute radiation syndrome (ARS) within three months of the accident. Nineteen more died from 1987 to 2004 from different causes. A further analysis of 61,000 emergency room workers who had lower doses of radiation estimates around 116 cases of illnesses attributable to radiation (WNA 2016).

Fukushima – nuclear power reactor

It is too early to determine the global scope of the Fukushima disaster. A Stanford study estimated Fukushima cancer-related mortality to be around 130 people and cancer-related morbidity to be around 180 people (Hoeve and Jacobson 2012). The Stanford study also

estimated a nuclear accident using their own region, which is 25% as dense as Fukushima, and their projections are around 600 mortalities.

Radiation contamination of the environment may cause further issues in the future if not dealt with quickly and effectively. Fallout from radioactive plumes and clouds contaminates the topsoil with radioactive dust. To reduce future human health risk this soil must be collected and stored. Fukushima cleanup collected 10 million trash bags full of contaminated soil (ZeroHedge 2016). The seemingly endless fields of black plastic bags shown in Figure 18 are a grim reminder of the Fukushima disaster.

Figure 18 - Contaminated Soil in Fukushima (ZeroHedge 2016)

Response of the World Nuclear Association and other agencies

The World Nuclear Association contends "The nuclear fuel cycle does not give rise to significant radiation exposure for members of the public, and even in two major nuclear accidents – Three Mile Island and Fukushima – exposure to radiation has caused no harm to the public." (WNA 2016) WNA goes on to state "Radiation protection standards assume that any dose of radiation, no matter how small, involves a possible risk to human health. This deliberately conservative assumption is increasingly being questioned. Fear of radiation causes much harm. Expressed particularly in government edicts following the Fukushima accident (and also Chernobyl), fear has caused much suffering and many deaths" (WNA 2016). The deaths and suffering the WNA refers to relates to individuals being injured / killed during evacuation procedures.

Clearly the World Nuclear Association has a different perspective on the dangers of radiation than the public. One primary issue with the WNA report is their focus on immediate and local casualties. Further, the WNA completely avoids the global dispersion of radionuclide release from Fukushima by narrowing the impacted area to around Fukushima and local radiation levels. In addition, illnesses related to ingestion of radionuclides through marine life were not considered in the WNA article, surprisingly so, especially since there were large amounts of radiation released through contaminated water leakage into the sea (TEPCO, 2013). Apparently, the WNA aims to establish that the evacuation and "fear of radiation" was more dangerous than the radiation itself (WNA 2016) due to the casualties related to evacuating the

area. WNA analysis only supports the supposition that the government used poor evacuation techniques and not that the threat of radiation was “non-existent”.

What does that say about confidence in WNA analysis of nuclear disaster?

The perspective is further complicated by the inaccurate, false, and late reporting to possibly impacted individuals about the disasters by (Inajima and Okada 2011, Tokyo 2011, Dedman 2014, Hirose 2016). TEPCO established a false sense of security by releasing recovery schedules based on incomplete information, without knowing the severity of the damage or state of the reactors it would’ve been impossible to develop an accurate recovery timeline (Inajima and Okada 2011). (Tokyo 2011) reveals the government delayed giving information to the public, authorities grossly underestimated tsunami risks, and Tepco was untrained to handle emergencies such as a nuclear shutdown, leading to worsening conditions at the plant. TEPCO’s own President, Naomi Hirose even issued an apology, stating Fukushima was a “cover-up” and their actions were “extremely regrettable” (Hirose 2016). Following the disaster, even U.S. nuclear agencies “made a concerted effort to downplay the risks of earthquakes and tsunamis to America’s aging nuclear plants.” (Dedman 2014). These failures underscore the need of interested third parties to have access to low-cost, reliable, and independent tools that may accurately simulate the impacts of various disaster and response scenarios.

Reducing Radiation Exposure to Emergency Responders and their Equipment

While health issues outside the immediate disaster area may be debated, there is little to no debate about the threat of radiation poisoning to on scene emergency responders. Using

lead-based underwear and carbon wet-suits may reduce individual radiation exposure and contamination as shown in figure 18. Wet suits may stop 100% of beta radiation. Lead underwear may prevent gamma ray exposure to pelvic area and lower spine (Demetriou 2013).

Figure 19 – Lead Based Underwear & Carbon Wet-Suits (Demetriou 2013)

Effect of Radiation on Equipment Electronics

Use of equipment to mitigate a nuclear power disaster is essential. Humans operate UAVs remotely and are thereby removed from exposure to radiation but the electronics on-board the UAV are still exposed. Exposing electronics to irradiated environments poses a risk to their functionality and usability. Damage to these electronics occurs in two forms: Cumulative effects and Single-Event-Effects (SEEs) (Makowski 2006, Vanderbilt University 2016). Cumulative effects are gradual and occur throughout the lifecycle of the electronic device with the Total Ionizing Dose (TID) being the tolerance limit of the accumulated radiation the device can handle. In theory it is possible to foresee when a failure will happen from cumulative-effect radiation (Patrick 1981, Faccio 2001, Vanderbilt University 2016). Single Event Effects (SEEs) are caused by the energy deposited by one single particle. A device sensitive to SEEs can exhibit failure at any moment during its operation, in order to determine the possibility of SEE failure researchers use probability. Types of SEEs are (Vanderbilt University 2016):

Single Event Upsets (SEUs)

- An energetic particle passing through a digital electronic device causes an unplanned change in its logic state. Device may be re-written to intended state.

Single Event Latchups (SELs)

- The device is latched into one logic state and will not change states in response to a logic signal. Operability of the device can be recovered by cycling the power.

Single Event Burnouts (SEBs)

- The current is not limited, and the device is destroyed.

In determining electronic failure, TID and SEE should both be considered especially since "gamma rays are almost always accompanied by alpha or beta particles" (Training 2007), indicating that radiation that causes TID electronic failure is accompanied by radiation that causes SEE damage. The analysis performed in this study includes TID and not SEE damage leaving room for future research to include probability of failure rates caused by SEE damage.

When designing electronic systems that will be used in ionizing-radiation environments one must consider the tolerance of the electronics involved (semi-conductors, resistors, capacitors, avionics) and ensure their functionality is not hindered by radiation induced degradation (Srour and Mcgarrity 1988). The Air Force recognizes the importance of increasing avionics tolerance to radiation and recommends that these systems be capable of withstanding a Total-Ionizing-Dose of 2300 Rads (Patrick 1981).

The Navy's Air Systems' EMI Corrective Action Program shed some light on how age affects shielding capability. Inspections on operating aircrafts revealed multiple cases of "foreign object damage, excessive chaffing of wires, and improper splicing and terminations." (DoD 2010) Measurements over a ten-year period show shielding degradation in Table 3.

Table 3 – Shielding Degradation relative to Age of Aircraft

Age of Aircraft	Shielding Degradation
New	**10-15%** Out of Specification
5 Years	**40-60%** Out of Specification
10 Years	**70-80%** Out of Specification

(DoD 2010)

Table 4 identifies assurance designators for electronics hardened against levels of radiation from no hardening to hardening up 10^6 Rads. Coupling Shielding degradation with hardness levels can provide insight into the possible causes of early term failure exhibited by other unmanned systems (Limer 2016, Treacy 2016). As recent as February 2017, unmanned systems in use to locate melted fuel are failing to live up to operational guidelines. These unmanned systems were designed to last 10 hours (at 100 Sieverts/hr) and are reaching their tolerance limit of 1000 Sieverts in just 2 hours (Newser 2017). The inconsistency between design parameters and operational expectancy is drastic. These inconsistencies may also be present in UAVs however their lack of use in irradiated environments has not brought these issues to light yet. By investigating early term failures in other unmanned systems, we gain insight into possible UAV failures.

Table 4 – Radiation Hardness Assurance (RHA) Levels

RHA Level Designator (See 3.6.2.1)	Radiation and Total Dose (Rads (Si))
/ or –	NO RHA
M	3000
D	10^4
P	3×10^4
L	5×10^4
R	10^5
F	3×10^5
G	5×10^5
H	10^6

(DoD 2002)

Unmanned Systems used in Fukushima

Recovery operations at Fukushima primarily used unmanned ground systems for: operational “environmental improvement and site repair”, investigative “grasp the site’s condition”, and operational/investigative hybrid purposes. Secondarily, recovery operations also used unmanned aerial and aquatic systems. Appendix F lists the unmanned systems deployed at Fukushima.

Failures of unmanned systems at Fukushima provide motivation for improved modeling and simulation of ionizing radiation risk prior to operations. In one case, an unmanned system at Fukushima experienced radiation spikes reaching 4 Sieverts per hour (400 Rads per hour) (Guizzo 2011). Another unmanned system doing surveillance monitoring inside the reactor vessel nearly 4 years after the incident recorded readings up to 9.7 Sieverts per hour (970 Rads per hour). This particular system was expected to last 10 hours in the radioactive environment but resulted in failure in just 3 hours (Jiji 2015). The largest recorded radiation level was 530 Sieverts per hour (53,000 Rads per hour) inside containment building 2’s reactor vessel (Hruska 2017).

While much work has gone into small unmanned surveillance systems designed for radiation operations, the development and use of larger, rotary-wing, heavy lift UAVs such as the K-MAX in radiation operations is absent. At Fukushima, the only large aircrafts that emergency responders used were two lead-lined manned Japanese Chinook helicopters “to make four water drops each of 7.5 tons of seawater”, but only one drop hit the target (Hannaford 2011). The pilots of the manned helicopters wore protective clothing and were

limited to 40 minutes of flying above the power plant. Thus, there is clear motivation to investigate heavy lift UAV operations in irradiated environments that might improve mitigation efforts during a NPP disaster.

CHAPTER THREE: SOS, LVC, & LVC EXPERIMENTAL DESIGN

Given an understanding of the dangers of radiation to UAV electronics, one may ask, how might one model and simulate potential NPP disaster and response scenarios?

Chapter three discusses the generalizable approach to implementing SoS conceptual models and operational scenario similar to the nuclear disaster at Fukushima into LVC simulation framework. This chapter also discusses an introduction to the integration of ionizing radiation models into a distributed RASCAL-LVC simulation framework applied to nuclear disaster response, based on the SoS conceptual model approach proposed by (Davis, Proctor et al. 2016).

Researchers often use modeling and simulation to replicate scenarios that would be too costly or dangerous to conduct in live operations (Lyon 2014). In terms of cost and danger avoidance, M&S is an effective tool to conduct systems engineering of potential systems designed for nuclear disaster response & catastrophe mitigation in an irradiated environment. Including radiation in this process is important because of its negative effects on unmanned systems functionality. As discussed in Chapter 1 and 2, unmanned systems deployed at Chernobyl and Fukushima experienced failures due to radiation exposure. Further, heavily-lift rotary UAVs were not deployed, but rather manned helicopters that proved both dangerous to human life and ineffective. These failures further validate the need for pre-disaster, model and simulation verification of system capability and hence creation of models and simulation

capable of assessing radiation effects on heavy lift UAV operating during possible future nuclear disasters.

Modeling and Simulation Systems

There are various M&S systems that can assist in recreating elements of the Fukushima Power Plant test case (Hill 2003, Baker 2012, Thunder 2014, NRC 2015):

NRC Computer Codes and RASCAL

- Development through a partnership between the NRC and Sandia National Laboratories

Corys Thunder

- Development by CORYS Inc, a global leader in power and rail training simulators

Hazard Prediction & Assessment Capability HPAC

- Development by Oak Ridge National Laboratory

Chemical-Biological Simulation Suite – CBSS

- Development by the U.S. Army

In order to develop an accurate recreation of events, these models and simulations must involve scientifically correct nuclear calculations. At the same time, understanding representational limits of each M&S system is important to determining their ability to integrate with unmanned systems operating in real time.

Nrc Computer Codes and RASCAL (NRC 2015)

The NRC in partnership with Sandia National Laboratories developed a suite of highly complex nuclear software. "The NRC uses computer codes to model and evaluate fuel behavior, reactor kinetics, thermal-hydraulic conditions, severe accident progression, time-dependent dose for design-basis accidents, emergency preparedness and response, health effects, and radionuclide transport, during various operating and postulated accident conditions." (NRC 2015) NRC computer codes listed in Appendix G provide the necessary models and calculations to simulate the various interactions that occur within nuclear power plants.

The NRC codes are highly complex, and each code typically uses its own interface (stand-alone design) where the user enters a set of parameters and the software provides an output. This input-output design is beneficial in determining discrete event calculations, but the stand-alone design typically lacks the ability to integrate with real-time simulations without extensive additional programming or software "work-arounds." This limitation on interoperability makes it difficult to incorporate these high-fidelity models into a distributed LVC simulation framework.

The nuclear codes from the NRC provide a means for precise calculation of the multitude of nuclear processes that occur within power plants. However, these codes alone do not provide a means of training or mission management for emergency responders. The nuclear codes are access controlled and require approval from the Nuclear Regulatory

Commission in order to use, but the NRC allows researchers with U.S. citizenship to use the codes.

NRC's RASCAL outputs nuclear radiation dispersion over time. The RASCAL code determines time-dependent dose projection releases from a simulated nuclear power plant accident during a radiological emergency. RASCAL is capable of computing dose releases from reactors, spent fuel storage pools, casks, fuel cycle facilities, and radioactive material handling facilities of the following radionuclides listed in Appendix E.

CORYS THUNDER

One simulation agency, Corys Thunder (interface below), integrates the NRC's MELCOR code into their nuclear reactor training simulator (Sanders and Panfil 2013). MELCOR extends the capabilities of Corys Thunder's full-scope desktop and glass-panel simulators to provide best-estimate Severe Accident training for operators, engineers and the Emergency Response organization (Thunder 2014). Recent advancements in MELCOR also allow Cory's to model accidents in spent fuel pools, such as a loss-of-coolant scenario (Thunder 2014).

Figure 20 – Corys Thunder MELCOR Simulation (Sanders and Panfil 2013)

Cory's Thunder simulator design focuses on the power plant's internal dynamics and provides an effective training tool for plant employees, however Cory's Thunder's design does not allow for the integration of externally deployed and operated unmanned systems or external agents (Sanders and Panfil 2013, Thunder 2014).

HPAC

Hazard Prediction and Assessment Capability (Hill 2003, OFCM 2003, Company 2004, Office of the Assistant Secretary of Defense for Nuclear Chemical 2016)

HPAC is defined as: “An atmospheric dispersion modeling tool developed for military operations. The Defense Threat Reduction Agency (DTRA) developed this tool to provide quick response to threats from weapons of mass destruction. This is accomplished by using a suite of programs to read in meteorological data and interpolate it to a user-defined grid, describe in detail the source configuration, and run a transport and diffusion code to generate output in a variety of ways (i.e. concentration, dose, etc.). The main code of use within HPAC for transport calculations is the second-Order Closure Integrated Puff (SCIPUFF) model. SCIPUFF describes diffusion processes using second-order turbulence closure by relating the dispersion rate to velocity fluctuation statistics.” (Company 2004)

The HPAC atmospheric dispersion model provides the capability to predict the effects of HAZMAT releases into the atmosphere and their impact on civilian and military populations. The HPAC model integrates into simulation software to create an accurate representation of dispersion related to hazardous agent releases (Office of the Assistant Secretary of Defense for Nuclear Chemical 2016). The software is controlled access to the defense community and is not being released to researchers. HPAC provides limited benefits in nuclear power plant radiation dispersion and is focused on the dispersion of weapons of mass destruction.

CBSS

Chemical-Biological Simulation Suite

"A set of distributed simulation software tools designed to represent all aspects of CB defense on the tactical battlefield, including applications to analyze strategies, and to provide cost-effective test programs and training of U.S. and allied soldiers." (Baker 2012)

The suite is able to:

- Develop effective CB defense material
- Evaluate tactics, techniques, and procedures (TTP)
- Provide constructive testing over a wide range of terrain, weather, and delivery conditions
- Provide broad scenario-based training
- Support live sensor testing at Dugway

(Baker 2012)

The CBSS Synthetic Natural Environment provides realistic digital representations of chemical, biological, and radiological threats in traditional and urban battlefield environments, by creating high-fidelity, three-dimensional hazard environments as a function of hazard delivery systems, time-varying meteorological conditions, and complex terrain. The model also includes representations of airborne vapor, aerosol concentrations, dosage, deposition, and air concentration contours (Baker 2012).

Although the CBSS is a highly effective tool for training military forces and improving tactical operations management, CBSS' primary focus is related to a chemical, biological, or

radiological attacks and not nuclear accidents from a power plant. Similar to HPAC, CBSS also has controlled access to the defense community.

PRESAGIS Modeling and LVC Simulation Suite

As noted above, M&S software capable of replicating the Fukushima scenario is limited in terms of availability and, when available, limited in scope of coverage. In particular, the NRC computer codes provide an accurate representation of the processes within the power plant and, most important to national response framework responding elements external to NPP, RASCAL provides radiation dispersion models. To design a Fukushima scenario in which UAVs are deployed as part of the external response team, RASCAL radiation prediction zones must be coupled with a software suite capable of terrain generation, developing UAV missions, integrating weather data, and scenario management. Presagis offers a variety of commercial-off-the-shelf (COTS) products for developing modeling & simulation and embedded applications. Appendix H lists the software tools Presagis offers. The tools are able to develop scenarios on a LVC simulation framework compliant to IEEE distribution standards.

> Tolk (2012) defines Live, Virtual, and Constructive simulations in the following way: "The easiest way to understand the three concepts is to look at people, systems, and the operation. If real people use the real systems to participate in a simulated operation, then we are talking about live simulations. If real people use simulated systems or simulators to participate in a simulated operation, then we are talking about virtual simulations. If simulated people use simulated systems to participate in a simulated operation, then we are talking about constructive simulations… Furthermore,

mixed forms are supported by mixing live, virtual, and constructive simulation technologies."

Using Presagis LVC simulation tools, scenarios may be built on Terra Vista synthetic natural environments derived from geographically specific terrain, including elevation post, imagery, and feature information, imported from the United Stated Geological Survey agency and other sources. Finally, STAGE enables scenario management (Presagis 2016). Scenarios built in the Presagis LVC simulation framework may enable concept exploration of system life cycle processes including systems engineering for various aircrafts, modeling and simulation of various environments, simulating operation of those aircrafts in various scenarios, etcetera.

LVC Simulation Framework

(Davis, Proctor, and Shageer 2016b) identify the lack of: interoperability within the nuclear simulation community but also identify the availability of a LVC simulation framework capable of testing the use of unmanned systems in NPP disaster response. (Davis, Proctor et al. 2016) propose a conceptual model shown in Figure 21, suitable for instantiation of a LVC simulation framework nuclear disaster systems analysis and training.

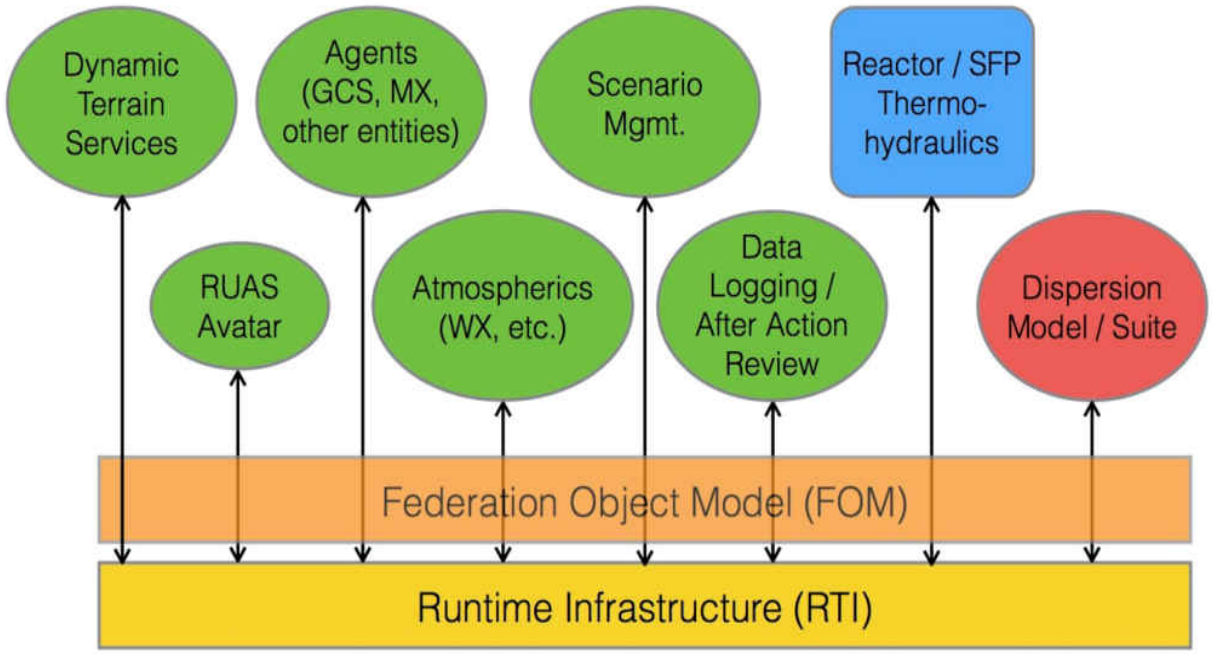

Figure 21 – Conceptual Model of a distributed, LVC-Simulation Framework (Davis, Proctor et al. 2016)

This proposed research seeks to build upon their work by integrating a radiation dispersion model into the LVC simulation framework. The scenario simulated in the (Davis 2017) research study is geographically oriented to the nuclear power plant in St. Lucie, FL and the nearby area (e.g. staging area, freshwater sources). This area is chosen given the geographic data available for this area and the lack of geographical data available for Japan. The St. Lucie power plant was also chosen because of the resemblance to Fukushima (coastal power plant) as well as listed by the NRC as one of the ten nuclear power plants subject to either a tidal bore or storm surge disaster. For simplicity, the St Lucie power plant containment buildings in the simulation are modeled after the Fukushima Dai-ichi containment buildings. These building models are chosen because due to the recent nature of the Fukushima incident, information on plant layout, structure of the containment buildings, timeline, and response

efforts is readily available (Guizzo 2011, Miller 2011, Foundation 2012, Fukushima 2012, Wang, Gauld et al. 2012, WNA 2012, TEPCO 2013). Figures 22 through 25 pictorially describe the scenario beginning with an overhead view of St Lucie NPP in Figure 22. Figure 23 shows NPP SFP water replenishment by UAV, which may also represent a boron/sand delivery. Figure 24 shows the bucket refill at a fresh water source, which may also represent a boron/sand pickup site. Figure 25 shows the scenario management interface.

Figure 22 – Terrain Generation (Davis, Proctor et al. 2016)

Figure 23 – SFP Replenishment by water bucket drops (Davis, Proctor et al. 2016)

Figure 24 – Rotary UAV Refill at a Fresh water source (Davis, Proctor et al. 2016)

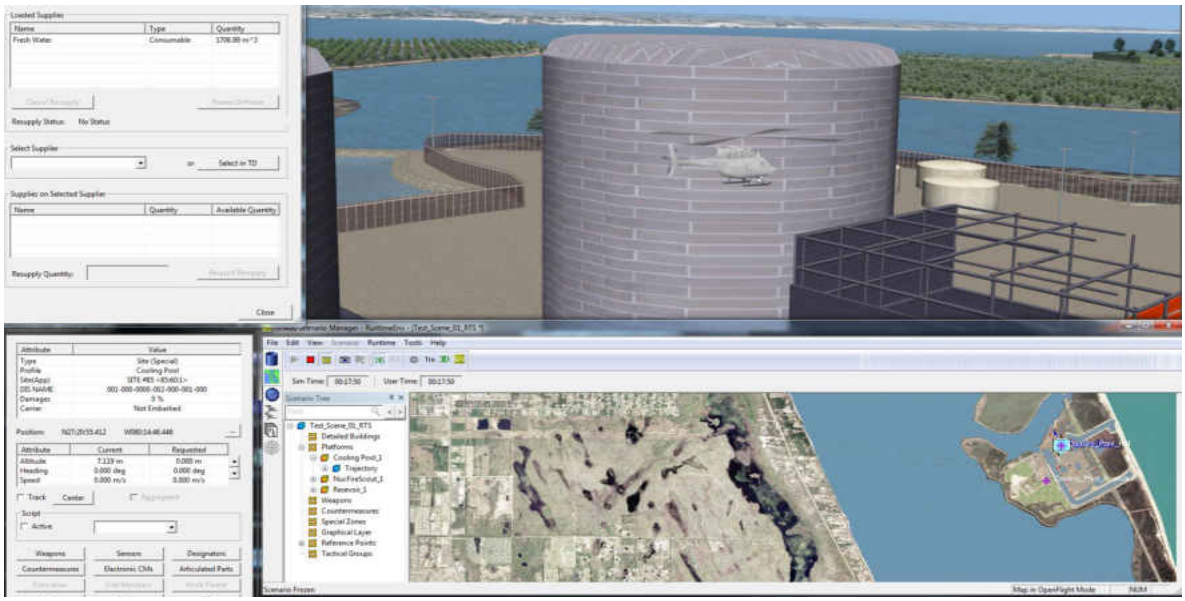

Figure 25 – View of Presagis' STAGE (Davis, Proctor et al. 2016)

Communication Protocols

Communication protocols establish interoperation within the LVC Simulation framework. The three protocols used within Presagis are:

- Distributed Interactive Simulation (DIS)
- Common Image Generator Interface (CIGI)
- nCom

Distributed Interactive Simulation (DIS) is an IEEE standard developed by the Simulation Interoperability Standards Group (SISO). DIS is widely used in real time, virtual world military simulations. DIS is a network protocol that uses Protocol Data Units (PDUs) to send information regarding position and orientation of entities in the world (OPEN-DIS 2016).

Common Image Generator Interface (CIGI) is an interface designed to promote a standard interface for a host device to communicate with an image generator (IG) in the simulation industry (Presagis 2016). In order to transmit entity and environmental data to the image generators of the UAV and Operations Stations, CIGI will be used.

nCOM is a communications layer that exists outside of standard protocols. nCom allows Presagis' tools to exchange data more effectively. This communications layer will display and log the "health" of the UAV and level of the SFP during runtime (Presagis 2016).

Modeling of Spent Fuel Pool Environment

Modeling the SFP is possible using various methods: liquid-heat transfer, fluid dynamics, or analysis of empirical data; all of which are mathematically intensive and difficult to integrate into a "live" simulation capable of training and mission rehearsal. Considering that the parameters of the research questions are concerned with water level in the SFP, a simpler model was chosen. (Davis and Proctor 2016) provide an option for modeling SFP levels, which accounts for evaporative loss as a mass transfer equation, founded on the principles in (Hugo and Kinsel 2014, Hugo 2015, Hugo and Omberg 2015). Implementing this model into the simulation allows for a simpler and more accurate representation of SFP dynamics (Hugo and Kinsel 2014). The Hugo model uses inputs available from standard weather data and predicted water temperatures within the SFP. The model from (Hugo and Kinsel 2014) is shown in Equation 1 (Hugo and Kinsel 2014):

$$\boldsymbol{E = 9.24\left(1 + 2v^{1.35}\right)^{0.67} \frac{T}{273K} \ln \frac{P - \phi P_{\text{sat, a}}}{P - \phi P_{\text{sat, w}}}} \quad \textbf{(1)}$$

Where,

$E =$ mass flux, kg/m^{2}sec

$v =$ air velocity, m/sec

$T =$ water temperature, K

$P =$ atmospheric pressure, Pa

$P_{\text{sat,a}} =$ saturation pressure of water at the ambient air temperature, Pa

$P_{\text{sat},w} =$ saturation pressure of water at the pool water temperature, Pa

$\phi =$ relative humidity, dimensionless

There are various methods of evaluation using a LVC simulation framework discussed in Appendix K. Table 5 provides a list of nine factors identified by (Davis and Proctor 2016)'s screening experiment.

Table 5 – Davis' Study Design

Factor Common Name	Mathematical Symbol	Component of Origin
Cruise Speed	V	UAV
Sling Load Capacity	C	UAV
Sortie Length	S	UAV
Number of Aircraft	A	UAV
SFP Wind Factor	v	Weather
Atmospheric Pressure	P	Weather
Relative Humidity	ϕ	Weather
Water Temperature	T	SFP Model
Air flow reduction ratio	r	SFP Model

(Davis and Proctor 2016)

(Davis, Proctor et al. September 2017) utilized a screening exam in order to build upon the works (Davis and Proctor 2016) and identified wind velocity as one of the statistically significant factors in UAV SFP water replenishment operations shown in Figure 26.

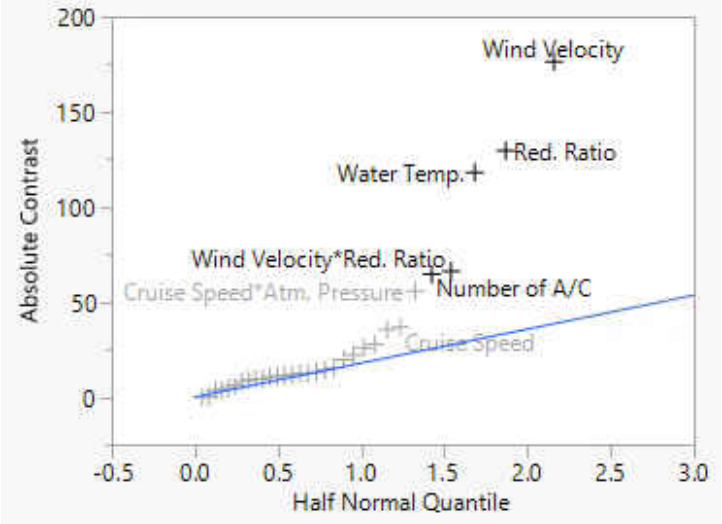

Figure 26 - Half Normal Quantile Plot of Effects

Using data in Figure 26 from (Davis, Proctor et al. September 2017)'s experiment, this study plotted wind velocity versus time to reach SFP critical water levels without UAV water replenishment interventions shown in Figure 27.

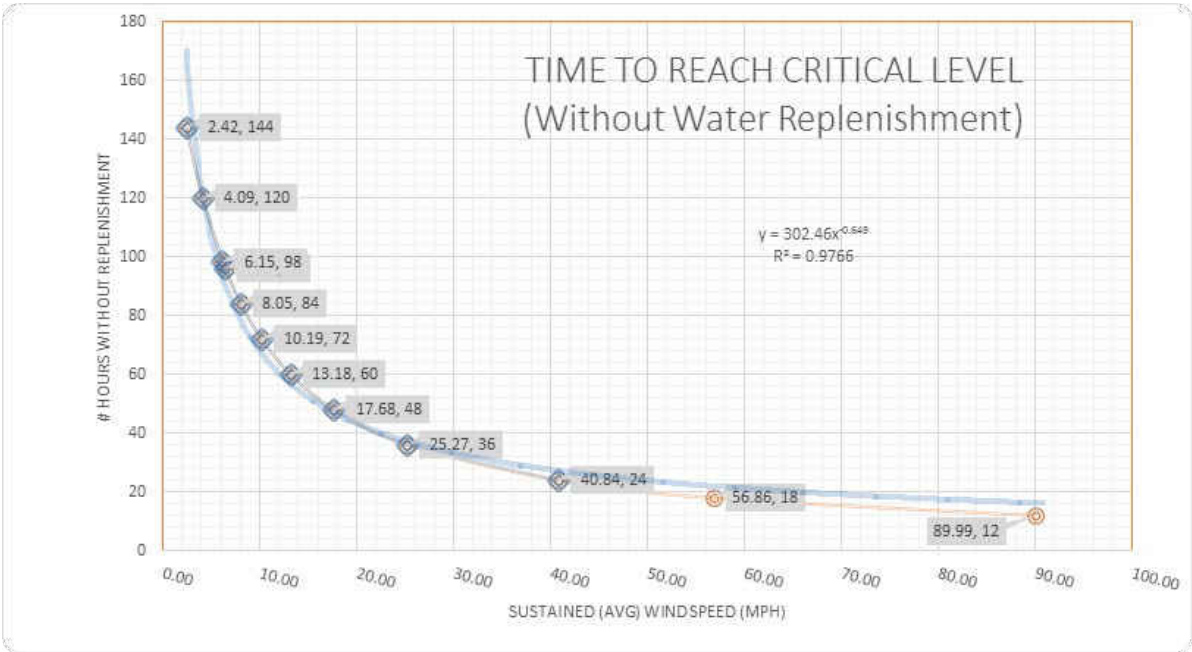

Figure 27 – Time to Reach SFP Critical Level Given Sustained Avg Wind Velocity

(Davis and Proctor 2016) extended the work of (Hugo and Kinsel 2014) by using the SFP evaporation model in a LVC simulation. (Davis, Proctor et al. September 2017) expanded upon the (Davis, Proctor et al. 2016) study by examining important variables by factor screening.

These extensions leave a gap in the research in that none of the extensions address the impact ionizing radiation has on UAV operations or identifies operational expectations for electronic tolerance to ionizing radiation. Further, lack of interoperability of RASCAL with the LVC simulation framework inhibits continuous representation of radiation in the framework. As shown in Figure 28, Presagis created a simulation architecture that models HPAC radiation in STAGE. This setup was completed for the Canadian military to develop scenarios for various operations in CBRN (chemical, biological, radiological, and nuclear) threat conditions. The HPAC dispersion model focuses on radiological and nuclear releases from chemical weapons (not NPP accidents); however, the success of the approach to export HPAC radiation data into the Presagis LVC simulation framework as dispersion zones provides validity and proof of concept of a similar effort to add RASCAL to the existing LVC framework.

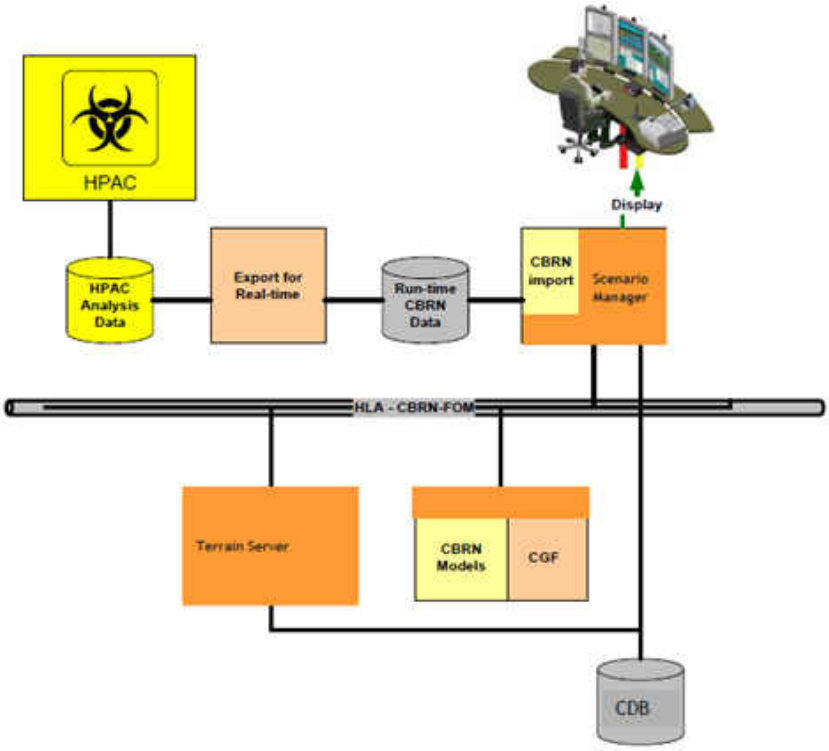

Figure 28 - Simulation Architecture of Presagis & HPAC (Presagis 2015)

Presagis recently introduced Ondulus IR, which gives the ability to add physics-based IR sensors to simulations (Presagis 2017). This sensor model dynamically computes radiation loading, cooling, conduction, convection & evaporation on objects. However, the approach is not suitable at this time for integration into a RASCAL_LVC framework. Therefore, dispersion of ionizing radiation clouds will require representation as radiation zones in STAGE.

CHAPTER FOUR: EXPERIMENTAL METHODOLOGY

Experimental Methodology

Reliability Assessment Methodology

Given the fore mentioned Presagis-HPAC architecture capability to model military CBRN scenarios, might RASCAL and the LVC simulation framework be leveraged to model, simulate and assess NPP disaster and response scenarios from an operational perspective? Can RASCAL NPP radiation models be incorporated into LVC simulation and if so, what advantages might it provide? Might an instantiated RASCAL-LVC framework improve estimation of operational expectations for Unmanned Aerial Systems' electronic system reliability when responding to a NPP disaster?

These research questions lead to additional research questions including: What technical hurdles exist to creating a RASCAL-LVC Simulation framework? What technical solutions exist to overcoming those hurdles? How generalizable is the experimental solution?

Building on the (Davis, Proctor et al. 2016) Systems-Of-Systems Conceptual Model and integrated LVC simulation framework, this research creates an enhanced RASCAL-LVC simulation framework by modeling and simulating NPP disaster radiation release based on the Nuclear Regulatory Commission's RASCAL simulation and meteorologically-based radioactive cloud dispersion in Stage. The resulting framework enables analysis of survivability envelopes of UAV electronics given different NPP disaster irradiated environments and response missions. Using factors identified in the (Davis 2017) screening experiment, three scenarios are

examined: (1) an In-And-Out Mission that simulates Parts Delivery, Surveillance, or passenger pickup/delivery; (2) a Fukushima-like Spent Fuel Pool water replenishment mission with radiation hot spot; and (3) an exploratory Chernobyl-magnitude Reactor Fire-extinguishing Mission with an open reactor radiation hot spot.

More generally, the enhanced RASCAL-LVC framework in capable of: (1) supporting human-in-the-loop training and mission rehearsal; (2) design and analysis of a broad spectrum of NPP disaster scenarios and mission responses; (3) analysis of various response vehicles within mission-scenario combinations; and (4) system engineering support to each system's life cycle.

Once a technical solution was achieved, case study questions investigated were: Given USAF electronic system hardening of 2300 Rads, how long does a flight of MQ-8C Fire Scout UAVs survive (1) a Fukushima-like In-And-Out Mission that simulates repeated parts delivery, surveillance, or passenger pickup/delivery? (2) a Fukushima-like Spent Fuel Pool water replenishment mission? (3) an exploratory Chernobyl-magnitude Reactor Fire-extinguishing Mission with radiation hot spot? Additionally, what are the survivability envelops for the specific systems tested? An experiment was designed to address these questions. At the conclusion of the experiment, what technical approach is recommended for future research?

To facilitate the above questions, this research outputs RASCAL radiation dispersion clouds that are integrated into a LVC simulation framework as STAGE radiation zones. This enables analysis of the operational suitability of various unmanned vehicles and their underlying electronics for NPP disaster response and mitigation in the presence of irradiated environments. A basic emergency response scenario package/part/personnel delivery/pickup

requires UAVs to fly an In-and-Out Mission through a cloud of radioactive materials that exists over a NPP releasing such materials atmospherically. A Fukushima-like SFP Cooling Mission exposes UAVs to cloud radiation but also hot spot radiation while hovering over a SFP within the NPP to deliver water. A Chernobyl-like Reactor Extinguishing Mission exposes UAVs to cloud radiation and hot spot radiation while hovering over a breached reactor core to deliver boron and sand.

Radiation intensity for these missions was determined based on publicly released information from the Fukushima NPP SFP cooling emergency and the Chernobyl accident. While these missions represent some of many possible unmanned systems operations, they provide valid cases as they were attempted at Fukushima and Chernobyl. Furthermore, aerial delivery was chosen as it is not likely to be impeded by nuclear disaster ground debris, loss of roads or bridges, or flooding such as seen at Fukushima or Chernobyl or probable in future chain of event disasters. In addition, water replenishment operations may be expected for Fukushima-like boiling water reactors as well as pressurized water reactors designed "to passively remove heat for 72 hours, after which its gravity drain water tank must be topped up for as long as cooling is required" (Morris 2015). Morris goes on to indicate "current operating fleet of PWR will need water much sooner than 72 hours."

The capability to determine ionizing radiation operational expectations for UAV electronics or any unmanned system during disaster response operations is critical to requirements for UAV survivability and hence operational success. Expectations for electronic tolerance are based on absorbed radiation observed during simulated operations. Though the approach

taken in this dissertation is applicable to all unmanned systems operations in a nuclear disaster, the specific research cases selected involve a flight of four rotary UAVs performing an In-and-Out Mission, a SFP Cooling Mission, and a Reactor Extinguishing Mission.

The use case includes specific mission objectives and parameters as described below.

Research Objectives

The particular focus of this research is electronic system survivability when responding to a NPP radiological emergency. **Sub-objectives are:**

1. Create a RASCAL-LVC simulation framework by incorporating radiation zones in STAGE based on the Nuclear Regulatory Commission's RASCAL simulation.
2. Demonstrate the utility of the RASCAL-LVC simulation framework in performing operational radiation risk assessment for identification of survivability expectations of unmanned systems, particularly UAVs.
3. Analyze the following tasks: In-and-Out Mission, a SFP Cooling Mission, and Reactor Extinguishing Mission

The Use Case

This research is based on simulating a NPP radiological emergency at St. Lucie NPP. The specific missions include an In-and-Out Mission, a SFP Cooling Mission, and a Reactor Extinguishing Mission. The missions simulate, respectively, the delivery of parts, the replenishment of water to an overheating SFP, or the dropping of boron/sand into an open and overheating nuclear reactor. All three missions may be performed by a UAV with the latter two missions being done using slung-load drops from a UAV operating in an irradiated environment.

The scope of the missions is to observe cumulative radiation doses absorbed by UAVs responding to the disaster.

Figure 29 is adapted from the conceptual model introduced in Figure 21. Figure 29 shows the specific models, tools, and techniques that will be used to execute the experimental design. Real-Time interoperability of RASCAL is currently unavailable as illustrated in the framework below by a break in the connection between RASCAL and the rest of the system (Shageer and Proctor 2020, IN REVIEW).

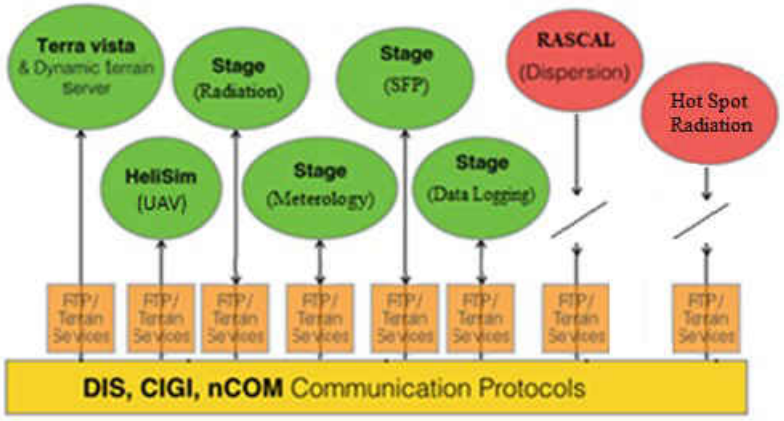

Figure 29 – Experimental implementation of the Distributed, LVC-RASCAL Simulation Framework for UAV Operational radiation risk assessment (Shageer and Proctor 2020, IN REVIEW)

The lack of RASCAL interoperability with the LVC simulation framework is another gap in capability. Electronic interoperability of RASCAL with LVC simulations or the integration of a dispersion model that is interoperable with LVC simulations would increase analysis productivity and effectiveness by removing the necessity for manual conversion of the dispersion model from RASCAL to the LVC simulation framework. Creating software to enable

electronic interoperability between RASCAL and the LVC simulation framework is beyond the scope of this dissertation.

The Presagis LVC software suite allows for the development of Fukushima scenarios; however, to determine the effect of radiation on unmanned systems over the course of extended operations, the integration of a radioactive dispersion model into a LVC simulation framework is crucial. The resulting RASCAL-LVC framework enables study of radiation absorption by unmanned systems during nuclear disaster scenarios. One benefit of the study is that this provides engineers expectations for recommended design tolerance to ionizing radiation of UAVs and their respective electronics while operating in irradiated environments. Additionally, emergency response planners may use electronic design tolerances in conjunction with the RASCAL-LVC framework to plan resources for operational missions. Using distributed, LVC simulation also provides life cycle insights discussed in Chapter 3 and enables analysis of non-parametric, dis-continuous, and non-monotonic observations not typically well addressed by tabletop math methods. Providing an assessment of operational radiation exposure of UAVs responding to a nuclear disaster will assist in providing future electronic ionizing radiation tolerance recommendations. Knowledge of expected exposure helps emergency managers prevent early-term failures as seen in unmanned ground robots responding to Fukushima. Since radiation dose is time-dependent, the simulation will: (1) monitor enduring contact of each UAV with radiation zones; (2) measure how long each UAV is in specific irradiated environments; (3) sum the radiation absorbed by each UAV, and (4) enable determination the cumulative dose has on operations degradation.

Since radiation is absorbed over time, the Fukushima and Chernobyl disasters provide a case study into the possible length of a real-world mission. In terms of the Fukushima observed timeline, the Nuclear and Industrial Safety Agency of Japan initiated an emergency at 16:00 March 11. After the failure of the manned helicopters to effectively cool SFP's over the course of five-days, the Tokyo Fire Department dispatched fire fighters with a 22-meter water tower early morning March 18. Given this span of time was approximately 126 hours; a reasonable operational scenario would replicate that length of time and determine UAVs ionizing radiation tolerance expectations while responding to a radiological emergency.

A failure of aerial SFP water replenishment occurs when water level drops to within three feet of the top of the fuel rods. This is the level used in NUREG-1738: "The end state … was an SFP water level 3 feet above the top of the fuel. This simplified end state was used because recovery below this level, given failure to recover before reaching this level, was judged to be unlikely given the significant radiation field in and around the SFP at lowered water levels" (Collins & Hubbard, 2001). Based on calculations shown in Figure 27 and assuming a constant 10 mph wind and no water replenishment, the SFP used in this research can be expected to reach critical water level after approximately 72 hours. Using recommended values from Davis et al's factor screening experiment (Davis, Proctor et al. September 2017), a sortie time of 180 minutes and Four-UAVs were chosen to ensure SFP wouldn't reach critical levels.

The Northrop Grumman MQ-8C Fire Scout unmanned helicopter is currently in use by the U.S. Navy for land and sea-based military operation (Northrop Grumman 2015). With

demonstrated capability, the Fire Scout might be effective for the proposed missions. Presagis' HeliSIM offers a model representative of the US Army OH-58 Kiowa Warrior, which is based on the same airframe as the Fire Scout (Deagel 2015). Similar flight profiles and performance makes these two aircrafts interchangeable. Slight modifications to the exterior design and sling load capacity to the Kiowa Warrior model makes the Warrior resemble the Fire Scout.

Because of the accident at Fukushima, data on plant layout, containment structure construction, timeline of the accident, and response efforts are readily available, the simulation uses containment building models from Fukushima Dai-ichi in place of the existing containment structures found at the St. Lucie NPP.

The Presagis Run Time Publisher (RTP) manages and publishes terrain data to subscribing models. The RTP is a backend process specifically designed to manage dataflow out of the Common Data Base (CDB) format either from a local source or a terrain server. CDB is the computer format in which the St Lucie NPP virtual world (synthetic natural environment) is instantiated within the computer system. The RTP formats the data in specific ways to optimize the data for the particular model making the request to use the data. The RTP operates similarly to a run time infrastructure (RTI) within an HLA federation except that the RTP focuses solely on terrain data. An instance of the RTP is needed on each computer running Presagis software in the experiment. Due to network limitations within the laboratory discovered during initial research efforts, the client / server structure that is one of the most appealing features of the CDB architecture will not be used. Rather, the CDB will be stored

locally on each of the participating computers. As such RTP / Terrain Services are shown in Figure 29 for each node of the larger simulation.

Representing NRC's RASCAL Nuclear Radiation Dispersion Model (NRC 2015) and UAV Absorbed Radiation

RASCAL's dispersion model outputs radiation intensity in the form of 2-Dimensional radiation zones as shapefiles and text files (horizontal plane). RASCAL determines the ionizing radiation dispersion footprint based on NPP location (latitude and longitude). RASCAL models single-reactor releases and outputs the dispersion footprint using a fixed latitude and longitude point based on reactor location. When modelling multiple reactors, a single center point ignores the distance between reactor buildings. The analysis performed in this dissertation research assumes the sufficiency of the center point dispersion model. This dissertation analysis defers to the expertise of the NRC as to the assumed lack of significance assigned to multiple radiation release points inferred by a fixed center point.

Transferring RASCAL output to the LVC simulation framework depends on the needs of the scenario being considered. RASCAL provides radiation intensity data as a list of reference points in a text file, each reference point has a respective latitude, longitude, and radiation intensity value associated with it as seen in Appendix N. RASCAL outputs values for a specific point in time (i.e. one hour after explosion), these "snapshots in time" are based on the various types of doses resulting from airborne releases (TEDE, thyroid, acute, etc) from three dose pathways - Inhalation, Cloudshine, and Groundshine. Given UAV operations are conducted in the air, Cloudshine Dose is appropriate for this research and will be implemented as zones in

STAGE (APPENDIX O). As explained further below, we implemented RASCAL generated "snapshots" for six-hour periods, because the RASCAL output is generated offline it's impossible to update radiation data in real-time. Six-hour blocks were chosen for computational efficiency and recommended by the NRC officials contacted prior to conducting this research. Since the entire recovery mission simulated is 126 hours, 21 Six-hour zones will be output from RASCAL and generated in STAGE.

Radiation absorbed by a UAV flying through a cloud of radiation is cumulative and measured in Rads absorbed over time. A worst-case scenario for radiation may be calculated as simply the maximum radiation release at a source per time period multiplied by the number of time periods being considered. This technique yields an unrealistically high estimate for radiation exposure. Over estimation of radiation exposure is potentially as bad as under estimation of radiation exposure as it may unnecessarily increase cost of electronic ionizing radiation tolerance measures.

To get a more accurate estimate for UAV radiation exposure, the method used by this research is to model incremental absorption based on UAV flight time through an irradiated environment (APPENDIX P). Cumulative absorbed radiation dose (ARD) is the primary experimental response variable used in this research to measure UAV absorbed dose during mitigation operations across the entire 126 period. ARD of any given Fire Scout during mitigation operations is based on encounter with, and time of exposure to (Texposure), the intensity of radiation (Rintensity) at each reference point within a given Snapshot is calculated in Equation 2. For Equation 2, time of exposure is in seconds. Reference point intensity is in

Rads/hour. There are 3600 seconds in an hour. The total radiation absorbed for a given Fire Scout over the course of a 126-hour mission is the summation of all the radiation absorbed each second at each reference point encountered in each Snapshot. This equation is based on the Total Cumulative Dose method used in the radiation exposure chart provided in Military Field Manual 3-3-1 Operational Exposure Guidance FM 3-3-1 Appendix A (Department of the Army 1994), which sums exposure over time. UAV radiation exposure is assumed limited to radiation contained in the radiation cloud that a UAV flies through.

$$ARD_{UAV_J} = \sum_{Snapshot=1}^{L} \sum_{RefPoint=1}^{K} \sum_{i=1}^{Texposure} \left(\frac{Rintensity_{RefPoint\ K,Snapshot\ L} \; x\, Texposure_{RefPoint\ K,Snapshot\ L}}{3600}\right) \quad \textbf{(2)}$$

Where
I= seconds
K= the number of reference points encountered in a given snapshot
L = the number of snapshots, which for this experiment is 21 over the course of a 126-hour mission
X = the number of a given UAV, which for this experiment is 1 through 4
ARD_{UAV_J} *= Radiation Damage to UAV$_x$*
$Rintensity_{RefPoint\ K,Snapshot\ L}$ *= Radiation Intensity of reference point K encountered in Snapshot L*
$Texposure_{RefPoint\ K,Snapshot\ L}$ *= Time of exposure of a UAV to radiation from Reference Point K within Snapshot L*

There are several limitations to the technique described above. UAV electronics failure is measured using TID, as this data was readily available. Electronic failure caused by neutron and proton displacement damage (Makowski 2006), enhanced low dose rate effects (Löchner 2011), and single event effects (Sawant 2012) was not considered, as failure rates for helicopter avionics were not available. UAV radiation exposure does not include prior radiation fallout that might contaminate the ground the UAV may fly over. When UAVs are outside of the radiation zones, the residual radiation on the surface of the airframe is assumed to not to continue to further irradiate the UAV. Neutron-induced radiation can cause various electronic failures and

cause objects to become chemically unstable, thus becoming a source of radiation; however, the effects of neutron-induced radiation are not included in this research. Future research could include failure rates caused by other forms of radiation damage, to increase accuracy and fidelity and determine whether neutron-induced radiation could cause UAVs to become a source of radiation after leaving irradiated environments. This simulation does model external decontamination of UAVs by washing prior to each sortie and refueling and maintenance cycle over the course of the operational mission. While removing radioactive dust on the surface of the UAV, these washings are assumed to not reduce absorbed radiation or reverse the damage that the electronics have undergone.

Integrating multiple reactor radiation releases

Since RASCAL only outputs single-reactor releases, if multiple reactors are dispersing simultaneously as seen in Table 6, combining the radiation intensity of reference points into one time period makes for efficient execution in a LVC simulation (Graniela and Proctor 2012).

Table 6 – Parameters determining Cloudshine Snapshots covering the 126-hour mission

	SNAPSHOT 1	**SNAPSHOT 2**	**…**	**SNAPSHOT 20**	**SNAPSHOT 21**
Time	MARCH 12 - 18:00	MARCH 13 - 00:00	…	MARCH 17 - 12:00	MARCH 17 - 18:00
Wind Direction	West	East	…	West	West
Operation Time	Night	Night	…	Day	Night
Time of Day	Evening	Midnight	…	Afternoon	Evening
Unit 1 Leak Rate (Release) %	25%	25%	…	0%	0%
Unit 2 Leak Rate (Release) %	0%	0%	…	1%	1%
Unit 3 Leak Rate (Release) %	0%	0%	…	1%	1%
Time since SCRAM	27.23	33.23	…	141.23	147.23

Units Releasing	1	1	…	2 & 3	2 & 3

For this experiment, in order to combine the intensity of radiation values to account for multiple reactors releasing radiation at the same time, an algorithm was needed in STAGE. The Radiation Intensity Addition Algorithm in Equation 3 is an add-on scripted plugin that accomplishes the integration of additional reactor releases given a single reactor's set of radiation reference points. When adding additional radiation intensity to another reactor's reference points, the following pre-conditions must be met:

For a two-reactor release scenario, if there is a pre-existing reference point that's within 24.3 meters (80 feet) or less of an additional reactor's reference point, the radiation intensity value of both reference points will be combined. If no pre-existing reference point is within range, the 2 closest points within 24.3 meters - 67 meters (220 feet) will share the value of the additional reactor's reference point based on the Radiation Intensity Addition Algorithm in Equation 3. If there is no pre-existing reference point within 67 meters, a new reference point will be created with its respective radiation intensity value.

$$Ref_{A_{Intensity,Snapshot}} + Ref_{New_{Intensity,Snapshot}} = Ref_{A_{Intensity,Snapshot}} + Ref_{New_{Intensity,Snapshot}} * \frac{Dist_{Total_{A+B}} - Dist_{A_{RefA,RefNew}}}{Dist_{Total_{A+B}}}$$

$$Ref_{B_{Intensity,Snapshot}} + Ref_{New_{Intensity,Snapshot}} = Ref_{B_{Intensity,Snapshot}} + Ref_{New_{Intensity,Snapshot}} * \frac{Dist_{Total_{A+B}} - Dist_{B_{RefB,RefNew}}}{Dist_{Total_{A+B}}} \quad (3)$$

Variables

$Ref_{A_{Intensity,Snapshot}}$ = Unit 1 Radiation release at Existing Point A

$Ref_{B_{Intensity,Snapshot}}$ = Unit 1 Radiation release at Existing Point B

$Ref_{New_{Intensity,Snapshot}}$ = Unit 2 additional Radiation release from New Point

$Dist_{A_{RefA,RefNew}}$ = Distance to Point A from New Point

$Dist_{B_{RefB,RefNew}}$ = Distance to Point B from New Point

$Dist_{Total_{A+B}}$ = Total Distance (Distance to point A + Distance to point B) from New Point

Experimental Design Factors

As seen in Figure 30, absorbed radiation dose, ARD, per equation 2 is the primary experimental response variable building on the experiment by (Davis 2017) that used SFP water level as the response variable. The Davis' experiment identified significant factors useful for this study. (Davis 2017) identify wind speed, sortie length, and number of Fire Scouts as significant factors stating, "Common to the runs 2, 8, 21, and 29 safety failures was high wind speeds and only one Fire Scout RUAV. Runs 13 and 32 safety failures had high wind speeds and four Fire Scout RUAV as well as a 360-minute sortie length – inferring high maintenance down time - and high-water temperature in common."

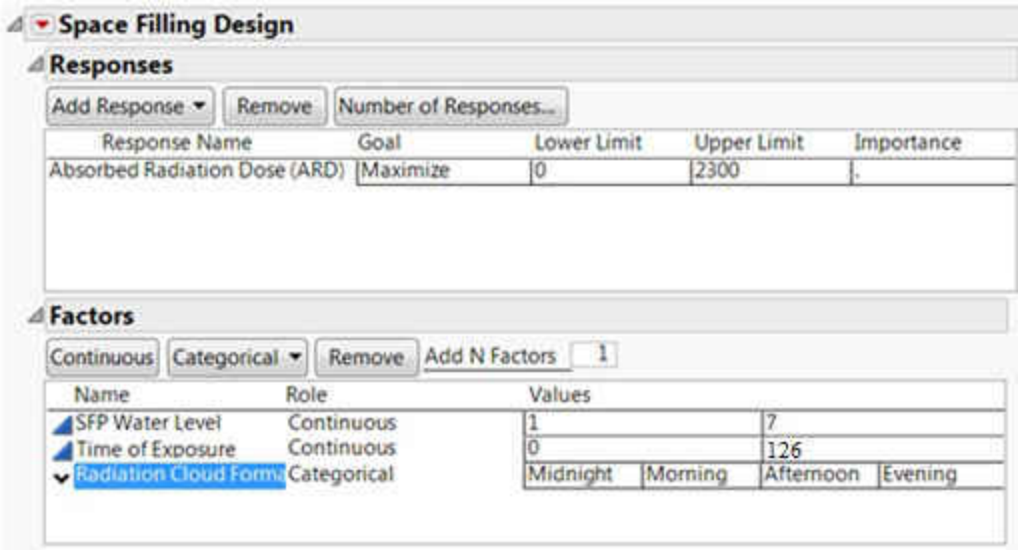

Figure 30 - Space Filling Design Responses and Factors

The objective of this research is not to optimize the number of Fire Scouts or sortie length necessary to avoid SFP critical water safety levels. Davis (2017) established a flight of four Fire Scouts provides high assurance of no SPF failure. That leaves identifying expectations for electronic radiation tolerance for this research. Factors significant to absorbed radiation dose (ARD) are meteorological and other factors associated with creation of radiation clouds and UAV contact with the radiation clouds. The other non-significant factors of the experiment use fixed values from (Davis 2017) study with a complete list of factors identified in Appendix A.

Wind velocity, radiation intensity, and wind direction determine the radiation cloud form and lethality. Radiation clouds vary during a given "snapshot". Since the Fukushima disaster is being recreated as if it occurred at the NPP at St Lucie, the Windrose in Figure 31 displays the likelihood and intensity of historical winds in the St Lucie area. The Windrose in Figure 31 is based on probabilities in the chart in Appendix I. Coastal winds typically follow a

pattern. The coastal winds pattern involves winds blowing primarily from the ocean from midnight until the afternoon and blowing primarily the opposite direction from noon till midnight. The direction and intensity of the winds used in the simulation will be based on the historical pattern for St. Lucie during the Spring (Wunderground 2017) provided in Graph 1. Detailed historical data is in Appendix J. The average wind velocity in Spring is equivalent to 9mph as seen in Figure 32.

Given a case study approach, the RASCAL cloud radiation input data are based on reactor data during the Fukushima disaster timeline that occurred between the time periods of March 11 to March 17. RASCAL converts the reactor release data into dispersion cloud outputs that match the combined output of ionizing radiation leaks at Fukushima. To balance accuracy with computation limitations given 126 hours in the mission, 21 "snapshot" RASCAL clouds (every six hours associated with the St Lucie wind direction and velocity pattern) will be updated in STAGE as radiation zones that the UAV must fly through. The resulting 21 STAGE radiation zones reflect RASCAL radiation cloud dispersion based on wind speed and direction patterns that corresponds to Spring historical averages.

For illustration purposes, Figures 34-37 represent the RASCAL output clouds based on an average day in the simulation (shown in 6-hour blocks) generated from wind speed, direction and intensity of radiation. Figure 38 shows the methodology used to transfer RASCAL output clouds to Stage. The approach adapts the methodology used by Presagis to transfer radiation data from HPAC to Stage previously discussed in Figure 28. Although wind velocity and direction will be updated in STAGE and RASCAL every six hours during the simulation, the wind

velocity factor used to calculate SFP evaporation rate from (Davis 2017) earlier experiments will remain constant as the average wind, without respect to direction, since it currently can only be altered prior to runtime. Emergency planners may use the approach described above and site-specific historical data – averages, worse case, or specific cases such winds during a hurricane - to determine wind speed and direction with resulting radiation dispersion models for their missions.

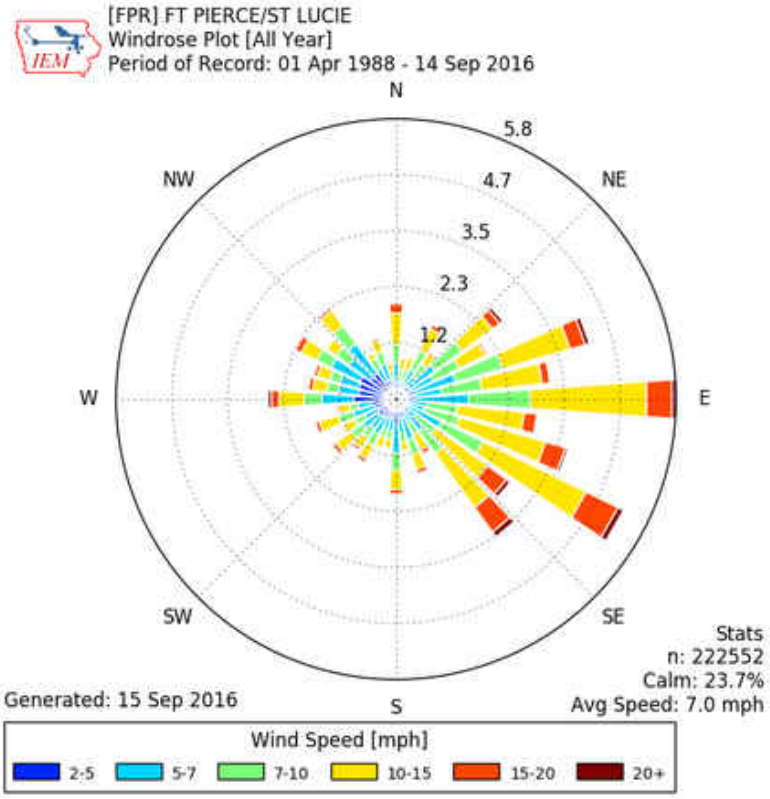

Figure 31 – Windrose (IEM 2017)

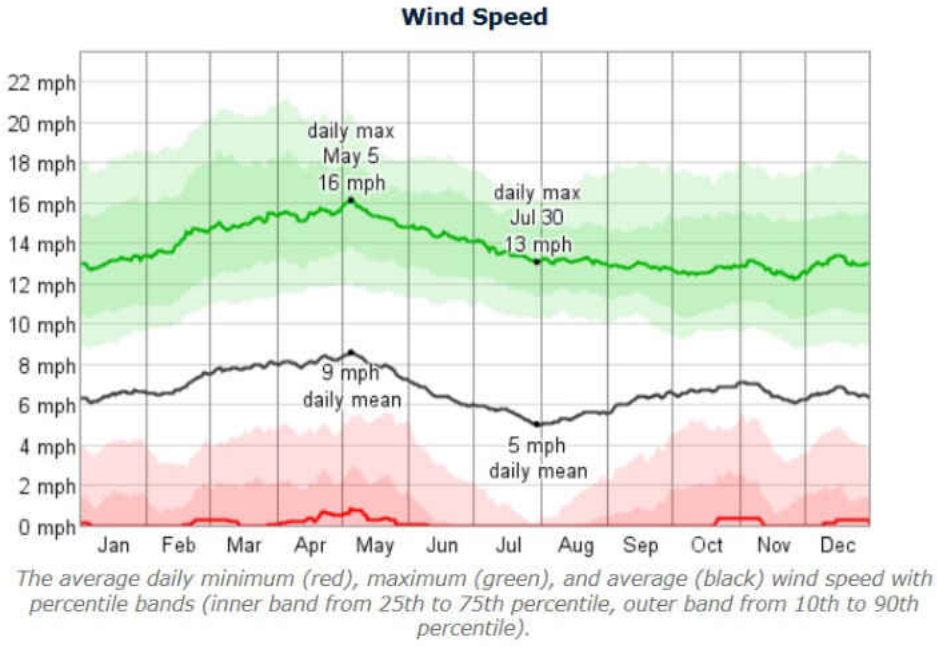

Figure 32 – Average Wind Velocity throughout the Year (WeatherSpark 2017)

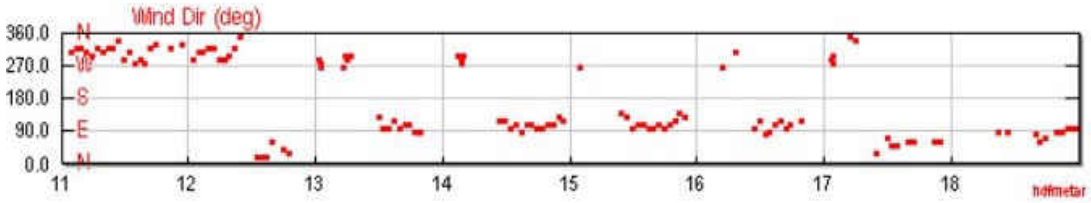

Figure 33 - Week of March 11 – 18, 2011 Daily Wind Trends (Wunderground 2017)

Snapshot 1

Wind Direction: 90 degrees

Time of Day: Evening (6 PM to 12 AM)

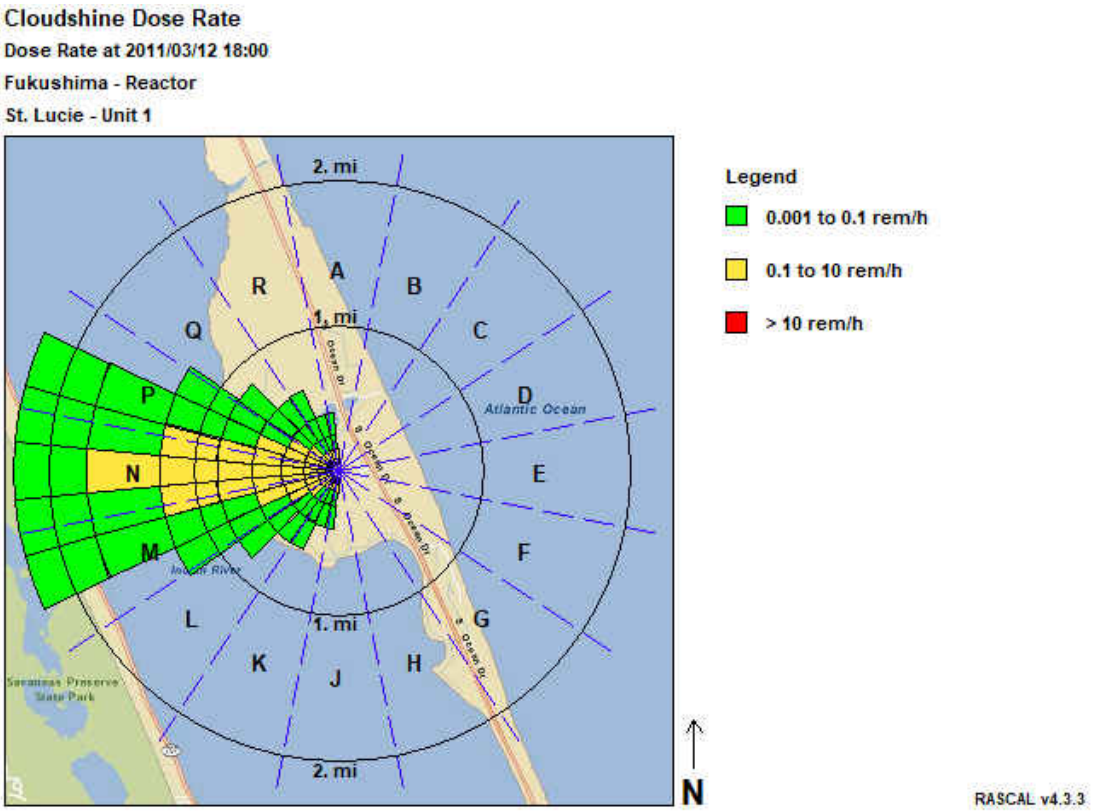

Figure 34 - RASCAL 90 Degree Evening Projection Zone (NRC 2015)

Snapshot 2

Wind Direction: 270 degrees

Time of Day: Midnight (12 AM to 6 AM)

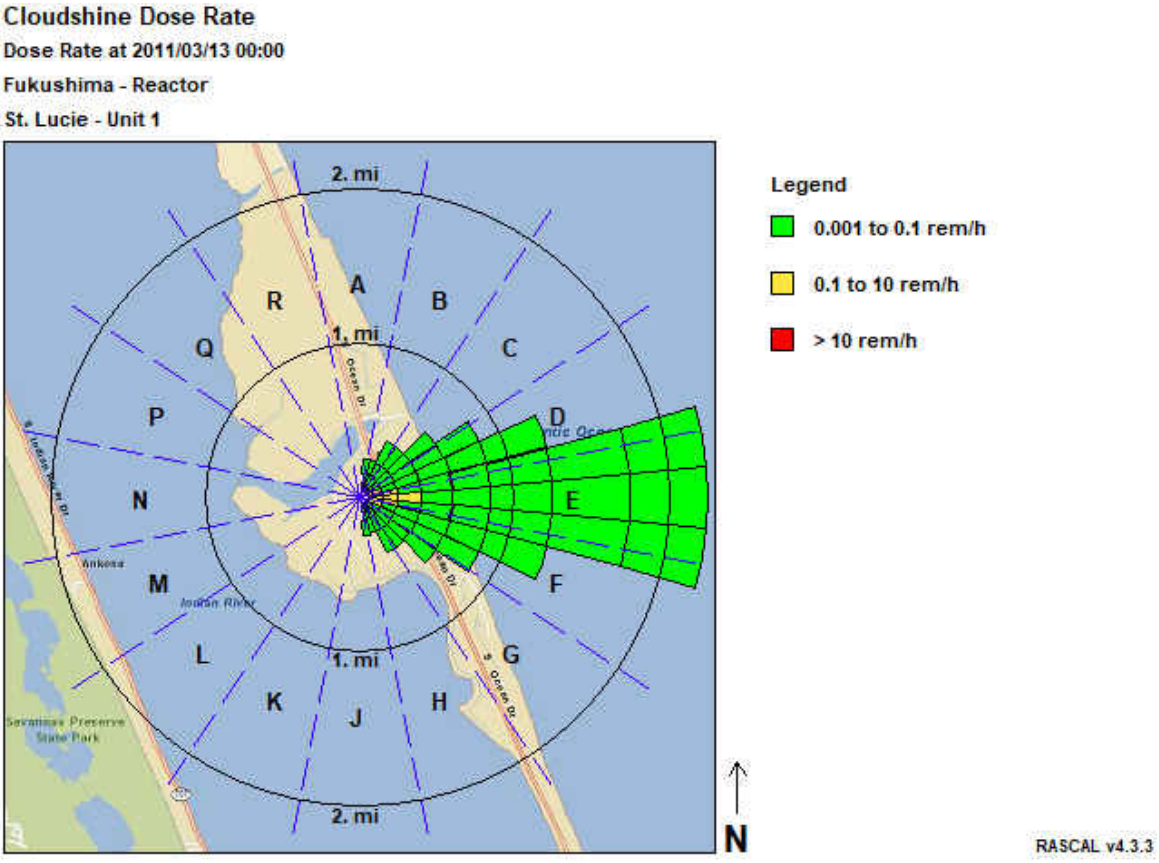

Figure 35 – RASCAL 270 Degree Midnight Projection Zone (NRC 2015)

Snapshot 3

Wind Direction: 270 degrees

Time of Day: Morning (6 AM to 12 PM)

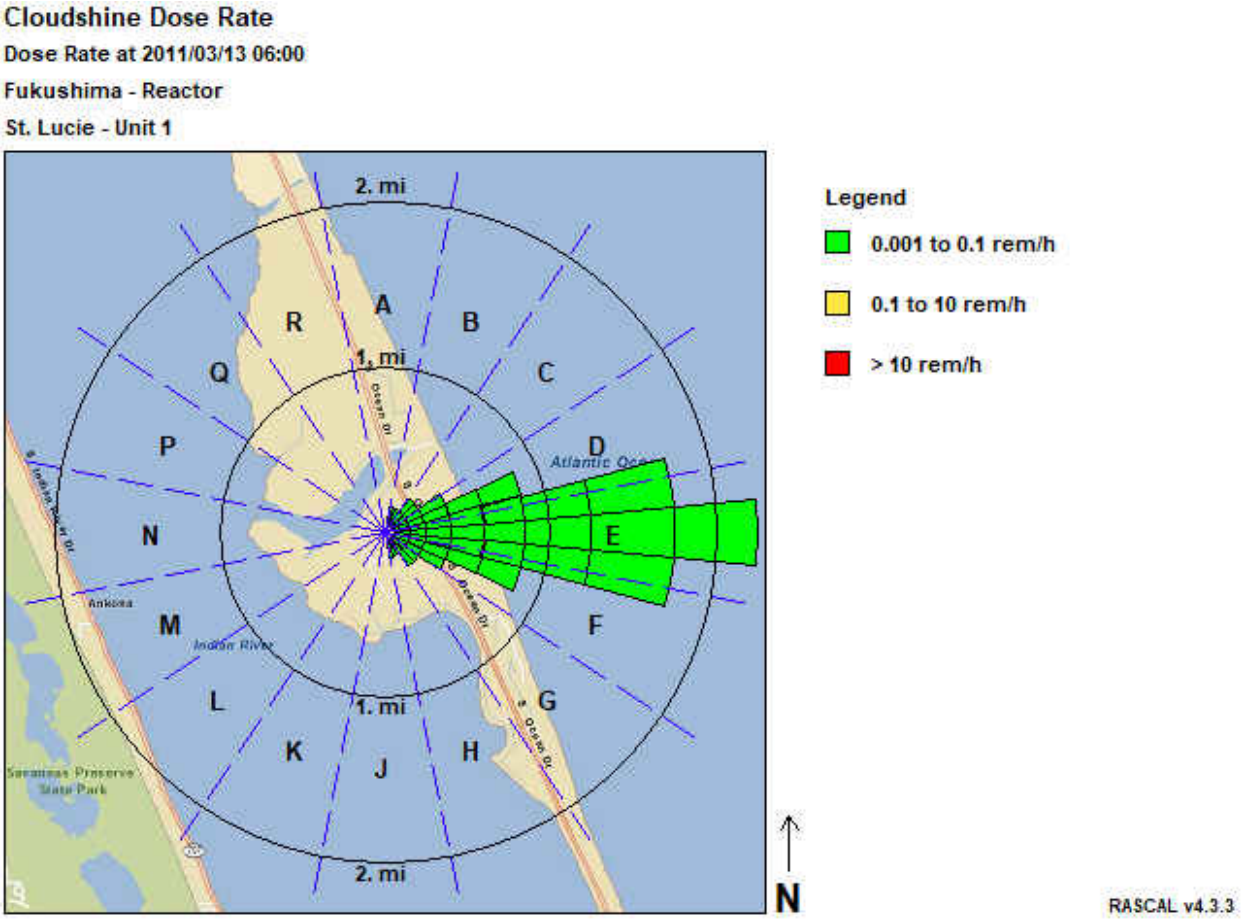

Figure 36 – RASCAL 270 Degree Morning Projection Zone (NRC 2015)

Snapshot 4

Wind Direction: 90 degrees

Time of Day: Afternoon (12 PM to 6 PM)

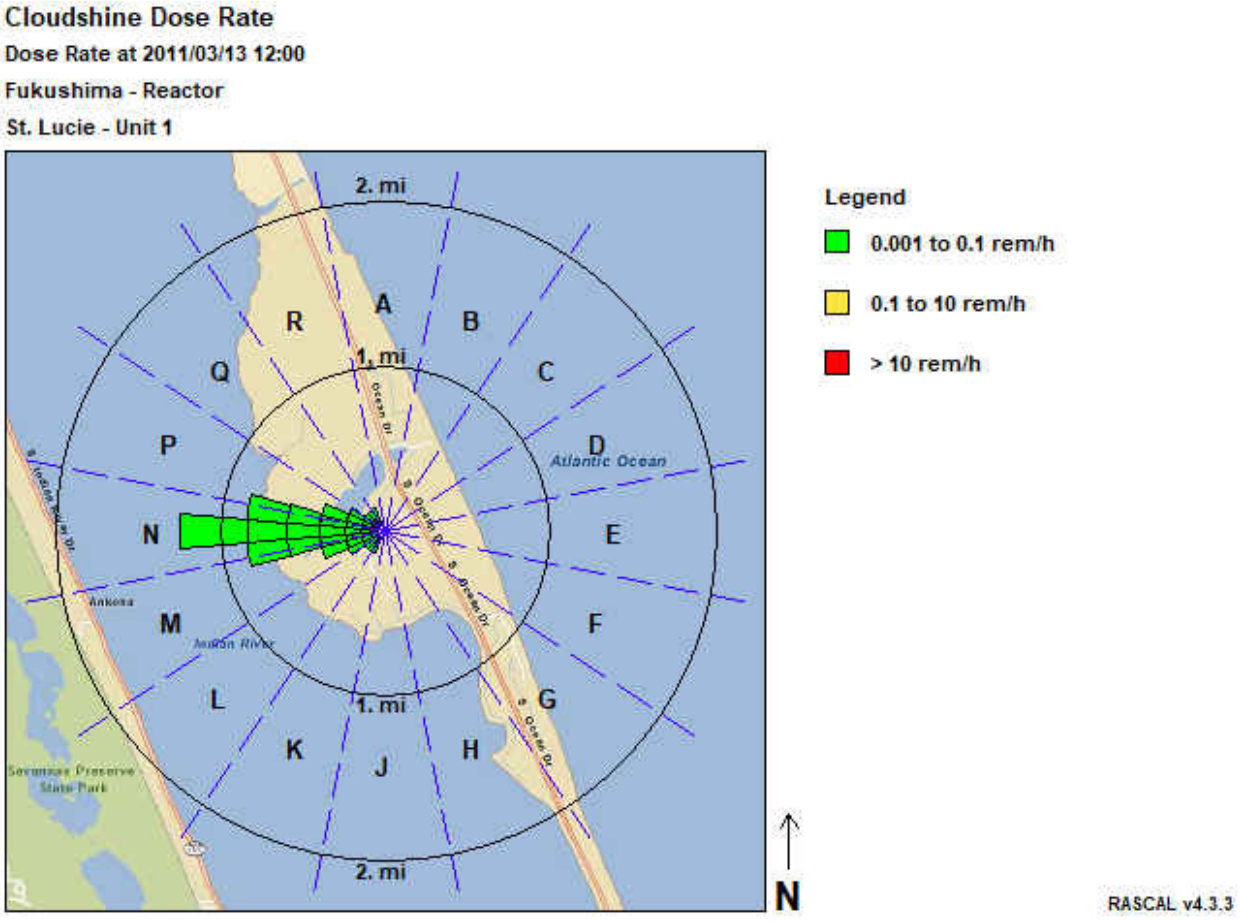

Figure 37 – RASCAL 90 Degree Afternoon Projection Zone (NRC 2015)

***RASCAL Output Rate: Rems/hr (1 rad inflicts 1 rem of Damage)**

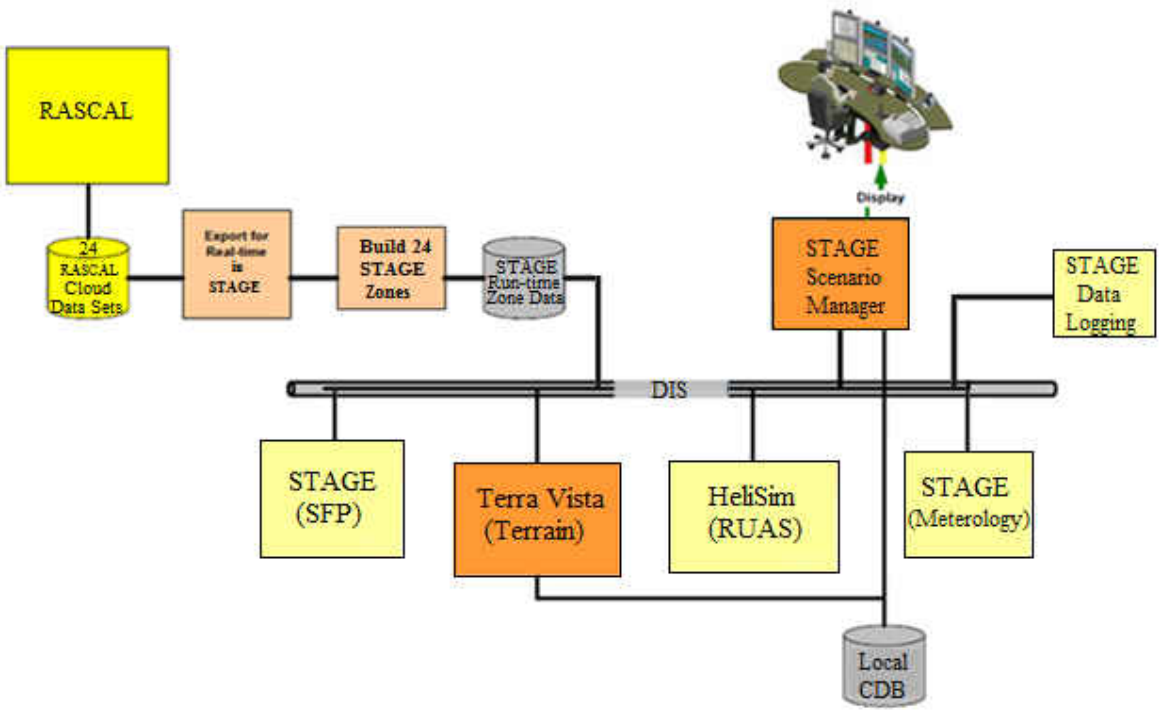

Figure 38 –RASCAL to STAGE Process Flow Diagram

Novel Experimental Design Approach

Experimental runs must assess UAV absorbed radiation dose (ARD) in an operational setting. The (Davis 2017) screening experiment indicated that the values chosen for the critical factors above will insure the SFP water level remains above the critical level throughout the time frame. That allows focus on ARD. Table 7 outlines the high, low and fixed values associated with certain factors in the design. The radiation cloud formation factor is likely critical to ARD since the UAV must fly through the radiation cloud formation in order to deliver parts, replenish SFP water, or drop sand/boron. A novel approach to representing the cloud

formations is to use, as indicated in Figures 34-37, the four periods of time during a given 24-hour day. For a 126-hour experiment, RASCAL outputs 21 unique but representative Midnight, Morning, Afternoon, and Evening cloud formations. Each cloud formation encompasses wind velocity, wind direction, and radiation intensity typically associated with those times of day. From an experimental perspective, the cloud formations are categorical data with four sub-categories.

Table 7 - Design Factors Values

Factor	Low Value	High Value	Fixed Values	Type
Cruise Speed (V)			25 m/s	Continuous
Sling Load Capacity (C)			450kg	Fixed
Sortie Length (S)			180 Min	Fixed
Number of UAVs (A)			4	Fixed
SFP Wind Factor (v)			9mph	Fixed
Atm. Pressure (P)			103000 Pa	Fixed
Relative Humidity (ϕ)			55%	Fixed
Water Temp. (T)			90	Fixed
Reduction Ratio (r)			0.3	Fixed
SFP Water Level (WL)	1m	7m		Continuous
Radiation Intensity per Cloud Zone (*Rint*)	0 Rem/hr	Determined by RASCAL		Continuous
Radiation Cloud Formation - Wind Velocity	N/A	Set in RASCAL transferred to Stage		Categorical
Radiation Cloud Formation - Wind Direction Degrees	N/A	Set in RASCAL transferred to Stage		Categorical
Radiation Cloud Formation - Radiation Intensity	0 Rem/hr	Determined by RASCAL transferred to Stage		Categorical
Time of Exposure per Cloud Zone (*Texp*)	0 Seconds	Determined in STAGE		Continuous

There are many tools available in the software community for developing Design of Experiments. JMP® is a recommended tool. JMP recommends a Space-Filling design for computer simulations. After inputting the response variables and factors, JMP recommends a 32 run Fast Flexible Filling design method. (Scott 2011) recommends an alpha of 10% in the early phase of experimentation, a power level of 80%, and a beta of 20% for all factors; the minimum acceptable R^2 values for the model are greater than .8, the greater the R^2 value, the more variability explained by the model.

The Fast-Flexible Filling Design table is included in Appendix C and the generated run Table is in Appendix D.

The factors listed in Appendix A are controlled in order to better understand the effect of the factors of interest. The factors in Appendix A are listed because of their relevance in the simulation. The design of the UAV and its respective values are held constant and were chosen based on real-world expectations. The radiation tolerance threshold levels are determined based on actual tolerance levels of aircrafts currently employed by the military and will be similar in design to those that would be deployed in the actual event. The assumptions from (Davis 2017)'s study are provided in APPENDIX M.

Data Collection

There will be 32 experimental runs. Each run lasts 126 hours of simulation time, divided into 21 six-hour-snapshots. Radiation damage from each "snapshot" will be collected and summed offline. In addition to damage from the RASCAL zones, time spent hovering above the

reactor will determine the radiation damage for the SFP-cooling mission, and fire-extinguishing mission. All the replications of experimental runs will then be averaged.

Summary of Key Assumptions & Scope Limitations

There are various key assumptions and scope limitations of this study. RASCAL zones are generated OFFLINE and imported separately as text files. Assumptions include: (1) The In-and-Out Mission, Fire-Extinguishing Mission, and SFP water replenishment mission are representative of heavy-lift UAV operations, given a NPP radiological emergency. (2) Input parameters in RASCAL represent Fukushima-like conditions allowing for a relevant and recent case study. (3) The dispersion zones neglect rainfall and any effects rain has on radiation intensity. (4) The dispersion models from RASCAL do NOT account for Electronic failure caused by neutron and proton displacement damage (Makowski 2006), enhanced low dose rate effects (Löchner 2011), and single event effects (Sawant 2012), as failure rates for helicopter avionics were not available. (5) Factor significance identified by (Davis 2017) are accurate. (6) SFP safety thresholds relate to the depth of the water above the top of the fuel rods housed in the SFP. (6) If the SFP can be maintained in a normal operating state with regard to water level and temperature over the 126-hour period, it is assumed cooling systems are restored or ground-based water delivery is established, making aerial delivery no longer necessary. (7) Northrop Grumman MQ-8C Fire Scout unmanned helicopter is assumed an acceptable UAV for water replenishment operations. (8) Six-hour snapshots of NRC RASCAL Cloudshine Dose output for given wind velocities and directions are assumed sufficient for this research.

There are various initial conditions to specify to allow for complete understanding of the results. The UAV will begin each run on the ground waiting to begin its first sortie. The SFP water level will be set at six meters above the top of the fuel assemblies (normal operating conditions is seven meters above the assemblies). The one-meter difference accounts for loss since the initial accident and evaporative loss until UAV response is initiated. Radiation damage and time spent hovering above the reactor will be recorded to provide a detailed post-trial analysis. ARD is a measure of the cumulative dose over time, accountable by monitoring time spent in zones and hovering, along with radiation intensity.

CHAPTER FIVE: DATA COLLECTION AND ANALYSIS

Given a coastal NPP radiological emergency, the experiment uses the RASCAL-LVC framework to examine exposure and survivability to radiation of electronics of a flight of four responding Fire Scout UAVs. Three scenarios were investigated. The In-and-Out Mission involved sorties that take the UAV flight repetitively in and out of radioactive clouds above the NPP. Analytically building on In-and-Out Mission results, electronic exposure and survivability is estimated below for the UAV flight conducting a Fukushima-like SFP Cooling Mission and Chernobyl-like Reactor Extinguishing Mission while hovering over hot spots. Complete data sets of all replications are available upon request. Radiation damage values provided are in Rads.

Cloudshine Radiation Absorbed over 126-hour In-and-Out Mission

The In-and-Out Mission considers only Cloudshine radiation absorbed by the Fire Scouts. 32 simulated In-and-Out Missions of 126-hour duration each involve a flight of four Fire Scouts totaling 128 Fire Scout missions simulated. Fire Scouts fly through RASCAL generated Cloudshine radiation Snapshots to the coastal NPP, do a short hover to simulate a delivery/pickup, and then fly out of the irradiated environment. Over the course of the 126-hour In-and-Out Mission, the average Fire Scout conducted 21 sorties, based on a 180-minute sortie time between maintenance and decontamination, and absorbed 3.62 Rads as seen in Appendix Q. The range of total radiation absorbed by Fires Scouts was from 2.23 Rads to 4.39

Rads, all far below 2300 Rads TID USAF standard for military electronics. Essentially Cloudshine radiation damage to Fire Scout electronics by itself is NOT significant as seen in Figure 39.

EXPERIMENT	UAV	TOTAL RADIATION
EXPERIMENTAL RUN 1	UAV - 1	3.432786
	UAV - 2	3.874358
	UAV - 3	4.390401
	UAV - 4	3.712625
EXPERIMENTAL RUN 2	UAV - 1	3.78349
	UAV - 2	3.234139
	UAV - 3	3.436424
	UAV - 4	3.560286
.....	.....	.....
EXPERIMENTAL RUN 31	UAV - 1	3.513701
	UAV - 2	3.403518
	UAV - 3	2.842145
	UAV - 4	2.811939
EXPERIMENTAL RUN 32	UAV - 1	3.266351
	UAV - 2	3.120064
	UAV - 3	3.467665
	UAV - 4	3.295453
	Average Total Radiation Dose per UAV	**3.621262508**

Figure 39 - Experimental Run Absorbed Radiation

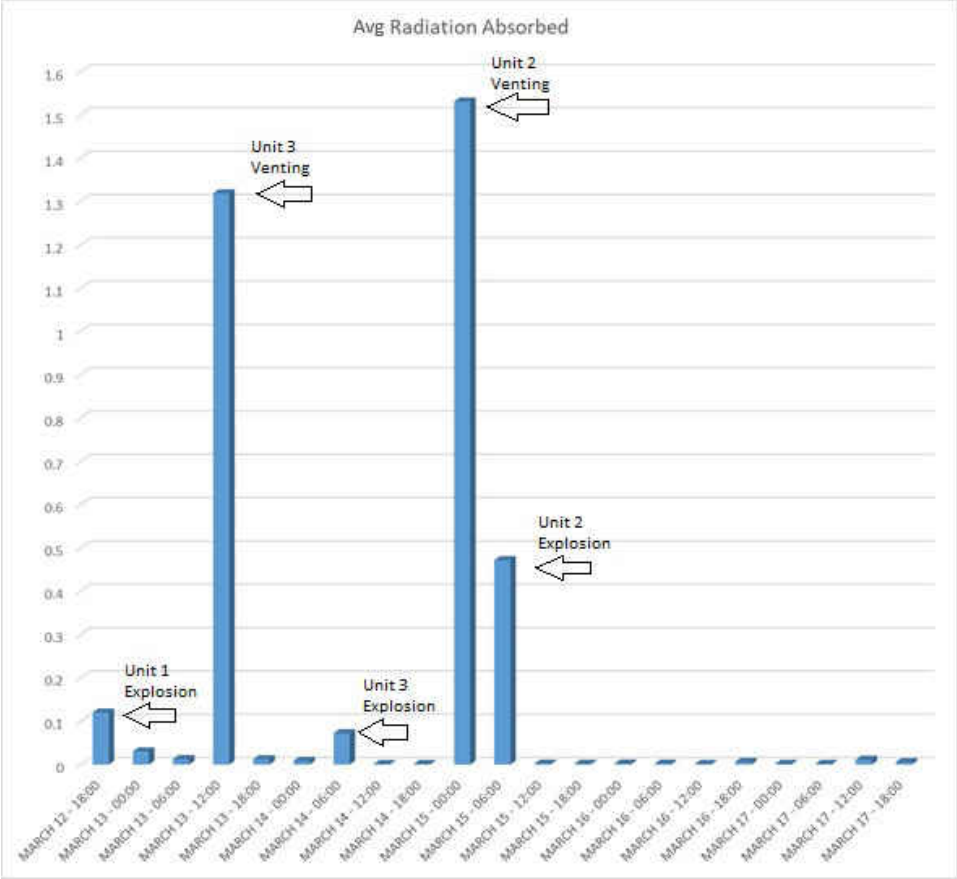

Figure 40 - Avg Radiation Absorbed during each snapshot

The average UAV radiation absorbed during the simulation shown in Figure 37 is consistent with reactor explosions and venting as shown in the Fukushima Timeline in Table 8. As summarized in Table 8, UAVs depart from the Staging area on March 12 18:00, 2.5 hours after the first explosion. The radiation being absorbed in each snapshot is reduced over time since the radiation intensity decreases as material is being released. It's not until March 13 12:00, when Unit 2 begins venting where we see another noticeable increase in UAV damage. While (Rocchi, Guglielmellli et al. 2014) shows that venting at Unit 3 occurs in three parts (lack of working sensors made it impossible to determine whether the vent closed or re-opened), in

the experiment venting was chosen for the entire 12pm-6pm snapshot. A 6 hour window was chosen because the data shows venting occurs between 2 – 10 hours. The experiment used the average of this range.

Table 8 - Simulated Fukushima Timeline

Timeline for theoretical coastal NPP emergency and simulation (IAEA 2013, Rocchi, Guglielmellli et al. 2014)	
March 11, 2011	Theoretical coastal NPP hit with Category 5 hurricane with maximum storm surge, flooding, and wind speeds. Offsite primary and onsite backup power disabled. Access bridges and roads knocked out. NPP facilities flooded and reactor and SFP cooling systems disabled.
March 12, 2011 **6:00 P.M.**	Unit 1 explodes at 3:30 pm Weather clears, enabling helicopter UAV response 2.5 hours later. LVC Simulation begins. ➔ Four STAGE Simulated UAVs leave staging area and head north to freshwater refill site ➔ RASCAL simulated Unit 1 radiation leak rate is set at 25% (drywell vent opened but never closed)
March 13, 2011	RASCAL simulated venting occurs at Unit 3 From: ➔ 9:20 am – 11:17 am ➔ 12:30 pm – 3:00 pm ➔ 8:10 pm – 1:00 am (3/14) Leak Rate is set to 25% during venting and 1 % between and after venting
March 14, 2011	Spent Fuel storage* pond at Unit 4 reactor is on fire at 8:54 am ➔ Radioactivity is being released* Explosion at Unit 3 Reactor at 11:00 am, ➔ Containment Building damaged, roof blown off ➔ RASCAL simulated Unit 3 leak rate is set to 50% for 1 hour
March 15, 2011	Explosion at Unit 4 reactor (6:00 am) and Explosion at Unit 2 Reactor (6:14 am) ➔ Unit 2 explodes during venting, RASCAL simulated leak rate set to 25% at 2:00 am and changed to 50% at 6:14 am

	➔ Unit 4 SFP fire at 12:50 pm ➔ RASCAL Simulated venting at Unit 2 stopped at 12:00 pm
March 16, 2011	Fire at Spent Fuel Pool in Unit 4 starts again ➔ Unit 4 SFP fire* begins again 24 hours later at 5:45 am
March 17, 2011 **Midnight**	Ground emergency response fully functioning. STAGE simulated UAV recovery operations cease. Simulation ends.
Continuous Operations Include	UAVs fly back and forth from water refill site to NPP containment facility ➔ Water buckets are loaded at refill site and dumped into SFP UAVs return as needed to the staging Area for 3 out of every 6 hours to perform: Refuel, Decontamination, and Maintenance

Hot Spot Radiation while Hovering during Fukushima-like SFP Cooling Mission

The Fukushima-like SFP Cooling Mission includes a radiation hot spot near the SFP. For reference, a hot spot value of 180 Rads/hr was recorded within the actual Fukushima NPP near the SFP. Clearly radiation emanating from that hot spot might have been absorbed by a Fire Scout while hovering over the SFP to drop water into the overheating SFP (Diblasio 2013). The simulation revealed that on average over the course of a 126-hour mission, a Fire Scout accomplishes 189 water drops totaling approximately 31.5 minutes above the radiation hot spot resulting in about 94.7 Rads of absorbed radiation shown in Figure 41. Given a 2300 Rads TID USAF standard electronics, a Fire Scout would survive their 126 mission.

Hot Spot Radiation of Hovering in Chernobyl-like Reactor Extinguishing Mission

The Chernobyl-like Reactor Extinguishing Mission also considers hot spot radiation that might have been absorbed while hovering over an open reactor to drop sand and boron into, respectively, extinguish the reactor fires and retard the nuclear reactions (Diblasio 2013, Sanchez 2016). In Chernobyl, hot spot radiation values were recorded as high as 17,540 Rads/hour (Sanchez 2016). Parenthetically a dose of 1000 Rads causes internal bleeding and death to a human within weeks (MensHealth 2011). Using the same 31.5-minute total hover time, a Chernobyl-like Extinguishing Mission inflicts radiation damage of around 9230 Rads shown in Figure 41. 2300 Rads TID USAF standard electronics of a Fire Scout would NOT survive a 126-hour mission and in fact survive less than 7.8 minutes of hover time. This is consistent with what was observed at Chenobyl where robot malfunctions were widespread.

UAV	Average Time Spent above Reactor (Minutes)	Radiation above Fukushima (180 Rads/hr)	Radiation Above Chernobyl (17,540 Rads/hr)
UAV 1	31.9375	**95.8125**	**9336.395833**
UAV 2	31.66145833	**94.984375**	**9255.699653**
UAV 3	31.328125	**93.984375**	**9158.255208**
UAV 4	31.39583333	**94.1875**	**9178.048611**
AVERAGE	31.58072917	**94.7421875**	**9232.099826**

Figure 41 - Hot Spot Radiation Results

CHAPTER SIX: CONCLUSIONS & FUTURE RESEARCH

After Fukushima, the countries in the world reconsidered the use of nuclear power. Germany ended its use of nuclear energy for commercial generation of electricity (Brendebach 2016). An Italian referendum voted 94% against the construction of new nuclear reactors in Italy (Engineering 2011). China suspended approvals of nuclear plants to revise safety standards (Staff 2011).

In contrast, the outcome of Fukushima, as devastating as it was, has not stopped the global use of nuclear power. There are countries currently adding nuclear power to satisfy their electrical needs. Saudi Arabia put in plans to develop two large nuclear power reactors by 2040 (WNA 2019). The UAE recently received approved building nuclear facilities (Ghosh 2020). The UAE plans to build four civilian nuclear reactors by 2023, making it the first Arab nation to operate a commercial nuclear power plant (Ghosh 2020). Since the use of nuclear power continues, the threat of a nuclear power plant disaster will remain though encouragingly an extremely infrequent event (Kyne 2015).

At the same time, the response to these disaster by the WNA, Tepco, U.S. Nuclear regulatory agencies, and the Japanese Government undermines public confidence in the accuracy of their pronouncements and shouts out for low cost, reliable, and independent tools that can reliably evaluate various NPP disaster and response scenarios. This dissertation puts forward the RASCAL-LVC framework as one such tool.

In order to prepare for these inevitable disasters, safe and effective responses, like unmanned systems, need to be considered. LVC simulation has proven to be a safe and effective approach to advance systems through life cycle phases to include training in the deployment phase as well as analysis during the concept, design, development, and test and evaluation phases. LVC simulation offers a low-cost assessment of equipment life expectancy for various operational missions conducted in the presence of ionizing radiation. Knowing life expectancy of equipment for operational scenarios is critical for emergency management planners. In order to address the threat of radiation during a NPP disaster, the independent RASCAL-LVC Framework shown below was conceptualized, created, and implemented.

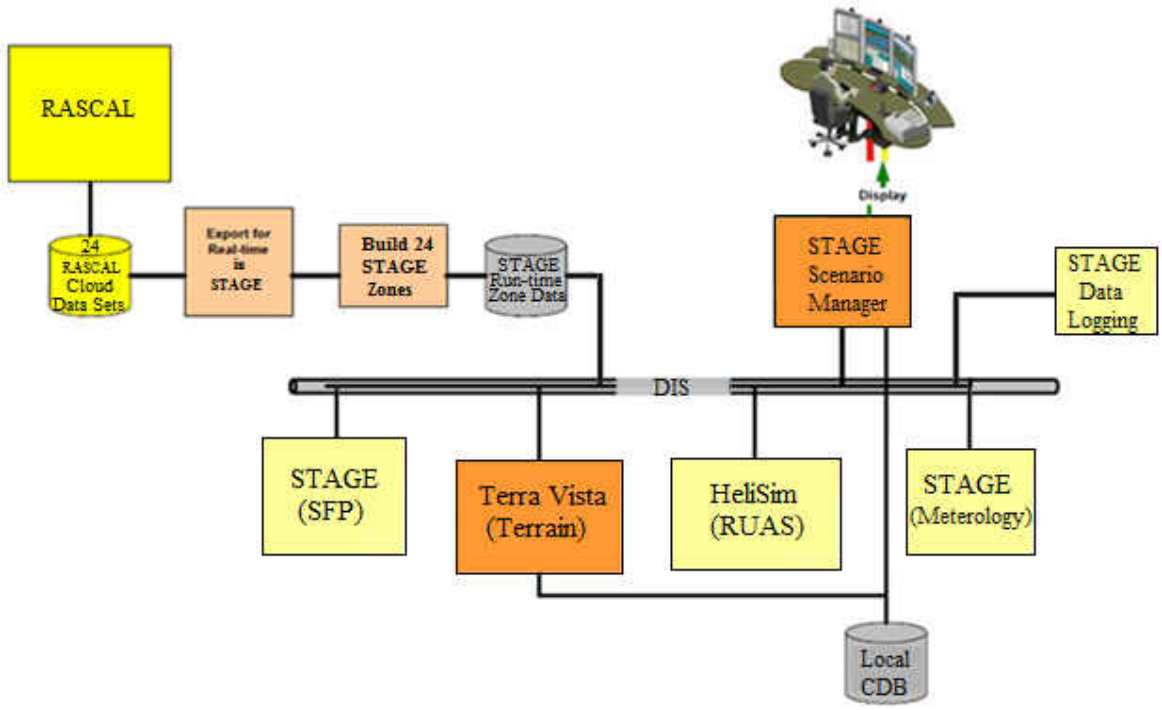

Figure 42 - RASCAL to STAGE Process Flow Diagram

The analysis performed with the framework revealed the survivability of Radiation Hardened Fire Scout UAVs operating in different disaster scenarios as shown in Table 9 below.

Table 9 - Fire Scout Performance

Survival of Flight of four Fire Scout UAVs for a 126-hour mission			
Mission Scenario	Fukushima in and out/# deliveries and pickup/potential tonnage delivered	Fukushima SFP Stabilization/# water drops/tonnage delivered	Chernobyl Reactor Extinguishing/# sand and boron drops/tonnage delivered
Survive	Yes	Yes	No
Number of Missions	756	756	156
Tonnage Delivered	340,200kg	340,200kg	70,200kg

With the increase in Nuclear power plants, and the yearly fluctuations in weather severity, emergency planners must develop safety nets and "back up" plans to prepare for the next disaster. Whether Hurricane Dorian was a product of climate change, global warming, or a natural occurrence in environment, one may ask, "What might have happened had Dorian pummeled a coastal NPP with the ferocity and duration that Dorian hit the Bahamas?" Extending the discussion beyond a Florida NPP site, had Dorian continued up the U.S. Atlantic coastline and struck Duke's Brunswick North Carolina NPP with Bahamas' intensity, the 23 foot storm surge seen in the Bahamas would have exceeded the 22 feet above sea level that Brunswick was prepared for (DiSavino 2018). Had Brunswick NPP lost both onsite and offsite power, would cooling be lost and a radiological emergency occur? Might it have escalated into

a Fukushima-like emergency? Chernobyl-like emergency? The Rascal-LVC framework created in this research could easily be extended to address the fore mentioned questions.

Given the mobility of UAVs to relocate rapidly to respond to an NPP emergency to the ten NPPs along the U.S. Gulf or Atlantic coast as well as their ability to access otherwise inaccessible areas, the research illustrates, investigates and presents results of the electronic survivability of a responding flight of four Fire Scout helicopters to three different radiological emergencies occurring at St Lucie.

When considering the Cloudshine results presented above, coastal meteorological conditions may contribute to the observed low radiation absorption levels as half the time the wind is blowing the atmospheric radioactivity out to sea. The Cloud is also dispersed resulting in low concentrations in the vast majority of the Cloudshine Snapshots. Additionally, Fire Scouts fly into the radioactive Cloud for only short periods and are decontaminated at a Staging area after each complete sortie. Decontamination is assumed to eliminate radioactive isotopes adhering to a Fire Scout during a sortie; reducing the gamma radiation damage those isotopes would have caused the electronics (Faccio 2001, Makowski 2006, Sawant 2012). To assess this damage, supplementary simulation tools would be necessary. Lastly, conservative containment leak rates were used due to loss of power to monitoring and sensor equipment (Huang and Jiang 2019) and the incorrect information disseminated by NPP owner, TEPCO (Inajima and Okada 2011).

Hover time is a significant contributor to damage to electronics. The hover times used above are based on trained and proficient forest service fire extinguishing missions (Base 2009,

Industries 2016). Since few if any are trained for a SFP Cooling Mission using a remotely operated helicopter, hover time estimates may be low and skewed. Virtual simulation helps pilots and crew train the task in a safe environment creating faster and more uniform performance (Systems 2019). Future live or virtual simulation may better estimate hover times then constructed behaviors used in this simulation (Proctor and Paulo 1996).

Using observed hot spot measurements, Chernobyl atmospheric radiation intensity was approximately 100 times as intense as Fukushima inferring on average 362 Rads of Cloudshine electronic damage rather than the insignificant 3.62 Rads seen at Fukushima. The resulting reduced 1938 Rads of electronic survivability would reduce hover time to about 6.6 minutes before electronic failure. That infers about 39 ten second hovers each delivering 450 kg of boron and sand totaling 17,550 kg before UAV demise. A flight of four Fire Scouts could deliver 70,200 kgs before demise. Whether 70,200 kgs of sand and boron are enough to extinguish the reactor fires and retard the nuclear reaction requires additional research. For emergency management planners, higher standards of radiation hardening of electronics sufficient to respond to a Chernobyl-like NPP emergency is also an alternative.

UAV electronics failure was measured using TID, as this data was readily available. Electronic failure caused by neutron and proton displacement damage (Makowski 2006), enhanced low dose rate effects (Löchner 2011), and single event effects (Sawant 2012) was not considered, as failure rates for helicopter avionics were not available. Future research could include failure rates caused by other forms of radiation damage to increase accuracy and fidelity.

The flexibility and utility of the LVC simulation framework enables future research into usability and electronic survivability of not only UAVs, but also unmanned ground and waterborne emergency response vehicles. Critical to ground vehicle usability will be modeling of dynamic changes to terrain and manmade features due to storm destructive impacts.

Additional research leveraging the LVC framework may determine Groundshine location and intensity as well as subsequent movement of radioactive materials once on the ground due to wind and rain. This may aid potential emergency response recovery planning and implementation.

Future research may also embed hot spots and enable RASCAL to interoperate in real time with LVC simulations enabling greater fidelity in representing radiation.

APPENDIX A:
DESIGN FACTORS WITHIN THE SIMULATION

Table 10 - Design Factors Within the Simulation

Factor	Type	Component of Origin	Category
Radiation Level	Continuous	RASCAL	Tested
Wind Direction	Categorical	Weather	Tested
Distance to Site	Continuous	UAV	Tested
Time of Day	Categorical	Weather	Tested
Cruise Speed	Continuous	UAV	Tested
Sling Load Capacity	Continuous	UAV	Tested
Sortie Length	Continuous	UAV	Tested
Number of UAVs	Discrete Numeric	UAV	Tested
UAV Survivability	Continuous	UAV	Controlled
UAV Sortie Regen Time	Continuous	UAV	Controlled
Water Drop Height	Continuous	UAV	Controlled
Bucket Fill Efficiency	Continuous	UAV	Controlled
Delivery Efficiency	Continuous	UAV	Controlled
Wind Velocity	Continuous	Weather	Tested
Atmospheric Pressure	Continuous	Weather	Tested
Relative Humidity	Continuous	Weather	Tested
Ambient Temperature	Continuous	Weather	Tested
Daily Precipitation	Continuous	Weather	Controlled
Water Temperature	Continuous	SFP Thermohydraulics	Tested

Factor	Type	Component of Origin	Category

Air Flow Reduction Ratio	Continuous	SFP Thermohydraulics	Tested
SFP Depth over Fuel	Continuous	SFP Thermohydraulics	Controlled
SFP Surface Area	Continuous	SFP Thermohydraulics	Controlled
SFP Water Volume	Continuous	SFP Thermohydraulics	Controlled
Fresh Water Temperature	Continuous	Terrain Services	Controlled
Fresh Water to SFP Distance	Continuous	Terrain Services	Controlled
Staging to SFP Distance	Continuous	Terrain Services	Controlled
Computers Involved	Categorical		Blocked

APPENDIX B:
NORMALIZED SPACE FILLING DESIGN

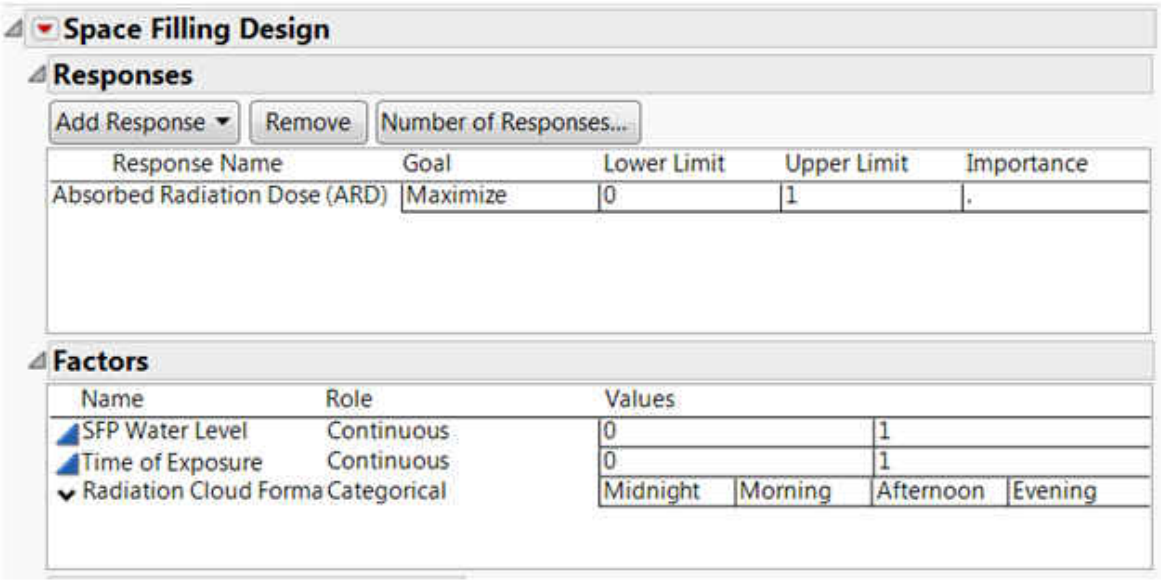

Figure 43 - Normalized Space Filling Design

APPENDIX C:
FAST FLEXIBLE FILLING DESIGN

3 Factors

Fast Flexible Filling Design

Design

Run	SFP Water Level	Time of Exposure	Radiation Cloud Formations
1	0.37942	0.34022	Midnight
2	0.29328	0.50433	Afternoon
3	0.72849	0.37190	Evening
4	0.48075	0.57660	Morning
5	0.58282	0.00673	Evening
6	0.26117	0.04016	Morning
7	0.63809	0.30071	Afternoon
8	0.51564	0.19888	Midnight
9	0.01095	0.43186	Midnight
10	0.10633	0.60403	Morning
11	0.07005	0.13481	Evening
12	0.17463	0.24012	Afternoon
13	0.99656	0.40592	Midnight
14	0.84171	0.47255	Morning
15	0.93688	0.54954	Afternoon
16	0.76407	0.63625	Evening
17	0.69373	0.09877	Afternoon
18	0.81337	0.16337	Midnight
19	0.96934	0.06118	Morning
20	0.90410	0.25777	Evening
21	0.14741	0.97757	Midnight
22	0.04423	0.83812	Afternoon
23	0.33733	0.79955	Morning
24	0.22309	0.68075	Evening
25	0.67369	0.76635	Morning
26	0.55810	0.71325	Midnight
27	0.43379	0.87454	Afternoon
28	0.61145	0.94913	Evening
29	0.87830	0.90106	Morning
30	0.79009	0.99817	Midnight

Figure 44 - Fast Flexible Filling Design

APPENDIX D:
FAST FLEXIBLE FILLING GENERATED TABLE

	SFP Water Level	Time of Exposure	Radiation Cloud Formations	Absorbed Radiation Dose (ARD)
1	0.3794229385	0.3402238504	Midnight	•
2	0.2932831333	0.5043258371	Afternoon	•
3	0.7284906426	0.3719026473	Evening	•
4	0.4807488324	0.576598089	Morning	•
5	0.5828249239	0.006729515	Evening	•
6	0.2611720878	0.0401593453	Morning	•
7	0.6380869825	0.3007117157	Afternoon	•
8	0.5156353342	0.1988750888	Midnight	•
9	0.0109502422	0.4318597697	Midnight	•
10	0.1063348395	0.6040328431	Morning	•
11	0.0700492873	0.134809817	Evening	•
12	0.1746344201	0.240122133	Afternoon	•
13	0.9965560492	0.4059220747	Midnight	•
14	0.8417103226	0.4725458028	Morning	•
15	0.9368794159	0.5495402756	Afternoon	•
16	0.7640673224	0.6362511432	Evening	•
17	0.6937260097	0.0987716726	Afternoon	•
18	0.8133748485	0.1633721986	Midnight	•
19	0.969337819	0.0611840946	Morning	•
20	0.9040987296	0.2577659687	Evening	•
21	0.1474080659	0.9775720647	Midnight	•
22	0.0442345535	0.8381210965	Afternoon	•
23	0.3373316028	0.7995494644	Morning	•
24	0.2230895622	0.6807485006	Evening	•
25	0.6736885681	0.766354139	Morning	•
26	0.5580952356	0.713249346	Midnight	•
27	0.4337923311	0.874539912	Afternoon	•
28	0.6114516671	0.9491291792	Evening	•
29	0.8782951097	0.9010630783	Morning	•
30	0.7900853871	0.9981652257	Midnight	•

Figure 45 - Fast Flexible Filling Generated Table

APPENDIX E:
RASCAL RADIONUCLIDE / HALF-LIFE LIST

Radionuclide	Half-life (d)	Decay Constant (1/d)	RASCAL 4.3 Model Production	
			BWR (Bq/MWt)/d	PWR (Bq/MWt)/d
H-3	4.51E+03	1.54E-04	5.770E+08	5.811E+08
Co-58	7.08E+01	9.79E-03	1.500E+11	1.401E+11
Co-60	1.92E+03	3.61E-04	9.716E+09	1.045E+10
Kr-85m	1.87E-01	3.71E+00	8.925E+14	8.291E+14
Kr-85	3.91E+03	1.77E-04	1.146E+10	1.110E+10
Kr-87	5.30E-02	1.31E+01	6.298E+15	5.846E+15
Kr-88	1.18E-01	5.87E+00	3.913E+15	3.622E+15
Rb-86	1.87E+01	3.71E-02	8.925E+10	9.817E+10
Sr-89	5.05E+01	1.37E-02	1.263E+13	1.169E+13
Sr-90	1.06E+04	6.54E-05	9.395E+10	9.053E+10
Sr-91	3.96E-01	1.75E+00	2.052E+15	1.908E+15
Sr-92	1.13E-01	6.13E+00	7.674E+15	7.229E+15
Y-90	2.67E+00	2.60E-01	4.796E+13	4.224E+13
Y-91	5.85E+01	1.18E-02	1.418E+13	1.336E+13
Y-92	1.48E-01	4.68E+00	5.902E+15	7.108E+11
Y-93	4.21E-01	1.65E+00	1.586E+15	1.513E+15
Zr-95	6.40E+01	1.08E-02	1.835E+13	1.789E+13
Zr-97	7.04E-01	9.85E-01	1.639E+15	1.606E+15
Nb-95	3.52E+01	1.97E-02	3.363E+13	3.284E+13
Mo-99	2.75E+00	2.52E-01	4.663E+14	4.596E+14
Tc-99m	2.51E-01	2.76E+00	4.518E+15	4.498E+15
Ru-103	3.93E+01	1.76E-02	2.774E+13	2.873E+13
Ru-105	1.85E-01	3.75E+00	4.047E+15	4.336E+15
Ru-106	3.68E+02	1.88E-03	1.331E+12	1.446E+12
Rh-105	1.47E+00	4.72E-01	4.860E+14	5.132E+14
Sb-125	1.01E+03	6.86E-04	1.321E+10	1.408E+09
Sb-127	3.85E+00	1.80E-01	1.527E+13	1.597E+13
Te-127m	1.09E+02	6.36E-03	9.172E+10	9.562E+10
Te-127	3.90E-01	1.78E+00	1.492E+14	1.561E+14
Te-129m	3.36E+01	2.06E-02	1.253E+12	1.276E+12

Figure 46 – RASCAL Radionuclide/Half-Life List (Commission 2015)

Radionuclide	Half-life (d)	Decay Constant (1/d)	RASCAL 4.3 Model Production	
			BWR (Bq/MWt)/d	PWR (Bq/MWt)/d
Te-129	4.83E-02	1.44E+01	4.301E+15	4.371E+15
Te-131m	1.25E+00	5.55E-01	1.077E+14	1.102E+14
Te-132	3.26E+00	2.13E-01	2.995E+14	2.975E+14
I-131	8.04E+00	8.62E-02	8.458E+13	8.484E+13
I-132	9.58E-02	7.24E+00	1.037E+16	1.035E+16
I-133	8.67E-01	7.99E-01	1.617E+15	1.599E+15
I-134	3.65E-02	1.90E+01	4.239E+16	4.184E+16
I-135	2.75E-01	2.52E+00	4.866E+15	4.827E+15
Xe-133	5.25E+00	1.32E-01	2.638E+14	2.659E+14
Xe-135	3.79E-01	1.83E+00	1.486E+15	1.228E+15
Cs-134	7.53E+02	9.21E-04	3.254E+11	3.592E+11
Cs-136	1.31E+01	5.29E-02	4.929E+12	4.908E+12
Cs-137	1.10E+04	6.30E-05	1.249E+11	1.247E+11
Ba-139	5.74E-02	1.21E+01	2.152E+16	2.108E+16
Ba-140	1.27E+01	5.46E-02	9.727E+13	9.595E+13
La-140	1.68E+00	4.13E-01	7.734E+14	7.552E+14
La-141	1.64E-01	4.23E+00	6.867E+15	6.713E+15
La-142	6.42E-02	1.08E+01	1.713E+16	1.673E+16
Ce-141	3.25E+01	2.13E-02	3.489E+13	3.444E+13
Ce-143	1.38E+00	5.02E-01	7.607E+14	7.383E+14
Ce-144	2.84E+02	2.44E-03	3.464E+12	3.406E+12
Pr-143	1.36E+01	5.10E-02	7.535E+13	7.366E+13
Nd-147	1.10E+01	6.30E-02	4.169E+13	4.130E+13
Np-239	2.36E+00	2.94E-01	5.598E+15	6.030E+15
Pu-238	3.20E+04	2.17E-05	4.020E+09	4.517E+09
Pu-239	8.78E+06	7.89E-08	2.991E+08	2.816E+08
Pu-240	2.39E+06	2.90E-07	4.670E+08	4.372E+08
Pu-241	5.26E+03	1.32E-04	1.440E+11	1.419E+11
Am-241	1.58E+05	4.39E-06	2.343E+08	1.946E+08
Am-242	6.68E-01	1.04E+00	1.604E+14	1.577E+14
Cm-242	1.63E+02	4.25E-03	4.336E+11	4.315E+11
Cm-244	6.61E+03	1.05E-04	3.689E+09	6.095E+09

APPENDIX F:
UNMANNED VEHICLES AT FUKUSHIMA

Operational Robots

Operational robots aid responders in various ways from assisting in the decontamination of the containment buildings to removing heavy objects that make mobility difficult. Examples include:

Dry ice Blast Decontamination Equipment for High Places

This robot decontaminates radioactive contaminants attached to ducts, piping, and walls by spraying dry ice powder on them and scraping it off (IRID 2015).

- **Development by Toshiba**
- **Decontaminates high places using a dry ice blast**
- **Introduced in November 2015**
- **Implemented in the Recovery Phase of the NPP**

Figure 47 - Dry Ice Blast Decontamination Equipment (TEPCO 2016)

Equipment to Remove Shielding Blocks (TEMBO)

This robot is used to remove blocks and iron plates previously of use to cover a pipe that leads to Fukushima Daiichi Unit 2's PCV so that a smaller investigational robot may enter the pipe. (IRID 2015)

- **Development by Mitsubishi Heavy Industries**
- **Modified fork-lift with mechanical arm/hand**
- **Moves blocks up to 50kg in weight**
- **Introduced in June 2015**
- **Implemented in the Recovery Phase of the NPP**

Figure 48 - Used to Remove Shielding Blocks (TEPCO 2016)

High Pressure Water Decontamination Robot

This robot is used for decontamination by using high pressure water jets (TEPCO 2016).

- **Development by Hitachi GE**
- **High Pressure water jets decontaminate contact surface**
- **Introduced in 2014**
- **Implemented in the Recovery Phase of the NPP**

Figure 49 - High Pressure Decontamination Robot (TEPCO 2016)

Maintenance Equipment Integrated System of Telecontrol Robot (MEISTeR)

This robot is capable of concrete drilling, cutting of handrails and piping, removal of obstacles, decontamination, and repair work. (Industries 2014)

- **Development by Mitsubishi Heavy Industries**
- **7 Freely Articulating Joints**
- **Dual-Arm Design**
- **Introduced in February 2014**
- **Implemented in the Recovery Phase of the NPP**

Figure 50 - MEISTeR (TEPCO 2016)

Dry Ice Blast Decontamination Robot

This robot uses dry ice to vacuum up radiation, it blasts tiny grains of dry ice to help detach radiological substances (PHYS 2013)

- **Development by Toshiba**
- **2 Boxy Machines the size of large refrigerators**
- **Caterpillar-tracked Design**
- **Introduced in February 2013**
- **Implemented in the Recovery Phase of the NPP**

Figure 51 - Dry Ice Blast Decontamination Robot (TEPCO 2016)

Decontamination Robot (Modified DXR 140 Demolition Machine)

The robot implements a “chemical mop” resembling a kitchen sponge mop for cleaning surfaces. It also uses a suction nozzle to suck up radioactive dust. The robot will vacuum the building’s walls, cable trays, ducts and control-panel surfaces. (Hornyak 2014)

- **Design by Husqvarna and modifications by Toshiba**
- **360-degree Rotational Arm**
- **Suitable for decontamination in high places**
- **Equipped with 12 Cameras and a dosimeter**

Figure 52 - Floor Decontamination Robot (TEPCO 2016)

Robot equipped with laser scanning

The robot is applied to acquire 3D laser scanning data inside the reactor buildings (TEPCO 2016).

- **Development by Hitachi GE**
- **Dual-Traction movement allows for stair climbing**
- **Allows for 3D Mapping of the interior**
- **Introduced in 2014**
- **Implemented in the Recovery Phase of the NPP**

Figure 53 - 3D Laser Scanning Robot (TEPCO 2016)

Floor Decontamination Robot (The Racoon)

The robot vacuum cleaner is designed to help with decontamination within Fukushima Daiichi Unit 2 in preparation for workers re-entering the building (News 2013).

- **Design in cooperation with ATOX**
- **Powered by two mobile relay units**
- **Scrubs and Jet washes the concrete through a suction/water delivery system**
- **Introduced in November 2013**
- **Implemented in the Recovery Phase of the NPP**

Figure 54 - The Raccoon Floor decontamination (TEPCO 2016)

ASTACO-SoRa robot

The ASTACO-SoRa robot can operate wirelessly from a dedicated control panel, a laser sensor detects the width of passages and any objects in the way. This robot also stores radiation monitoring data on the operator's station. (Falconer 2012)

- **Development by Hitachi GE**
- **Dual-armed heavy-duty design**
- **Each arm powerful enough to lift 150kg**
- **Introduced in July 2013**
- **Implemented in the Recovery Phase of the NPP**

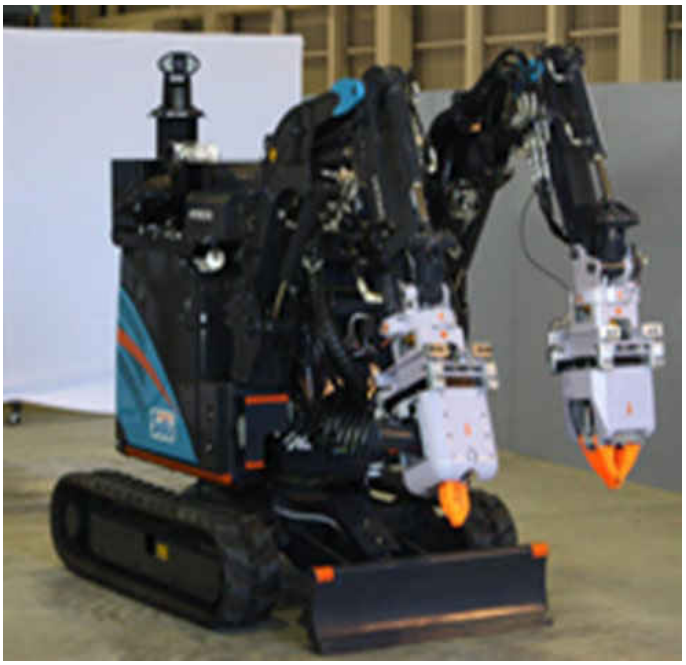

Figure 55 - Debris Removal Robot (ASTACO-SoRa) (TEPCO 2016)

Investigational Robots

Investigational robots are used in Fukushima to help responders fully grasp the site's condition. The investigational robots are small compared to operational robots as they require the ability to navigate through tight spaces. Examples below:

Shape-Shifting PCV Interior Inspection Robot

This robot is developed to investigate hard-to-access areas of the plant. It consists of three segments: the robot's main body and two compact crawlers. The robot can assume a long, straight shape for passing through narrow spaces, such as pipes (News 2015).

- **Development by IRID & Hitachi GE**
- **Able to pass through 10cm pipes**
- **Designed for high-radiation environments**
- **Introduced in April 2015**
- **Introduced in the Recovery Phase of the NPP**

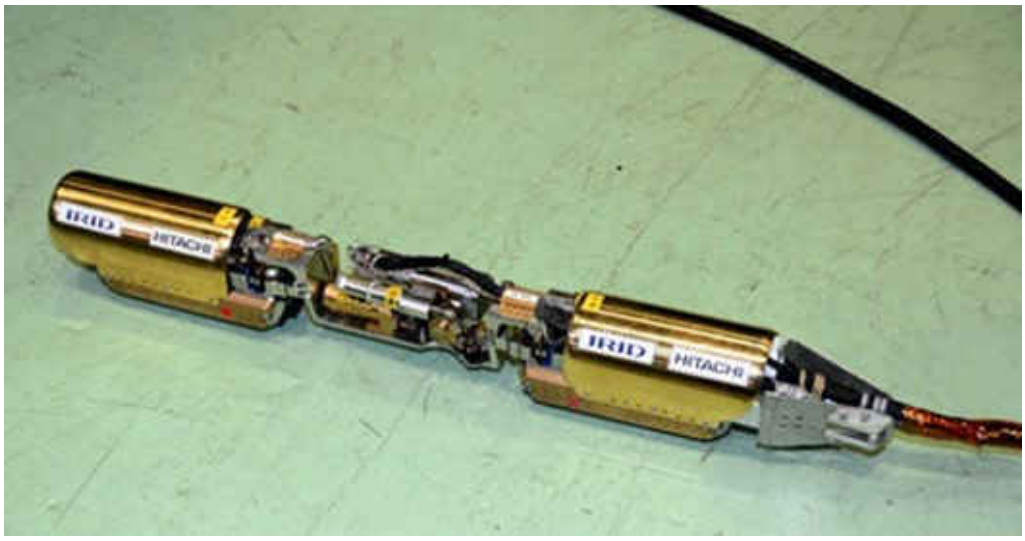

Figure 56 - Shape-Shifter PCV Inspection Robot (News 2015)

PCV Equipment Hatch Investigative Device

The miniature devices is beneficial in inspecting the hatch leading to the primary containment vessel (TEPCO 2016).

- **Development by TEPCO**
- **Equipped with integrated smartphone**
- **Easily navigational through small spaces**
- **Introduced in November 2015**
- **Implemented in the Recovery Phase of the NPP**

Figure 57 - PCV Equipment hatch Investigative Device (TEPCO 2016)

Kanicrane

The Kanicrane robot is used to investigate radiation sources on the upper part of the 1st floor of the reactor buildings (TEPCO 2016).

- **Development by Hitachi GE**
- **Developed in Remote Decontamination Project**
- **Introduced in May 2014**
- **Implemented in the Recovery Phase of the NPP**

Figure 58 – Kanicrane (TEPCO 2016)

Rosemary

Rosemary is equipped with a gamma camera (N-Visage) that detects radiation dosage rates inside the reactor building. Rosemary operates this camera via a wireless system since it is not equipped with an extension and retraction device for communication cables.

- **Development by IRID & Hitachi GE**
- **Operates in conjunction with Sakura**
- **Introduced in July 2014**
- **Used to inspect Radioactive Sources in Unit 1 Reactor Building**
- **Implemented in the Recovery Phase of the NPP**

Figure 59 - Rosemary (IRID 2014)

Sakura

Sakura supports Rosemary in a coordinated inspection effort inside the building by the robot pair, acting as a wireless transmission station (IRID 2014).

- **Development by IRID & Hitachi GE**
- **Operates in conjunction with Rosemary**
- **Introduced in July 2014**
- **Wireless Base Station**
- **Implemented in the Recovery Phase of the NPP**

Figure 60 - Sakura Wireless Base Station (IRID 2014)

High Access Survey Robot

This robot uses combination of cameras, laser range finders, and dosimeters on the tip of the extendable arm. The robot produces detailed video images, collects 3D structural data, and identifies sources of radiation from areas that would be otherwise inaccessible.(Falconer 2013)

- **Development by AIST and Honda**
- **Robot Arm (Honda) has 11 joints and extends up to 7 meters**
- **Introduced in June 2013**
- **Implemented in the Recovery Phase of the NPP**

Figure 61 - High Access Survey Robot (Falconer 2013)

Hybrid Robots (Operational and Investigational)

iRobot 710 Warrior

The 710 Warrior is designed for exploring irradiated environments, reconnaissance and surveillance missions and can lift loads of up to 220 lbs (100 kg) and carry payloads of more than 150 pounds (68 kg) over rough terrain (WIRE 2012).

- **Development by iRobot**
- **Provides Enough Power to Pull a Car**
- **Introduced in June 2011**
- **Obstacle avoidance sensors, compass and GPS**
- **Implemented in the Response Phase of the NPP**

Figure 62 - iRobot 710 Warrior (WIRE 2012)

Quince Robot

Quince is a rescue robot designed for CBRNE disasters. It assists in photographing the details of containment buildings, creating radiation dose maps, and sampled radioactive materials floating in the air (FuRo 2011).

- **Development by IRSI and Chiba Institute of technology**
- **Cumulative Radiation tolerance of 20 Sieverts**
- **Introduced in June 2011**
- **Implemented in the Response Phase of the NPP**

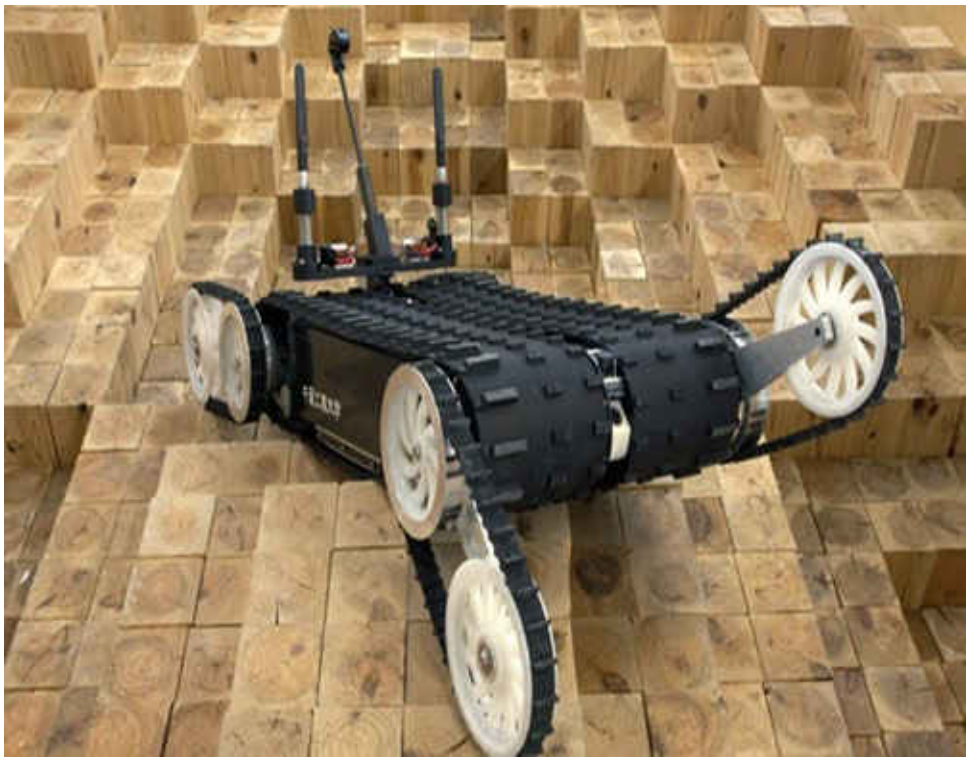

Figure 63 - Quince Robot (FuRo 2011)

iRobot Packbot

The 510 PackBot is a multi-mission tactical mobile robot designed for use by first responders to carry out dangerous missions in high-threat scenarios.

- **Development by iRobot**
- **Provided live interior images**
- **Recorded Temperature Readings**
- **Introduced in April 2011**
- **Implemented in the Response Phase of the NPP**

Figure 64 – iRobot Packbot (TEPCO 2016)

Unmanned Aerial Vehicles

Autonomous unmanned helicopter: RMAX G1 Yamaha

The RMAX G1 Yamaha is implemented as a radiation survey system to provide mapping of dose-rate distribution (Motors 2013).

- **Development by Yamaha**
- **Flight Altitude: 80 m**
- **Flight Range < 3 km**
- **Air Speed: 30 km/h**
- **Flight time: 90 min**
- **Max Payload: 10 kg**
- **Introduced in April 2011**
- **Implemented in the Response Phase of the NPP**

Figure 65 - Yamaha RMAX (Motors 2013)

Unmanned Airplane for Radiation Monitoring System (UARMS)

The unmanned airplane is designed for aerial radiation monitoring with the support of a ground station for wireless control

- **Development by JAXA**
- **Flight Altitude: 150 m**
- **Air Speed: 108 km/h**
- **Flight time: 360 min**
- **Max Payload: 10 kg**
- **Flight Range: > 10km**
- **Introduced in November 2014**
- **Implemented in Recovery Phase of the NPP**

Figure 66 - Unmanned Airplane (JAXA 2015)

Honeywell RQ-16 T-Hawk – Micro Air Vehicle (MAV)

Four T-Hawk drones are deployed at Fukushima to conduct video surveillance and nuclear radioactivity readings (Technology 2007).

- **Development by Honeywell**
- **Weight: 17 lbs (backpack portable)**
- **Flight Time: 50 min**
- **Vertical takeoff and landing**
- **Designed for Day/Night operations**
- **Intelligence, Surveillance, and Reconnaissance Mission**
- **Introduced in April 2011**
- **Implemented in the Response Phase of the NPP**

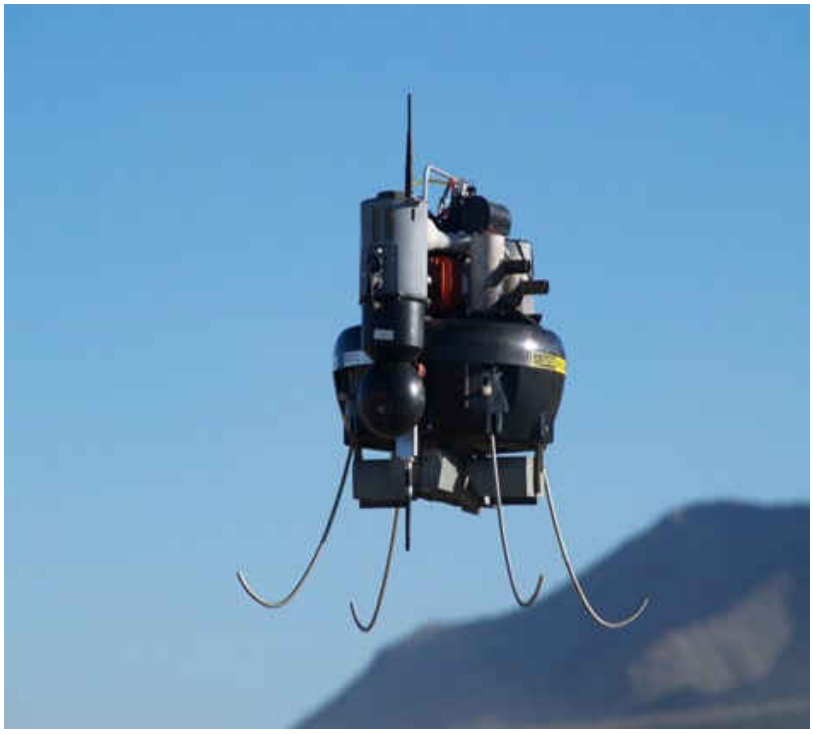

Figure 67 - Honeywell T-Hawk MAV (Aerospace 2009)

Unmanned Aquatic Systems

LEO: Underwater Remotely Operated Vehicle (ROV)

The LEO is part of an underwater investigation program using remotely operated vehicles to help in the effort to remove bodies and rubble from the seafloor (OSUMI 2014)

- **Developed by Tokyokyuei Corp**
- **Underwater Surveillance for Debris Cleanup**
- **Introduced in July 2011**
- **Works in conjunction with a fishing boat base station**
- **Implemented in the Response Phase of the NPP**

Figure 68 - LEO Underwater ROV (OSUMI 2014)

RTV – 100

The RTV-100 is part of an underwater investigation program using remotely operated vehicles to help in the effort to remove bodies and rubble from the seafloor (Maki 2011, OSUMI 2014)

- **Developed by Mitsui Engineering**
- **Underwater Surveillance for Debris Cleanup**
- **Introduced in April 2011**
- **Implemented in the Response Phase of the NPP**

Figure 69 - RTV-100 (Maki 2011)

APPENDIX G:
NRC SIMULATION CODES

Each will be discussed in detail below.

- Probabilistic Risk Assessment Codes
- Fuel Behavior Codes
- Reactor Kinetic Codes
- Thermal-Hydraulics Codes
- Severe Accident Codes
- Radiological Protection Computer Codes
- Radionuclide Transport Codes

(NRC 2015)

Probabilistic Risk Assessment Codes

SAPHIRE -- Systems Analysis Programs for Hands-on Integrated Reliability

- Used for performing probabilistic risk assessments.

Fuel Behavior Codes

- **FRAPCON-3 --** Steady-state and mild transient analysis of a fuel rod under normal conditions.
- **FRAPTRAN --** Transient and design basis accident analysis of a fuel rod in off-normal conditions.

Reactor Kinetic Codes

PARCS: **Purdue Advanced Reactor Core Simulator**

- Solves the time-dependent two-group neutron diffusion equation in three-dimensional Cartesian geometry using nodal methods to obtain the transient neutron flux distribution. The code may be used in the analysis of reactivity-initiated accidents in light-water reactors where spatial effects may be important. It may be run in the stand-alone mode or coupled to other NRC thermal-hydraulic codes.

Thermal-Hydraulics Codes

TRACE: TRAC/RELAP Advanced Computational Engine.

- A modernized thermal-hydraulics code designed to analyze large/small break LOCAs and system transients in both pressurized- and boiling-water reactors (PWRs and BWRs).

SNAP: Symbolic Nuclear Analysis Package

- A graphical user interface with pre-processor and post-processor capabilities, which assists in developing TRACE and RELAP5 input decks and running the codes.

RELAP5: Reactor Excursion and Leak Analysis Program

- A tool for analyzing small-break LOCAs and system transients in PWRs or BWRs. It has the capability to model thermal-hydraulic phenomena in 1-D volumes.

Severe Accident Codes

MELCOR -- Integral Severe Accident Analysis Code: Fast-Running, parametric models.

MACCS: MELCOR Accident Consequence Code System

- Used to perform probabilistic offsite consequence assessments for hypothetical atmospheric releases of radionuclides. The code models atmospheric transport and dispersion, emergency response and long-term protective actions, exposure pathways, early and long-term health effects, land contamination, and economic costs.

SCDAP/RELAP5: Integral Severe Accident Analysis Code: Uses detailed models.

IFCI -- Integral Fuel-Coolant Interactions Code.

VICTORIA -- Radionuclide transport and decommissioning codes provide dose analyses in support of license termination and decommissioning.

Radiological Protection Computer Codes

RADTRAD: Radionuclide Transport, Removal and Dose Estimation.

- The RADTRAD code uses a combination of tables and numerical models of source term reduction phenomena to determine the time-dependent dose at specified locations for a given accident scenario. The RADTRAD code can be used to assess occupational radiation exposures, typically in the control room; to estimate site boundary doses; and to estimate dose attenuation due to modification of a facility or accident sequence.

RASCAL: Radiological Assessment Systems for Consequence Analysis.

- The RASCAL code evaluates releases from nuclear power plants, spent fuel storage pools and casks, fuel cycle facilities, and radioactive material handling facilities and is designed for use by the NRC in the independent assessment of dose projections during response to radiological emergencies.

VARSKIN -- Computer code for calculating Skin dose.

- The code is used to perform confirmatory calculations of skin dose (from both beta and gamma sources) estimates at any skin depth or skin volume, with point, disk, cylindrical, spherical, or slab (rectangular) sources, and even enables users to compute doses from multiple sources.

Radiological Toolbox

- The NRC developed the radiological toolbox as a means to quickly access databases needed for radiation protection, shielding, and dosimetry calculations. The toolbox is essentially an electronic handbook with limited computational capabilities beyond those of unit conversion. The toolbox contains radioactive decay data, biokinetic data, internal and external dose coefficients, elemental composition of a large number of materials, radiation interaction coefficients, kerma coefficients, and other tabular data of interest to the health physicist, radiological engineer, and others working in fields involving radiation.

HABIT

- The HABIT code is an integrated set of computer programs used mainly to estimate chemical exposures that personnel in the control room of a nuclear facility would be exposed to in the event of an accidental release of toxic chemicals.

GALE: Gaseous and Liquid Effluent

- Estimates the quantities of radioactivity released by a plant through liquid and atmospheric discharges during routine operations for pressurized-water reactors (PWR) and boiling-water reactors (BWR).

DandD -- A code for screening analyses for license termination and decommissioning.

Radionuclide Transport Codes

RESRAD -- Applies to the cleanup of sites

RESRAD-BUILD – Applies to the cleanup of buildings and structures.

(NRC 2015)

APPENDIX H:
PRESAGIS LVC SUITE

Creator

Presagis' creator is used in designing optimized 3D models for real-time simulation, creator allows content developers to work natively with OpenFlight data to output highly optimized models with advanced surface materials and multiple levels-of-detail (Presagis 2016).

Terra Vista

Terrain generation software that gives integrators and database developers the tools they need to build database environments for ground, air, maritime, sensor, urban, and military operations in urban terrain (Presagis 2016).

STAGE

STAGE gives developers the power to create more sophisticated simulation scenarios across large areas for operations, training, and analysis. STAGE offers an extendable standards-based environment that comes complete with tools to develop rich scenarios (Presagis 2016).

FlightSim

Provides comprehensive flight models for military, commercial, and unmanned aircraft design and testing, with an emphasis on safety-critical simulations. FlightSim allows the user to test both aircraft design and aircraft performance under controlled simulated conditions, specify subsystems behavior, and tailor flight simulations through custom aerodynamics and environmental parameters (Presagis 2016).

HeliSim

Rotary-wing flight models for a wide range of military, civilian, and unmanned scenarios. HeliSIM allows the user to build comprehensive helicopter flight models easily. HeliSim allows the user to test both aircraft design and performance under simulated conditions (Presagis 2016).

Vega Prime

Comprehensive visualization toolkit that supports high-quality 3D databases, and the ability to configure, create, and deploy game-quality simulation applications. Vega Prime provides integrators and simulation developers the tools needed to create high-performance visuals for the most sophisticated of environments (Presagis 2016).

Interoperability

Interoperability is facilitated between STAGE, Flight Sim, HeliSim and Vega Prime through either Distributed Interactive Simulation (IEEE 1278) or High-Level Architecture (IEEE 1516).

APPENDIX I:
WINDROSE FREQUENCY DISTRIBUTION (SPEED X DIRECTION)

Calm - 23.7%		Wind Speed (miles per hour)						
		0.0- 1.9	2.0- 4.9	5.0- 6.9	7.0- 9.9	10.0-14.9	15.0-19.9	20.0- inf
NORTH	355-005	0.000	0.424	0.470	0.418	0.693	0.204	0.045
	005-015	0.000	0.223	0.205	0.234	0.253	0.028	0.004
NNW	015-025	0.000	0.206	0.218	0.278	0.280	0.023	0.005
	025-035	0.000	0.338	0.405	0.468	0.539	0.099	0.018
NE	035-045	0.000	0.294	0.324	0.370	0.303	0.024	0.003
	045-055	0.000	0.390	0.686	0.745	0.833	0.198	0.085
	055-065	0.000	0.386	0.546	0.653	0.652	0.057	0.009
ENE	065-075	0.000	0.485	0.896	1.079	1.578	0.346	0.097
	075-085	0.000	0.390	0.636	0.904	1.369	0.182	0.014
EAST	085-095	0.001	0.446	1.153	1.371	2.583	0.563	0.079
	095-105	0.000	0.252	0.444	0.671	1.489	0.278	0.034
ESE	105-115	0.000	0.214	0.445	0.789	1.991	0.456	0.060
	115-125	0.002	0.303	0.817	1.015	2.526	0.784	0.133
SE	125-135	0.001	0.169	0.391	0.523	1.425	0.521	0.103
	135-145	0.000	0.275	0.576	0.617	1.487	0.666	0.134
	145-155	0.000	0.261	0.309	0.300	0.390	0.087	0.019
SSE	155-165	0.000	0.440	0.484	0.336	0.355	0.092	0.010
	165-175	0.000	0.418	0.333	0.207	0.188	0.028	0.006
SOUTH	175-185	0.000	0.572	0.606	0.385	0.438	0.095	0.013
	185-195	0.000	0.406	0.295	0.184	0.198	0.023	0.006
SSW	195-205	0.000	0.408	0.273	0.187	0.227	0.044	0.005
	205-215	0.000	0.458	0.400	0.285	0.325	0.087	0.024
SW	215-225	0.000	0.466	0.341	0.255	0.278	0.074	0.020
	225-235	0.000	0.511	0.400	0.315	0.420	0.097	0.039
	235-245	0.000	0.434	0.340	0.247	0.280	0.045	0.013
WSW	245-255	0.001	0.509	0.483	0.340	0.436	0.088	0.029
	255-265	0.000	0.565	0.289	0.199	0.249	0.050	0.023
WEST	265-275	0.001	0.976	0.695	0.397	0.553	0.168	0.080
	275-285	0.000	0.850	0.450	0.266	0.304	0.103	0.042
WNW	285-295	0.000	0.884	0.439	0.233	0.292	0.083	0.018
	295-305	0.002	0.918	0.709	0.355	0.388	0.137	0.033
NW	305-315	0.000	0.709	0.592	0.362	0.265	0.036	0.004
	315-325	0.000	0.728	0.809	0.490	0.421	0.062	0.011
	325-335	0.000	0.456	0.315	0.248	0.139	0.012	0.004
NNW	335-345	0.000	0.446	0.390	0.266	0.255	0.061	0.012
	345-355	0.000	0.268	0.205	0.180	0.163	0.019	0.005

Figure 70 - Windrose Frequency distribution (IEM 2017)

APPENDIX J:
WIND DIRECTION AND INTENSITY AVERAGES
(Wunderground 2017)

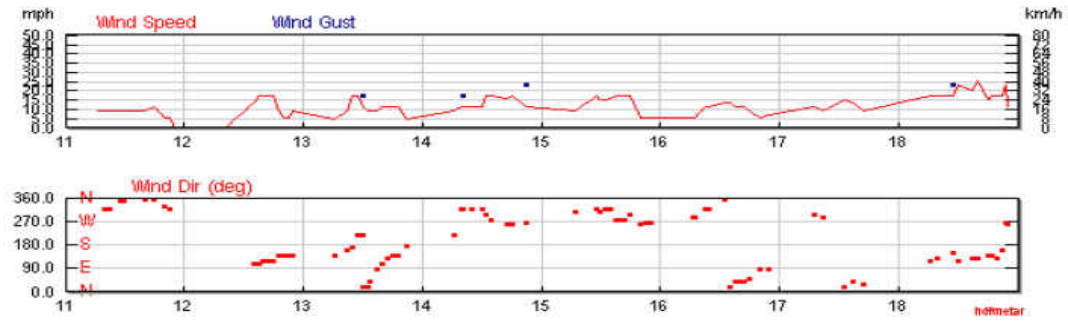

Figure 71 – 1988 Wind Direction and Intensity Average

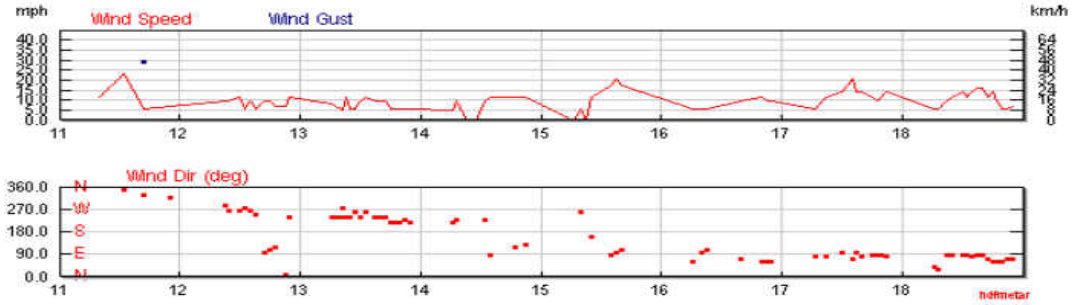

Figure 72 - 1989 Wind Direction and Intensity Average

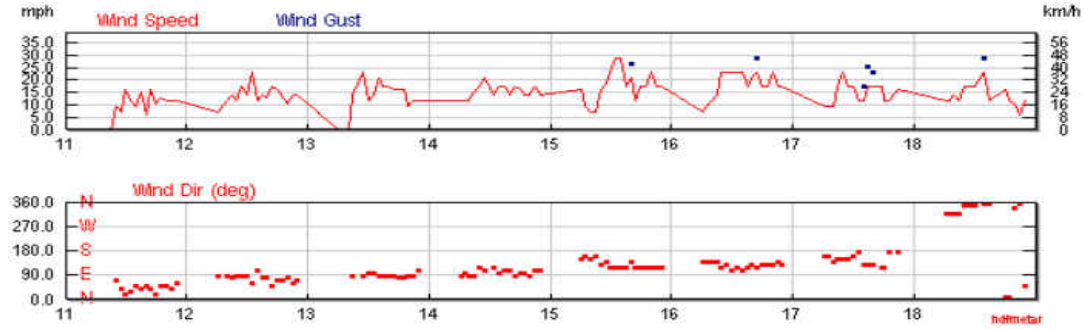

Figure 73 - 1990 Wind Direction and Intensity Average

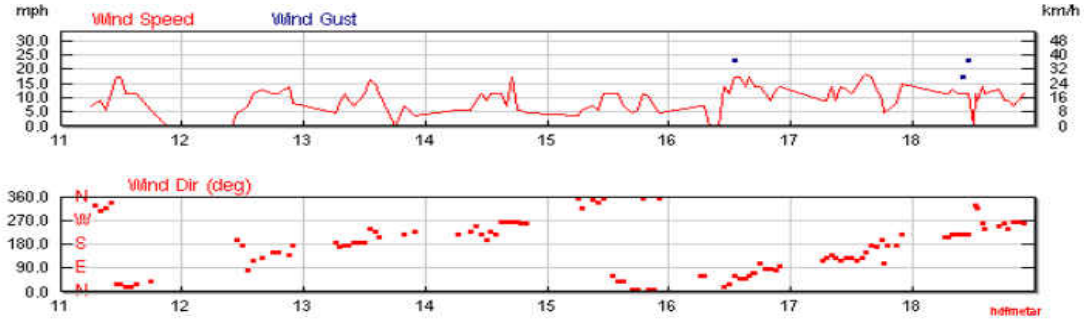

Figure 74 - 1991 Wind Direction and Intensity Average

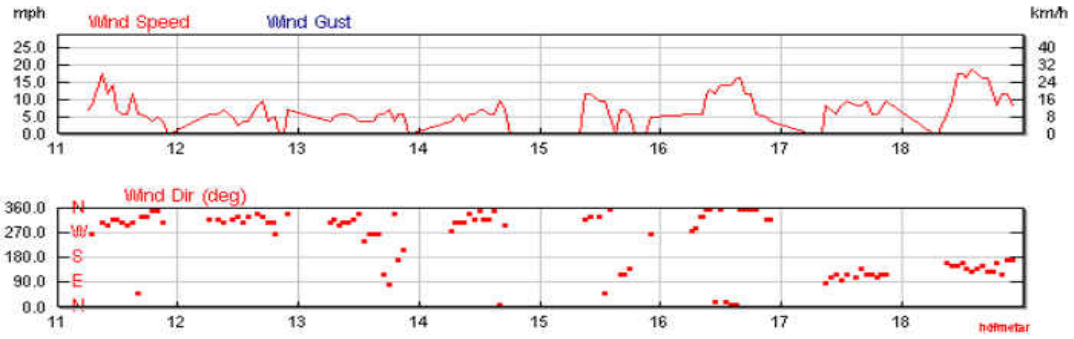

Figure 75 - 1992 Wind Direction and Intensity Average

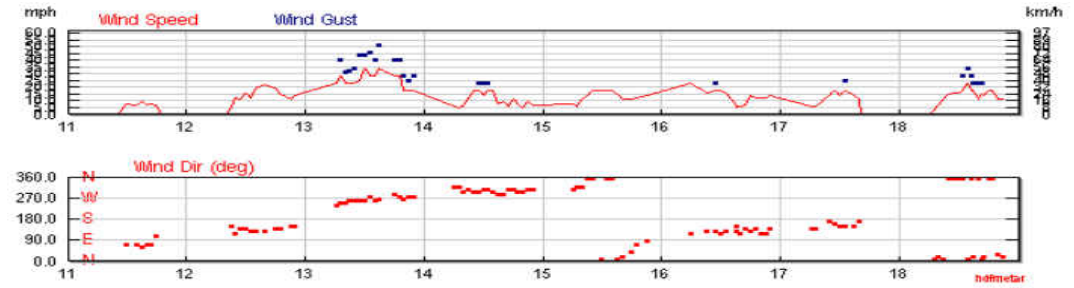

Figure 76 - 1993 Wind Direction and Intensity Average

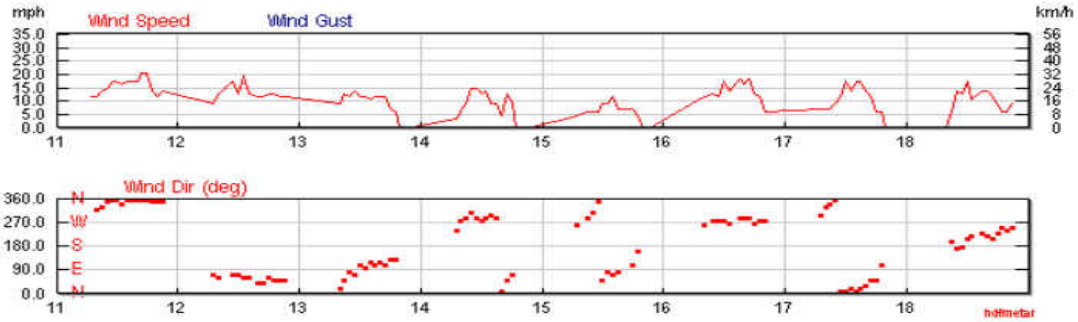

Figure 77 - 1994 Wind Direction and Intensity Average

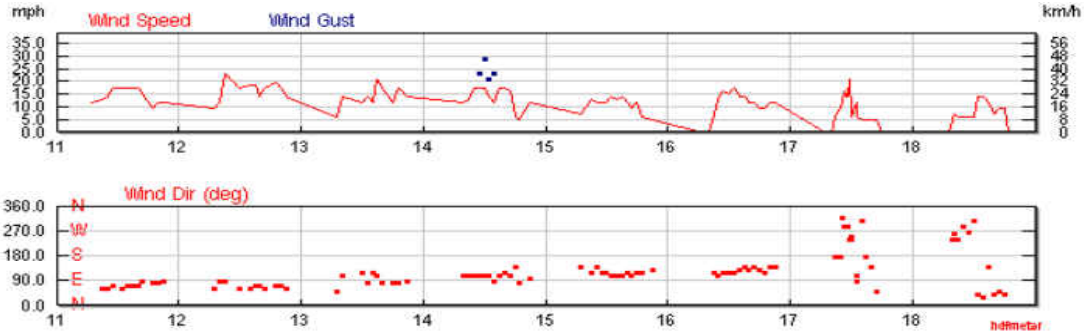

Figure 78 - 1995 Wind Direction and Intensity Average

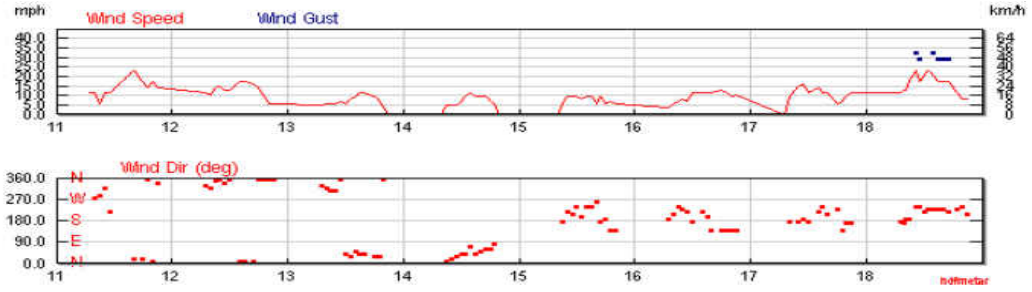

Figure 79 - 1996 Wind Direction and Intensity Average

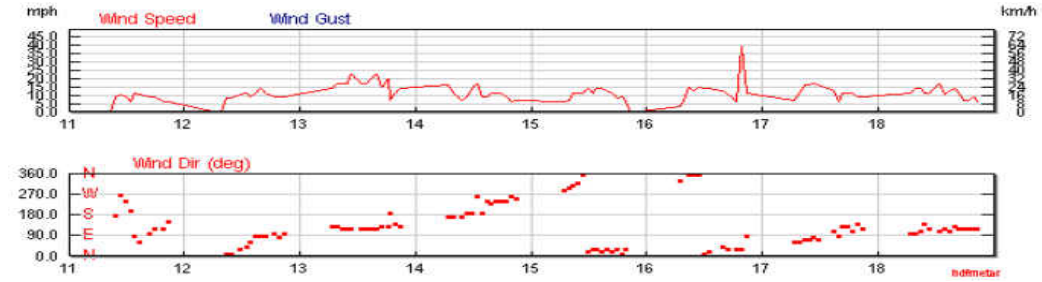

Figure 80 - 1997 Wind Direction and Intensity Average

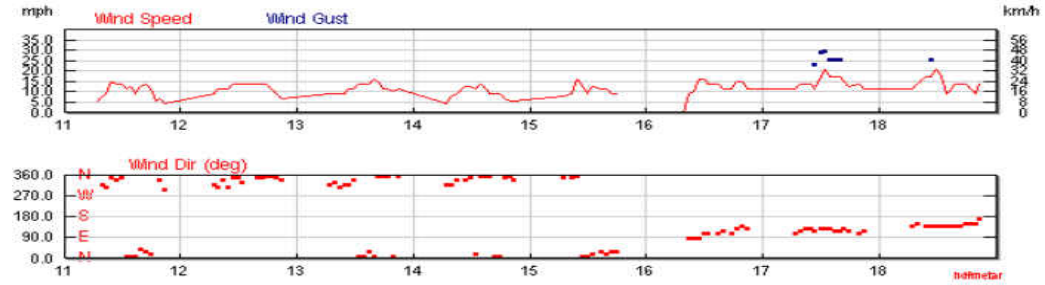

Figure 81 - 1998 Wind Direction and Intensity Average

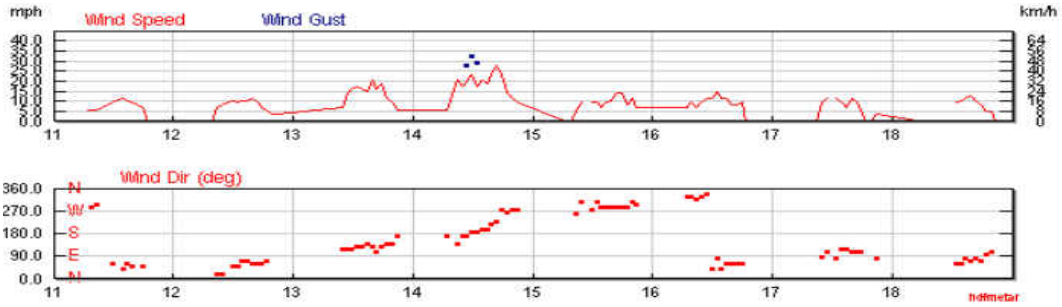

Figure 82 – 1999 Wind Direction and Intensity Average

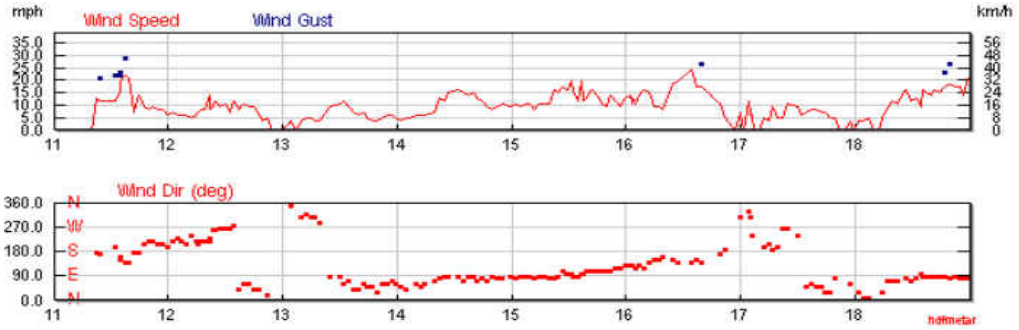

Figure 83 - 2000 Wind Direction and Intensity Average

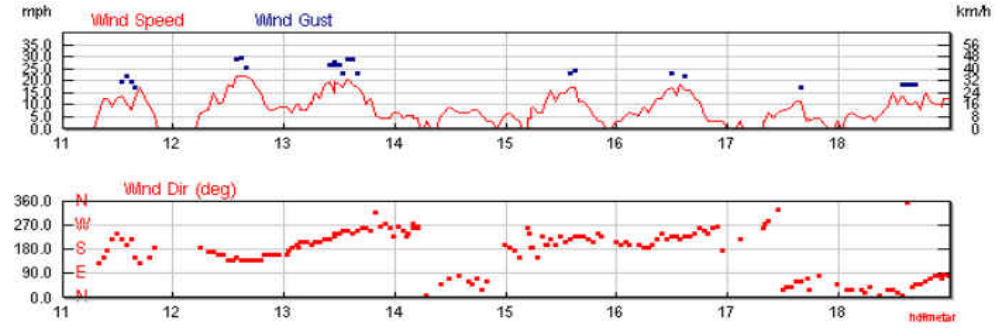

Figure 84 – 2001 Wind Direction and Intensity Average

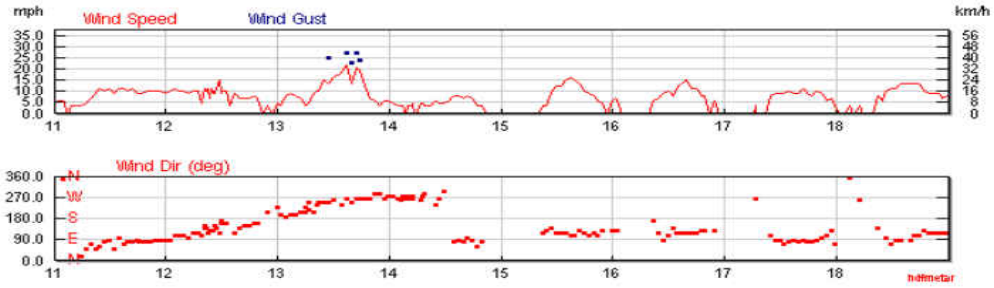

Figure 85 - 2002 Wind Direction and Intensity Average

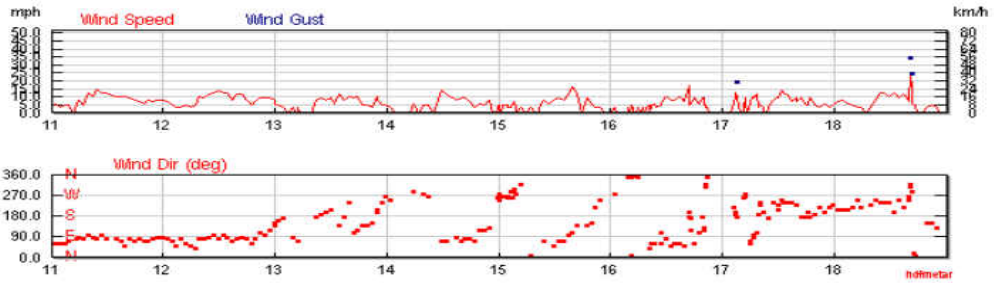

Figure 86 – 2003 Wind Direction and Intensity Average

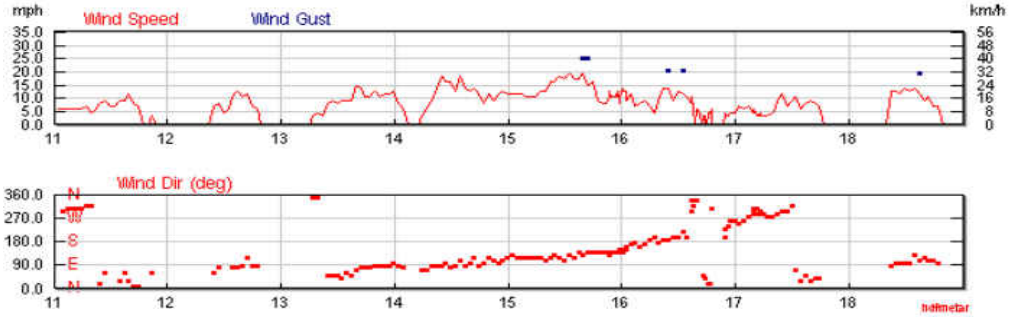

Figure 87 - 2004 Wind Direction and Intensity Average

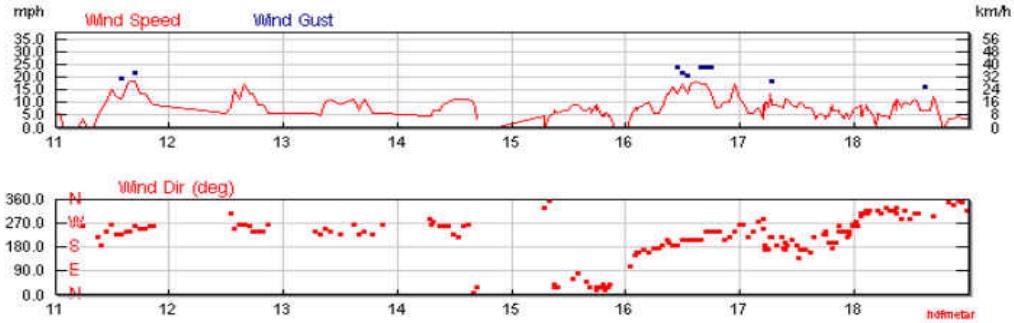

Figure 88 - 2005 Wind Direction and Intensity Average

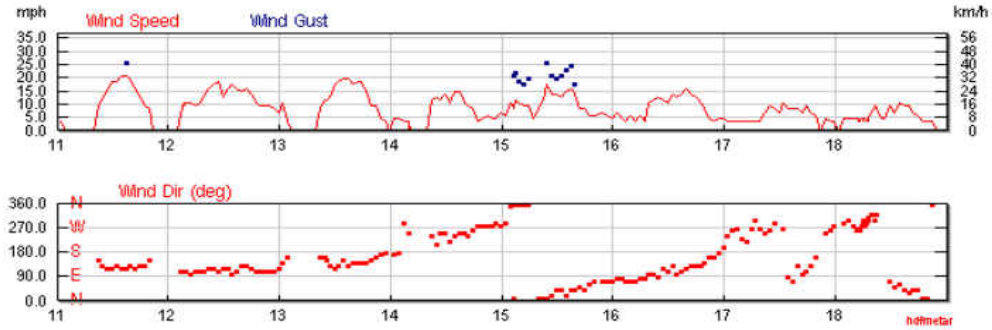

Figure 89 - 2006 Wind Direction and Intensity Average

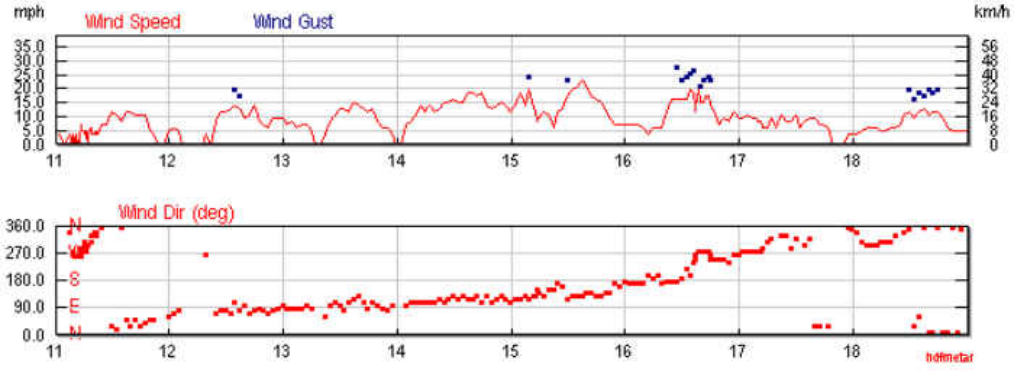

Figure 90 - 2007 Wind Direction and Intensity Average

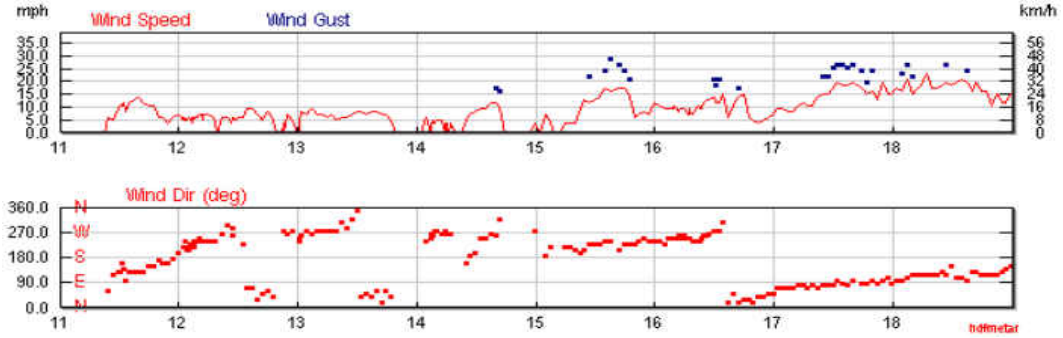

Figure 91 - 2008 Wind Direction and Intensity Average

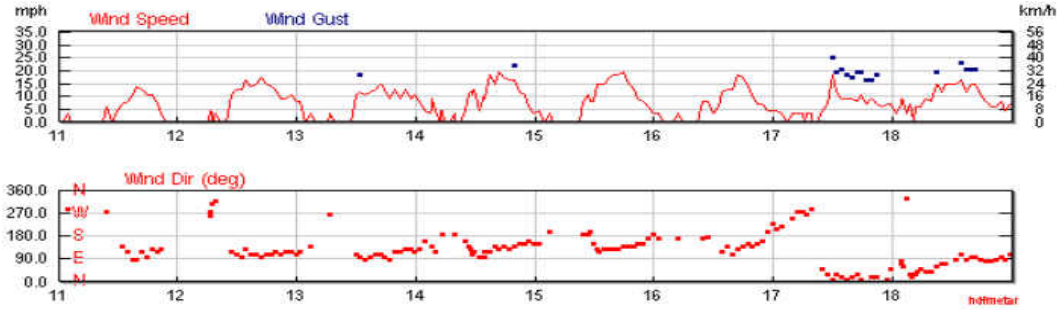

Figure 92 - 2009 Wind Direction and Intensity Average

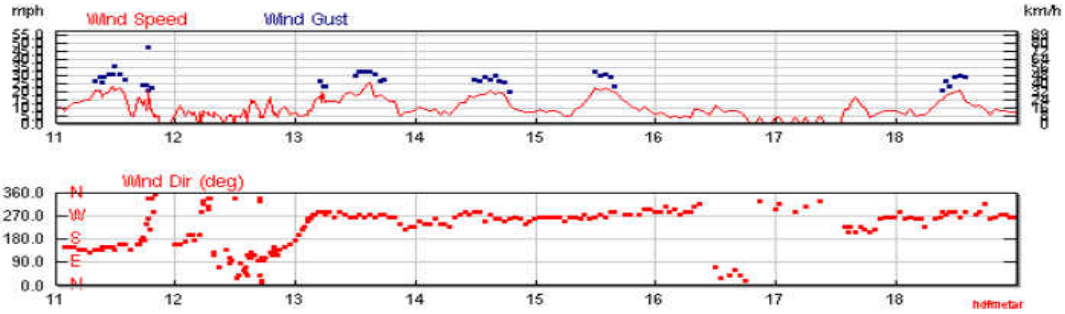

Figure 93 - 2010 Wind Direction and Intensity Average

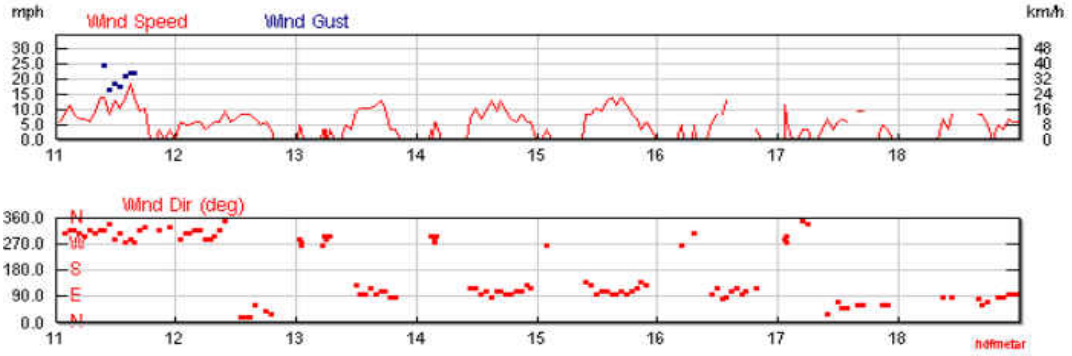

Figure 94 - 2011 Wind Direction and Intensity Average

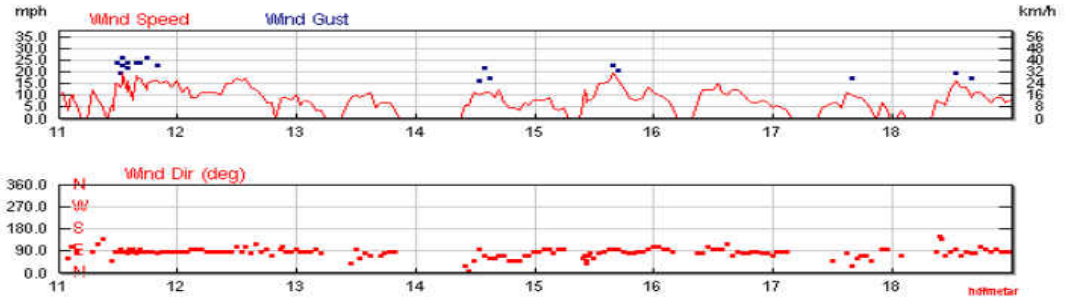

Figure 95 – 2012 Wind Direction and Intensity Average

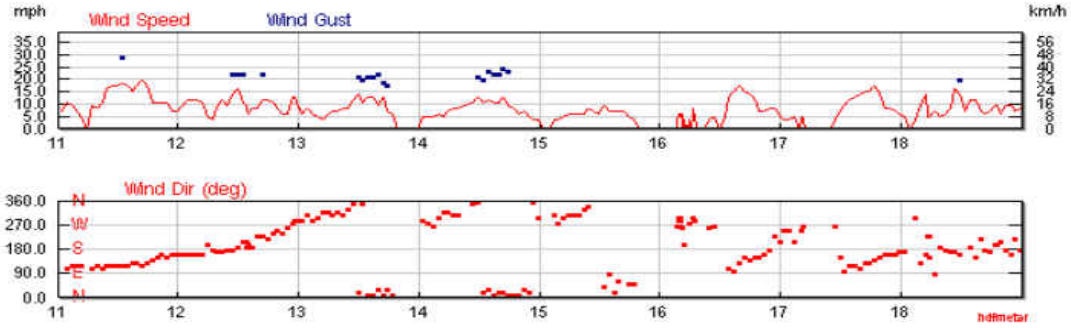

Figure 96 - 2013 Wind Direction and Intensity Average

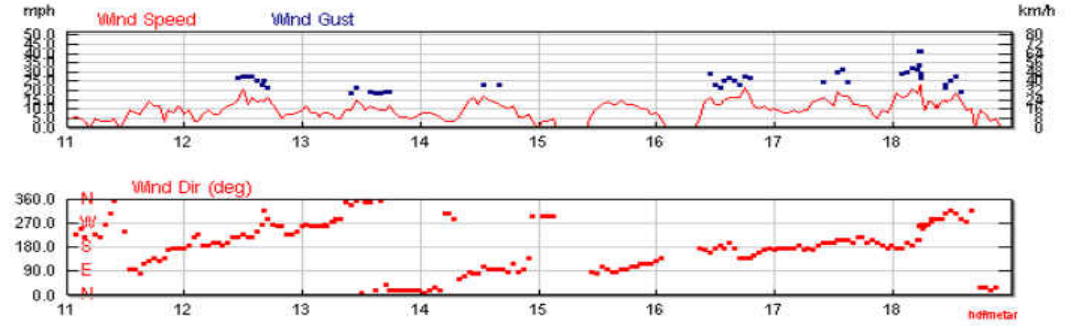

Figure 97 - 2014 Wind Direction and Intensity Average

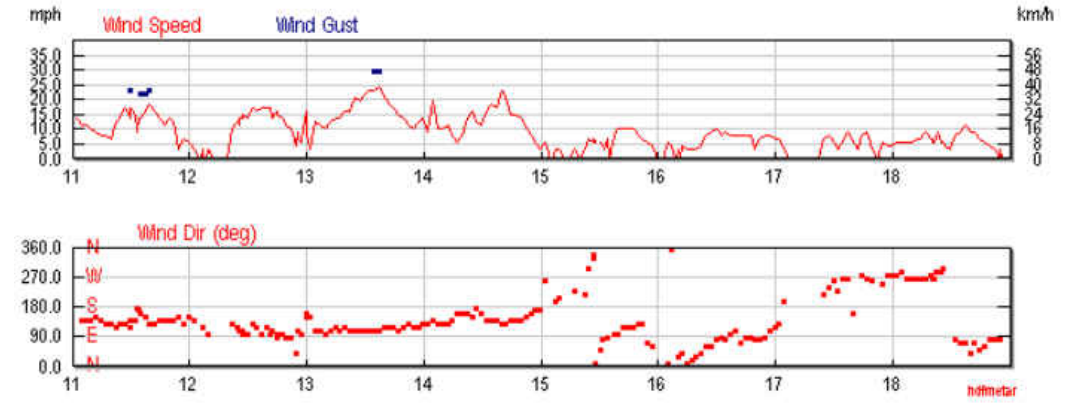

Figure 98 – 2015 Wind Direction and Intensity Average

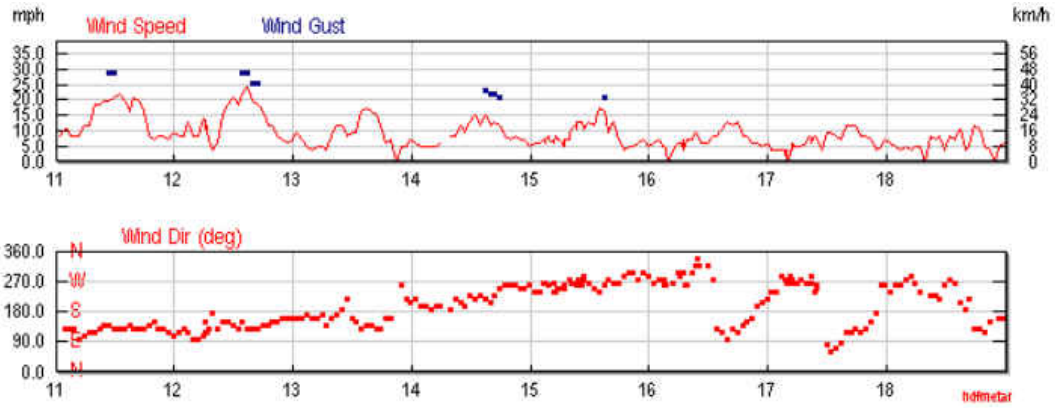

Figure 99 - 2016 Wind Direction and Intensity Average

APPENDIX K:
METHODS OF EVALUATION USING A LVC SIMULATION FRAMEWORK

There are various methods for enhancing and evaluating UAV effectiveness for particular mission sets that have been proposed in the literature (Blyenburgh 2000, Saggiani and Teodorani 2004) including the use of simulation (Zittel 2001, Bernabei, Sassanelli et al. 2014, Hodicky 2014), distributed, live, virtual, constructive (LVC) simulations "have been primarily an exercise and demonstration technology to date" (Hodson and Hill 2014).

Design of Experiments (DOE) is a simple "planned approach for determining cause and effect relationships" (Anderson and Whitcomb 2007). It is important to define the language of experimental design used throughout the rest of this study. The response variable is the parameter of interest. The parameters that can affect the response variable are called factors. These factors are assigned a value from within a range of interest for each run of the experiment. The combination of certain parameter values for a particular run is called a treatment. These terms related to formation, execution, and analysis of the experimental design are from (Montgomery 2013), a highly regarded reference text on experimental design and analysis.

(Haase, Hill et al. 2014) provide an LVC-experimental design similar to that of (Coleman and Montgomery 1993)'s designed industrial experiment planning process. While the proposed research is only one component of LVC, the suggested planning and execution process is still applicable. Consisting of seven steps:

- **Recognition and statement of the problem**
- **Selection of the response variable**
- **Choice of factors, levels, and range**

- **Choice of experimental design**
- **Performing the experiment**
- **Statistical analysis of the data**
- **Conclusions and recommendations**

Minor regrouping of these steps fits them to the standard dissertation model. Step 1 fits with Chapters 1 and 2 where the problem of interest is identified and followed with background information. Steps 2-4 are typical of where methodology is detailed. Step 5 is actually performing the experiment. Steps 6 and 7 relate to data and analysis respectively.

(Haase, Hill et al. 2014) warn simulation experimenters to scope their experiments carefully; because of vast capabilities available in simulation tools, there is tendency to build larger, more complex environments than required.

(Hodson and Hill 2014) identify various sources in the literature on experimental design: (Steinberg and Hunter 1984, Cortes, Duff et al. 2011, Johnson, Hutto et al. 2012), but none included "LVC simulation as a context for experimentation." They discuss experimental design for LVC simulations at a conceptual level but don't identify particular designs a practitioner may find useful. This gap in the literature goes back to (Haase, Hill et al. 2014), who offers particular experimental designs well suited to LVC simulation testing. The recommended designs suitable for LVC simulation testing are: orthogonal and nearly orthogonal arrays, optimal designs, and split-plot designs.

Orthogonal arrays (OA) are applicable to multiple fields of study (Hedayat, Sloane et al. 1999). "An orthogonal design… is a $n \times m$ matrix with entries from a set of q levels such that

the m columns are pairwise orthogonal. The columns and rows can be identified with factors and experimental runs, respectively" (Georgiou, Stylianou et al. 2014). By definition the strength of an OA is limited to two; meaning only two values must appear in each of their combinations of levels. This strength measurement can be increased by increasing the number of factors that appear in each of their level combinations (Hedayat, Sloane et al. 1999). Full factorial experimental designs are OAs, but the size of the experiment increases geometrically as the number of factors increases (Anderson and Whitcomb 2007). OAs are widely recognized in the literature and their ability to identify main effects and two factor interaction influence on response variables in a relatively small number of runs makes them useful for factor screening experiments (Hedayat, Sloane et al. 1999, Haase 2011, Haase, Hill et al. 2014).

Nearly orthogonal arrays otherwise known in experimental design as fractional factorial designs have the same basic characteristics as full factorial designs except that only some subset of the factors, or columns, are orthogonal (Hedayat, Sloane et al. 1999). Fractional factorial designs are popular among experimenters (Montgomery 2013) and are effective in screening many factors in search of an important few (Anderson and Whitcomb 2007). They are also more cost beneficial compared to full factorial designs. As the number of factors increases, the difference of required runs between full and fractional factorial designs grows drastically. Despite small sample sizes collected from fractional factorial experiments, properly designed and executed experiments can be very powerful and effective tools for evaluating main effects and two-factor interactions (Montgomery 2013).

Optimal Designs use model parameter variance reduction techniques to determine the design of the experiment. There are three types of designs: D-, G-, and I-optimal designs (Montgomery 2013). D-optimal designs minimize regression model coefficient variances and produce more accurate regression models from the collected data. G-optimal designs minimize the maximum prediction variance across the design region. Finally, I-optimal designs minimize the average prediction variance over the design space. General factorial 2^k designs are also optimal designs satisfying the criteria for each of the above design types.

Split Plot designs are described as "a blocked experiment, where the blocks themselves serve as experimental units for a subset of the factors." (Jones and Nachtsheim 2009) Such designs are used when complete randomization of the runs is difficult or impossible (Haase, Hill et al. 2014). While split plot designs offer a viable solution for experiments with randomization issues, (Jones and Nachtsheim 2009, Montgomery 2013, Haase, Hill et al. 2014) advise that caution should be taken to ensure the additional error and complex models are handled correctly.

In order to select the correct design, experiments must consider the characteristics of their simulation environment and problem of interest. The screening experiment performed by (Davis 2017) identified important factors for UAV slung-load water delivery operations to an overheating SFP. The design of this study uses the results of that screening experiment.

APPENDIX L:
RADIATION CONTAMINATION VS EXPOSURE

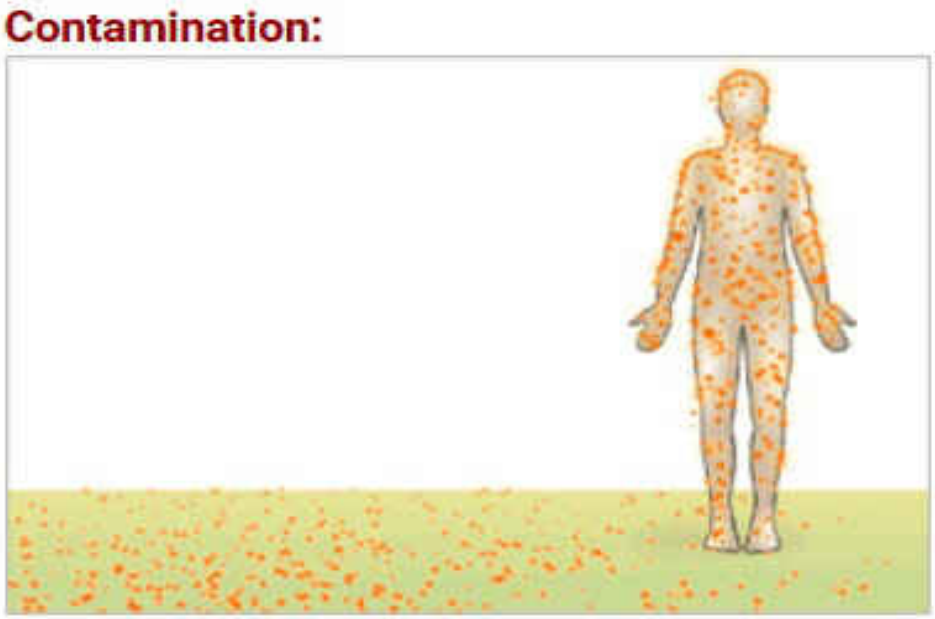

Figure 100 - Radiation Contamination (Management 2016)

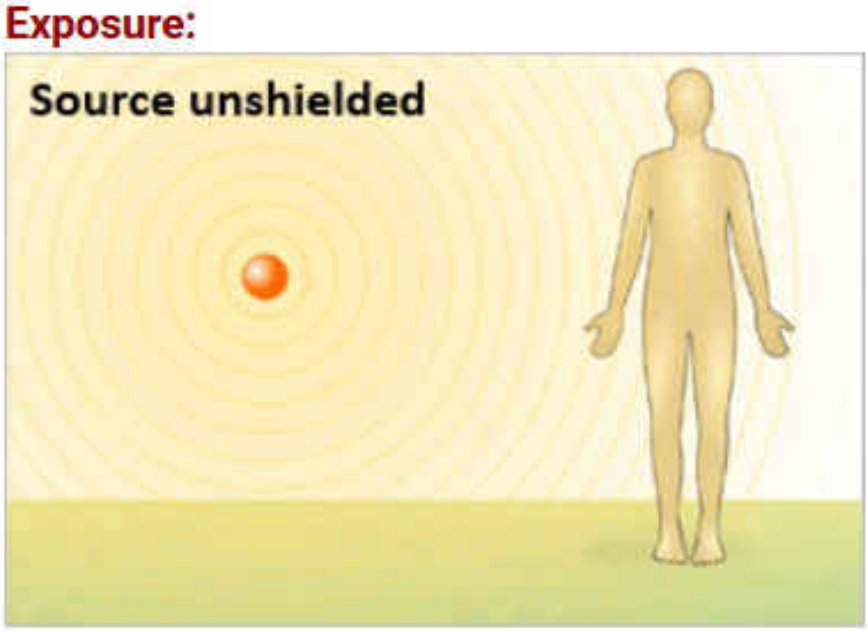

Figure 101 - Radiation Exposure (Management 2016)

APPENDIX M:
SIMULATION DESIGN ASSUMPTIONS

Assumptions from (Davis 2017) simulation study are as follows. The downtime associated with the UAVs (sortie regen time) and their effectiveness of water drops is based on various factors (water drop height, bucket fill/delivery efficiency) that are held constant throughout the simulation.

There are 2 points of water loss in the UAV – SFP replenishment system. The first point is when the UAV bucket picks up the freshwater load and flies towards the SFP, the second point of loss is when the water load is dropped onto the SFP from the UAV. These two points of water loss are established in Equation 4.

$$\text{Sling Load Capacity} \times 0.9 \times 0.8 = \text{Total Volume Delivered} \quad \textbf{(4)}$$

The power plant models associated with the simulation represent that of the Fukushima containment buildings. This includes the Unit 4 Spent fuel pool (SFP Depth over Fuel, SFP Surface Area, and SFP Water Volume), these values dramatically affect the outcome of the simulation, each power plant has different specifications for their individual SFPs but typical values are given in NUREG 1738 (Collins and Hubbard 2001). These values were chosen because of the recent nature of the Fukushima disaster and availability of data. There will be no consideration of the effect of rainfall on the SFP and this study will particularly be aimed at the UAVs ability to replenish the SFP given their electronic health and flight/load capabilities.

APPENDIX N:
RASCAL GENERATED OUTPUT

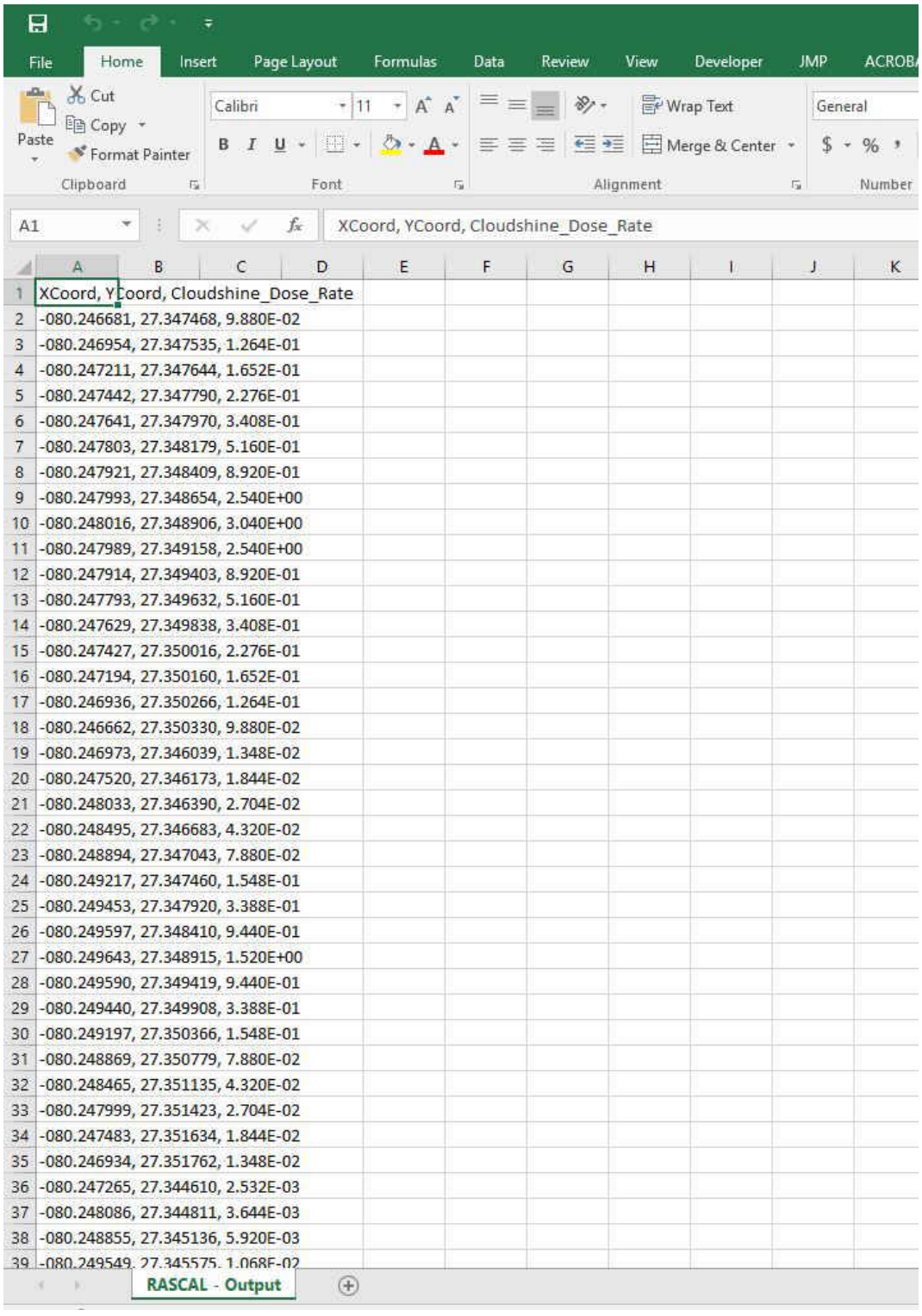

	A	B	C	D	E	F	G	H	I	J	K
1	XCoord, YCoord, Cloudshine_Dose_Rate										
2	-080.246681, 27.347468, 9.880E-02										
3	-080.246954, 27.347535, 1.264E-01										
4	-080.247211, 27.347644, 1.652E-01										
5	-080.247442, 27.347790, 2.276E-01										
6	-080.247641, 27.347970, 3.408E-01										
7	-080.247803, 27.348179, 5.160E-01										
8	-080.247921, 27.348409, 8.920E-01										
9	-080.247993, 27.348654, 2.540E+00										
10	-080.248016, 27.348906, 3.040E+00										
11	-080.247989, 27.349158, 2.540E+00										
12	-080.247914, 27.349403, 8.920E-01										
13	-080.247793, 27.349632, 5.160E-01										
14	-080.247629, 27.349838, 3.408E-01										
15	-080.247427, 27.350016, 2.276E-01										
16	-080.247194, 27.350160, 1.652E-01										
17	-080.246936, 27.350266, 1.264E-01										
18	-080.246662, 27.350330, 9.880E-02										
19	-080.246973, 27.346039, 1.348E-02										
20	-080.247520, 27.346173, 1.844E-02										
21	-080.248033, 27.346390, 2.704E-02										
22	-080.248495, 27.346683, 4.320E-02										
23	-080.248894, 27.347043, 7.880E-02										
24	-080.249217, 27.347460, 1.548E-01										
25	-080.249453, 27.347920, 3.388E-01										
26	-080.249597, 27.348410, 9.440E-01										
27	-080.249643, 27.348915, 1.520E+00										
28	-080.249590, 27.349419, 9.440E-01										
29	-080.249440, 27.349908, 3.388E-01										
30	-080.249197, 27.350366, 1.548E-01										
31	-080.248869, 27.350779, 7.880E-02										
32	-080.248465, 27.351135, 4.320E-02										
33	-080.247999, 27.351423, 2.704E-02										
34	-080.247483, 27.351634, 1.844E-02										
35	-080.246934, 27.351762, 1.348E-02										
36	-080.247265, 27.344610, 2.532E-03										
37	-080.248086, 27.344811, 3.644E-03										
38	-080.248855, 27.345136, 5.920E-03										
39	-080.249549, 27.345575, 1.068E-02										

Figure 102 - RASCAL Generated Output

APPENDIX O:
STAGE IMPORTED REFERENCE POINTS

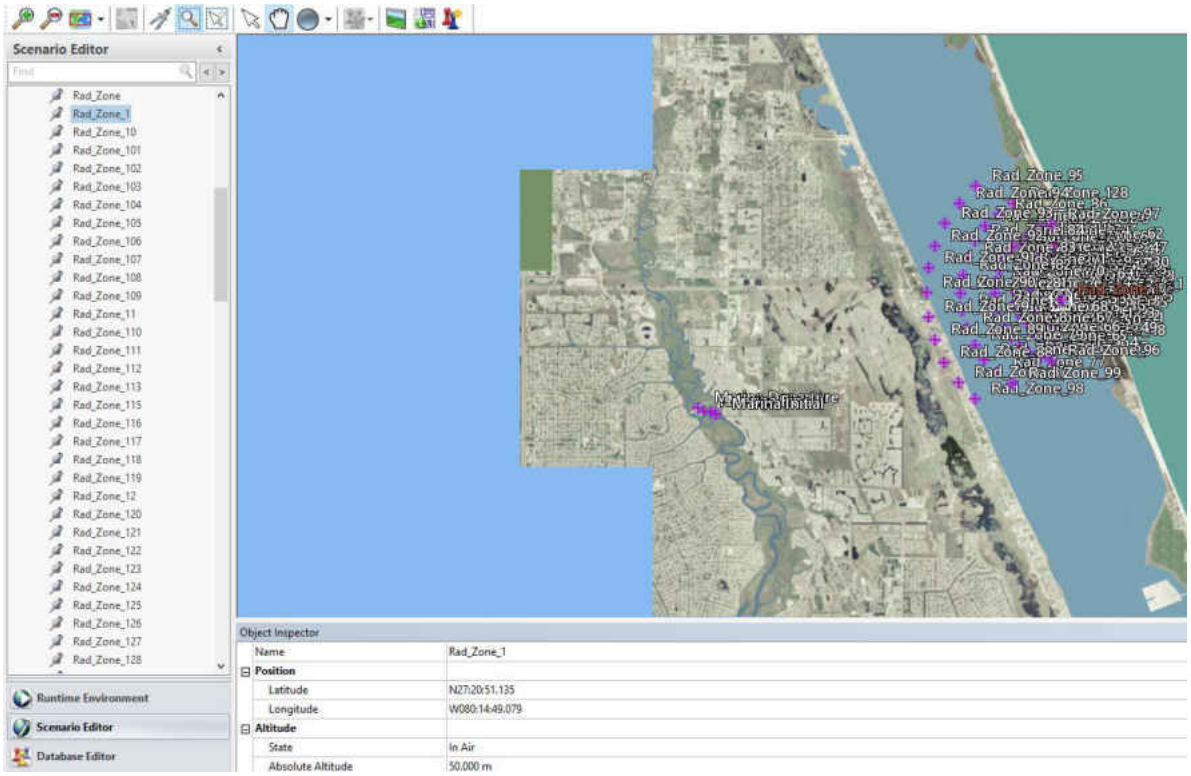

Figure 103 - STAGE Imported Reference Points

APPENDIX P:
UAV RADIATION ABSORPTION

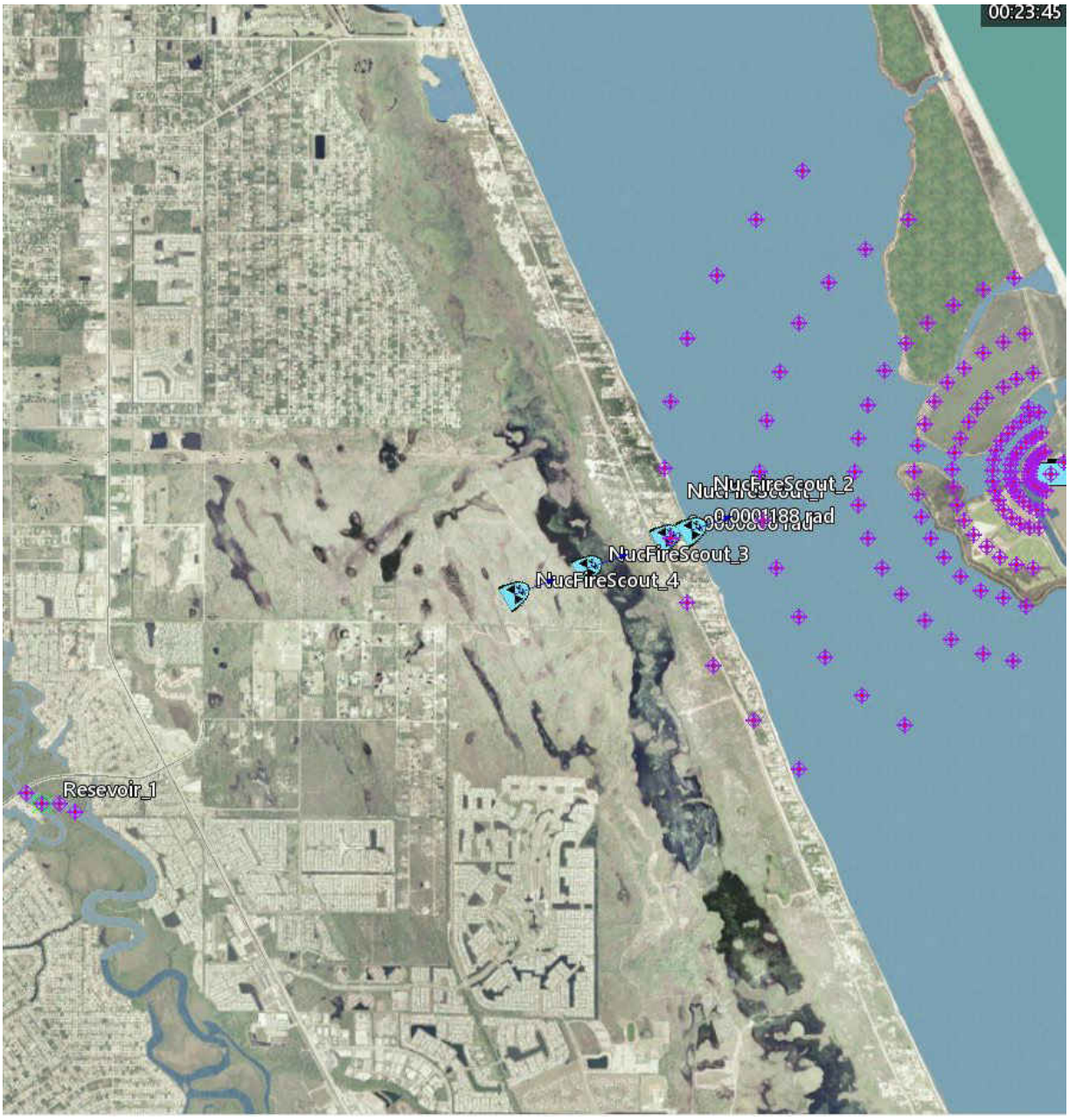

Figure 104 - UAV Radiation Absorption

APPENDIX Q:
EXPERIMENTAL RUNS

	UAV	TOTAL RADIATION
Time		
Wind Direction		
Operation Time		
Time of Day		
Unit 1 Leak Rate (Release) %		
Unit 2 Leak Rate (Release) %		
Unit 3 Leak Rate (Release) %		
Time since SCRAM		
Units Releasing		
EXPERIMENT 1	UAV - 1	3.432786
	UAV - 2	3.874358
	UAV - 3	4.390401
	UAV - 4	3.712625
EXPERIMENT 2	UAV - 1	3.78349
	UAV - 2	3.234139
	UAV - 3	3.436424
	UAV - 4	3.560286
EXPERIMENT 3	UAV - 1	4.022791
	UAV - 2	3.303094
	UAV - 3	4.043289
	UAV - 4	4.088223
EXPERIMENT 4	UAV - 1	3.817133
	UAV - 2	3.774641
	UAV - 3	3.682313
	UAV - 4	3.715492
EXPERIMENT 5	UAV - 1	3.513354
	UAV - 2	3.338623
	UAV - 3	3.50714
	UAV - 4	3.336147
EXPERIMENT 6	UAV - 1	3.741589
	UAV - 2	4.318205
	UAV - 3	3.791386
	UAV - 4	4.135876
EXPERIMENT 7	UAV - 1	4.052195
	UAV - 2	3.938904
	UAV - 3	3.845477
	UAV - 4	4.066784
EXPERIMENT 8	UAV - 1	3.922786
	UAV - 2	3.469533
	UAV - 3	3.991275
	UAV - 4	3.223869
EXPERIMENT 9	UAV - 1	4.000857
	UAV - 2	2.708054
	UAV - 3	4.124919
	UAV - 4	3.609788

Figure 105 - Experimental Runs (1-9)

EXPERIMENT 10	UAV - 1	3.550639
	UAV - 2	3.663405
	UAV - 3	3.659312
	UAV - 4	3.684445
EXPERIMENT 11	UAV - 1	4.157202
	UAV - 2	3.544103
	UAV - 3	3.867047
	UAV - 4	3.091117
EXPERIMENT 12	UAV - 1	3.542061
	UAV - 2	4.389069
	UAV - 3	3.326622
	UAV - 4	3.803122
EXPERIMENT 13	UAV - 1	3.467118
	UAV - 2	3.360693
	UAV - 3	3.827605
	UAV - 4	3.730745
EXPERIMENT 14	UAV - 1	3.752491
	UAV - 2	3.808483
	UAV - 3	3.516495
	UAV - 4	3.544973
EXPERIMENT 15	UAV - 1	4.081736
	UAV - 2	2.669884
	UAV - 3	3.901004
	UAV - 4	3.738544
EXPERIMENT 16	UAV - 1	3.863459
	UAV - 2	4.152056
	UAV - 3	3.12113
	UAV - 4	3.957
EXPERIMENT 17	UAV - 1	3.58656
	UAV - 2	3.946615
	UAV - 3	4.058834
	UAV - 4	3.448801
EXPERIMENT 18	UAV - 1	3.755747
	UAV - 2	3.039327
	UAV - 3	4.316695
	UAV - 4	3.629172
EXPERIMENT 19	UAV - 1	4.122649
	UAV - 2	3.757098
	UAV - 3	3.790013
	UAV - 4	3.780457
EXPERIMENT 20	UAV - 1	3.632629
	UAV - 2	3.465318
	UAV - 3	3.559738
	UAV - 4	3.684125

Figure 106 - Experimental Runs (10-20)

EXPERIMENT 21	UAV - 1	3.601648
	UAV - 2	3.580985
	UAV - 3	3.984258
	UAV - 4	3.701714
EXPERIMENT 22	UAV - 1	3.737945
	UAV - 2	3.218425
	UAV - 3	3.607031
	UAV - 4	3.517935
EXPERIMENT 23	UAV - 1	4.02606
	UAV - 2	3.162128
	UAV - 3	3.513222
	UAV - 4	3.865952
EXPERIMENT 24	UAV - 1	3.586819
	UAV - 2	3.020205
	UAV - 3	3.383468
	UAV - 4	4.017499
EXPERIMENT 25	UAV - 1	3.98025
	UAV - 2	3.215161
	UAV - 3	3.706235
	UAV - 4	3.995953
EXPERIMENT 26	UAV - 1	3.244304
	UAV - 2	3.320137
	UAV - 3	3.798554
	UAV - 4	3.679209
EXPERIMENT 27	UAV - 1	3.339069
	UAV - 2	4.10604
	UAV - 3	3.284194
	UAV - 4	3.175101
EXPERIMENT 28	UAV - 1	3.468281
	UAV - 2	3.822112
	UAV - 3	4.172947
	UAV - 4	3.498732
EXPERIMENT 29	UAV - 1	3.968833
	UAV - 2	3.539979
	UAV - 3	3.789816
	UAV - 4	3.334487
EXPERIMENT 30	UAV - 1	3.014856
	UAV - 2	2.904721
	UAV - 3	2.236531
	UAV - 4	2.826385
EXPERIMENT 31	UAV - 1	3.513701
	UAV - 2	3.403518
	UAV - 3	2.842145
	UAV - 4	2.811939
EXPERIMENT 32	UAV - 1	3.266351
	UAV - 2	3.120064
	UAV - 3	3.467665
	UAV - 4	3.295453
	Average Radiation Dose per Run	
	Average Total Radiation Dose per UAV	**3.621262508**

Figure 107 - Experimental Runs (21-32)

APPENDIX R:
COPYRIGHT PERMISSION

LIMITED COPYRIGHT LICENSE

This Agreement is made effective this 22 day of March, 2020, by and between Presagis Canada Inc., a Canadian corporation with an address at 4700 de la Savane, suite 300, Montreal, Quebec, Canada H4P 1T7 ("**Grantor**") and the individual or entity whose name and address appear below ("**Grantee**"). For good and valuable consideration, the receipt of which is hereby acknowledged, Grantee is hereby granted the non-exclusive, non-transferable, royalty-free, one-time right and license to reproduce, publish and display the copyrighted material owned by Grantor as set forth on and attached as **Exhibit A** (collectively, the "**Copyrighted Material**"), only for the limited, specific purpose described below (the "**Authorized Purpose**"):

Authorized Purpose:

*Reprint of screenshots from STAGE showing Grantee's reference points, various aerial in-flight photos of UAVs performing operational procedures, and STAGE's interface in order to complete Grantee's doctoral dissertation at University of Central Florida entitled CREATION AND ANLYSIS OF AN ENHANCED RASCAL-LVC FRAMEWORK CAPABLE OF SIMULATING IONIZING RADIATION DAMAGE TO EMERGENCY RESPONDERS DURING A NUCLEAR POWER PLANT DISASTER: A CASE STUDY IN UNMANNED AERIAL VEHICLE ELECTRONIC SYSTEM SURVIVABILITY (the "**Dissertation**").*

Grantee may reproduce, print and/or publish the Copyrighted Material in accordance with the Authorized Purpose only, Grantor acknowledging that the Authorized Purpose include Grantee's Dissertation being (i) translated in different languages, (ii) the object of future revisions or editions and (iii) published on the Internet. Grantee may not reproduce or use the Copyrighted Material in any other medium or in connection with any other publications, advertising or promotional materials, or for any other purpose. Except as expressly stated herein, Grantee shall acquire no right in the Copyrighted Material by virtue of this Agreement. The Grantor shall retain and expressly reserves for itself all other of its rights, including but not limited to the right to sell or license the Copyrighted Material to any other party for any purpose (including without limitation use in books and other publications) and any media (including without limitation the Internet). **This license is granted on an "AS IS' basis and Grantor makes no representation or warranty, whether express or implied, with respect to the Copyrighted Material.** Grantee agrees to indemnify, defend and hold Grantor harmless for and from any claims, damages, losses and expenses (including attorney's fees) arising out of Grantee's unauthorized use of the Copyrighted Material or in connection with claims asserted by any third parties based on their use of the information contained in any publication of Grantee that features the Copyrighted Material.

Grantee will include the following credit line with the Copyrighted Material used by Grantee in connection with the Authorized Purpose, or on a credit or copyright page within the publication that features the Copyrighted Material: *© Presagis Canada Inc., 2020. Reprinted with permission. All rights reserved.*

GRANTOR:

Jean-Michel Brière
General Manager
Date: March 23, 2020

GRANTEE:

Buder Shageer

Buder M. Shageer
Date: 03/22
Address:
12700 Woodbury Glen Dr,
Orlando, FL 32828

REFERENCES

Aerospace, A. (2009). "T-Hawk MAV." from http://www.avidaerospace.com/t-hawk-mav/.

Alexis, K., et al. (2009). Coordination of helicopter UAVs for aerial Forest-Fire surveillance. Applications of intelligent control to engineering systems, Springer**:** 169-193.

American, S. (2014). "Radioactive Isotopes from Fukushima Meltdown Detected near Vancouver." from http://www.scientificamerican.com/article/radioactive-isotopes-from-fukushima-meltdown-detected-near-vancouver/.

Anderson, M. J. and P. J. Whitcomb (2007). DOE Simplified : Practical Tools for Effective Experimentation. Boca Raton, FL, CRC Press Taylor and Francis Group.

ANS (2011). Status of Spent Fuel in the Unit 1 through 6 and Common Spent-Fuel Pools at the Fukushima Daiichi Nuclear Power Station, American Nuclear Society Special Committee on Fukushima.

AP (2012). "Sandy Washes Away Much Of Jersey Shore Town." from https://www.accesshollywood.com/articles/sandy-washes-away-much-of-jersey-shore-town-125222/.

Baker, J. (2012). Capabilities Report 2012, West Desert Test Center, 2012-03-12.

Base, A. H. (2009). CDF helicopter water drops on a fire near Morgan Hill California: Time it takes to release bambi water load.

Bendix, A. (2019). "Chernobyl's 'sarcophagus' is getting dismantled because it's teetering on collapse. Photos reveal the structure's rise and fall.". Retrieved October 31,, 2019, from https://www.businessinsider.com/chernobyl-disaster-sarcophagus-construction-dismantling-2019-9#now-construction-workers-will-have-to-reinforce-the-sarcophagus-again-while-its-parts-get-disassembled-15.

Bernabei, G., et al. (2014). A PLM-Based Approach for Un-manned Air System Design: A Proposal. Modelling and Simulation for Autonomous Systems Workshop. J. Hodicky. Rome, Italy, Springer International Publishing. **LNCS 8096:** 1-11.

Bernard, M., et al. (2008). A slung load transportation system based on small size helicopters. Autonomous Systems–Self-Organization, Management, and Control, Springer**:** 49-61.

Blyenburgh, P. v. (2000). UAVs - Current Situation and Considerations for the Way Forward, Defense Technical Information Center.

Brantley, M. W., et al. (2002). "Expanding the trade space: an analysis of requirements tradeoffs affecting system design. (Tutorial)." Acquisition Review Quarterly(1): 1.

Brendebach, B. (2016). "Decommissioning of Nuclear Facilities: Germany's Experience." from https://www.iaea.org/newscenter/news/decommissioning-of-nuclear-facilities-germanys-experience.

Britannica, E. (2016). "Ionization."

Britannica, E. (2016). "Radioactive Isotope." from https://www.britannica.com/science/radioactive-isotope.

Campbell, S., et al. (2014). "An automatic COLREGs-compliant obstacle avoidance system for an unmanned surface vehicle." PROCEEDINGS OF THE INSTITUTION OF MECHANICAL ENGINEERS PART M-JOURNAL OF ENGINEERING FOR THE MARITIME ENVIRONMENT **228**(2): 108-121.

CCI (2016). "About Chernobyl." from http://www.chernobyl-international.com/about-chernobyl/.

Chernobyl, H. i. (2012). from http://chernobylfoundation.org/wp-content/uploads/2012/12/chernobyl-helicopter.jpg.

Coleman, D. E. and D. C. Montgomery (1993). "A Systematic Approach to Planning for a Designed Industrial Experiment." Technometrics **35**(1): 1-12.

Collins, T. E. and G. Hubbard (2001). Technical study of spent fuel pool accident risk at decommissioning nuclear power plants NUREG-1738, Washington, DC : Division of Systems Safety and Analysis, Office of Nuclear Reactor Regulation, U.S. Nuclear Regulatory Commission : Supt. of Docs., U.S. G.P.O. [distributor], 2001.

Commission, C. N. S. (2012). Introduction to Radiation.

Commission, U. S. N. R. (2015). RASCAL 4.3: Description of Models and Methods.

Company, W. S. R. (2004). "Use of the Hazard Prediction and Assessment Capability (HPAC) at the Savannah River Site." U.S. Department of Energy.

Cortes, L. A., et al. (2011). A Primer on Design of Experiments for US Navy T&E Managers. Naval Sea Systems Command. **20**.

DailyMail, R. (2011). "Courage of the Fukushima fifty: This is suicide, admit workers trying to avert a catastrophe." from http://www.dailymail.co.uk/news/article-1367125/Japan-tsunami-Fukushima-Fifty-suicide-mission-battle-nuclear-meltdown.html.

Davis, M. (2017). "An SoS Conceptual Model, LVC Simulation Framework, and a Prototypical Implementation of Unmanned System Interventions for Nuclear Power Plant Disaster Preparedness, Response, and Mitigation." University of Central Florida.

Davis, M. and M. Proctor (2016). "The Viability of Extraordinary Methods to Mitigate Compromised SFP Cooling." International Nuclear Safety Journal **5**(2): 16-25.

Davis, M., et al. (2016). "A Systems-Of-Systems Conceptual Model and Live Virtual Constructive Simulation Framework for Improved Nuclear Disaster Emergency Preparedness, Response, and Mitigation." Homeland Security & Emergency Management.

Davis, M., et al. (September 2017). "Disaster Factor Screening using SoS Conceptual Modeling and an LVC simulation framework." Reliability Engineering & System Safety **165**(368-375).

Deagel (2015). "ARH-70A." Retrieved 11 March 2016, 2016, from http://www.deagel.com/Combat-Helicopters/ARH-70A_a000133004.aspx.

Dedman, B. (2014). "U.S. Nuclear Agency Hid Concerns, Hailed Safety Record as Fukushima Melted." Investigations. from https://www.nbcnews.com/storyline/fukushima-anniversary/u-s-nuclear-agency-hid-concerns-hailed-safety-record-fukushima-n48561.

Demetriou, D. (2013). Japan launches anti-radiation underwear after Fukushima crisis. The Telegraph.

Department of the Army, D. C. o. S., G1 (1994). Nuclear Contamination Avoidance - Appendix A: Operational Exposure Guidance. D. o. t. Army. Washington, D.C.

Deverell, E. (2012). "Investigating the Roots of Crisis Management Studies and Outlining Future Trajectories for the Field." JOURNAL OF HOMELAND SECURITY AND EMERGENCY MANAGEMENT **9**(1).

Diblasio, N. (2013). Radiation levels spike at Fukushima nuclear plant. USA Today.

DiSavino, S. (2018). "U.S. nuclear power plants prepare for Hurricane Florence." Retrieved 2019.

DoD, D. o. D. (2002). Performance Specification - Integrated Circuits (Microcircuits) Manufacturing MIL-PRF-38535F. Defense.

DoD, D. o. D. (2010). ELECTROMAGNETIC ENVIRONMENTAL EFFECTS - REQUIREMENTS FOR SYSTEMS MIL-STD-464C. Defense.

Edwards, M. W. (1987). Chernobyl - One Year After. National Geographic, National Geographic. **171:** 632-653.

Engineering, P. (2011). "Italian referendum: 94 per cent vote 'no' to nuclear." from https://www.power-eng.com/2011/06/15/italian-referendum/.

Faccio, F. (2001). "Radiation Effects in the Electronics for CMS." European Organization for Nuclear Research CERN.

Falconer, J. (2012). Hitachi unveils clean-up robot destined for Fukushima Daiichi nuclear plant. Hitachi.

Falconer, J. (2013). "High-Access Survey Robot begins work at TEPCO nuclear plant." from http://www.gizmag.com/honda-aist-high-access-survey-robot-nuclear-plant/28063/.

Farradyne, P. (2005). Use of Unmanned Aerial Vehicles in Traffic Surveillance and Traffic Management, Florida Department of Transportation.

FEMA (2014). Response Federal Interagency Operational Plan. www.fema.gov, Department of Homeland Security. **1:** 474.

Force, U. S. A. (2007). "MQ-9 Reaper." from https://en.wikipedia.org/wiki/General_Atomics_MQ-9_Reaper#/media/File:First_MQ-9_Reaper_at_Creech_AFB_2007.jpg.

Foundation, S. P. (2012). "The Fukushima Nuclear Accident and Crisis Managament." 15-16.

Fukushima, H. i. (2011). "Japan Earthquake." from http://extras.mnginteractive.com/live/media/site21/2011/0317/20110317_071456_Japan%20Earthquake%20Nucl_Seba(2)_400.jpg.

Fukushima, T. A. N. S. S. C. o. (2012). "FUKUSHIMA DAIICHI: ANS Committee Report, Appendix G." American Nuclear Society.

FuRo, F. R. T. C. (2011). "Quince." from http://furo.org/en/works/quince.html.

Georgiou, S. D., et al. (2014). "Construction of orthogonal and nearly orthogonal designs for computer experiments." Biometrika **101**(3): 741-747.

Ghosh, P. (2020). "UAE Gains License To Start First Nuclear Power Plant In Arab Region." from https://www.ibtimes.com/uae-gains-license-start-first-nuclear-power-plant-arab-region-2924471.

Graniela, B. and M. D. Proctor (2012). "A network-centric terrain database regeneration architecture." The Journal of Defense Modeling and Simulation: Applications, Methodology, Technology: 1548512912444178.

Guizzo, E. (2011). "Fukushima Robot Operator Writes Tell-All Blog." IEEE SPECTRUM.

Haase, C. L. (2011). Tailoring the Statistical Experimental Design Process for LVC Experiments. Department of Operational Sciences. Air Force Institute of Technology, 2011-03. **Master of Operations Research:** 152.

Haase, C. L., et al. (2014). "Planning for LVC Simulation Experiments." Applied Mathematics **5**(14): 2153.

Hannaford, K. (2011). "Military Helicopters Finally Dump Seawater on Over-Heating Fukushima Reactors." from http://gizmodo.com/5782885/military-helicopters-finally-dump-seawater-on-over-heating-fukushima-reactors.

Hedayat, A., et al. (1999). Orthogonal arrays : theory and applications, New York : Springer, c1999.

Hill, A. (2003). Using the Hazard Prediction and Assessment Capability (HPAC) Hazard Assessment Program for Radiological Scenarios Relevant to the Australian Defence Force, 2003-03.

Hirose, N. (2016). "Fukushima meltdown apology: "It was a cover-up"." from https://www.cbsnews.com/news/fukushima-tepco-power-japan-nuclear-meltdown-apologizes-cover-up/.

Hodicky, J. (2014). HLA as an Experimental Backbone for Autonomous System Integration into Operational Field. Modelling and Simulation for Autonomous Systems: First International Workshop, MESAS 2014, Rome, Italy, May 5-6, 2014, Revised Selected Papers. J. Hodicky, Springer. **8906:** 121.

Hodson, D. D. and R. R. Hill (2014). "The art and science of live, virtual, and constructive simulation for test and analysis." Journal of Defense Modeling & Simulation **11**(2): 77.

Hoeve, J. and M. Jacobson (2012). "Worldwide health effects of the Fukushima Daiichi nuclear accident." Energy & Environmental Science.

Hornyak, T. (2014). "Robot wields mop in Fukushima nuclear plant cleanup." from http://www.pcworld.com/article/2362800/robot-wields-mop-in-fukushima-nuclear-plant-cleanup.html.

Hruska, J. (2017). "Fukushima's Reactor #2 is far more radioactive than previously realized." from https://www.extremetech.com/extreme/243904-fukushimas-reactor-2-far-radioactive-previously-realized-no-sign-containment-breach.

Hsu, J. (2014). "THE WEIGHT OF WAR." Popular Science **285**(5): 60-65.

Huang, Q. and J. Jiang (2019). "An overview of radiation effects on electronic devices under severe accident conditions in NPPs, rad-hardened design techniques and simulation tools. ." Progress in Nuclear Energy **114**: 105-120.

Hugo, B. R. (2015). Modeling Evaporation From Spent Nuclear Fuel Storage Pools: A Diffusion Approach. School of Mechanical and Materials Engineering, Washington State University. **Doctor of Philosophy:** 88.

Hugo, B. R. and W. C. Kinsel (2014). "Predicting evaporation rates from spent nuclear fuel storage pools." International Nuclear Safety Journal **3**(1): 50-56.

Hugo, B. R. and R. P. Omberg (2015). "Evaluation of the Fukushima Daiichi Unit 4 Spent Fuel Pool." International Nuclear Safety Journal **4**(2): 1-5.

Huh, J. and A. Haldar (2011). "A Novel Risk Assessment for Complex Structural Systems." IEEE Transactions on Reliability **60**(1).

IAEA, I. A. E. A. (2013). "Fukushima Nuclear Accident Update Log." from https://www.iaea.org/newscenter/news/fukushima-nuclear-accident-update-log-52.

IAEA, I. A. E. A. (2016). "Operational Reactors." from https://pris.iaea.org/PRIS/WorldStatistics/OperationalReactorsByCountry.aspx.

IEM (2017). "Wind Roses." from http://mesonet.agron.iastate.edu/sites/windrose.phtml?network=FL_ASOS&station=FPR.

Inajima, T. and Y. Okada (2011). Tepco Misleading Public Over Nuclear Crisis, Institute Says. Bloomberg.

Industries, M. H. (2014). "MEISTeR" Remote Control Robot Completes Demonstration Testing At Fukushima Daiichi Nuclear Power Station -- Performs Decontamination Work and Concrete Core Sampling.

Industries, S. (2016). "BAMBI MAX Operations Manual." Retrieved September 24th, , 2019, from https://www.sei-ind.com/wp-content/uploads/2009/03/WEB_Bambi_MAX_Operations_Manual_vC.pdf.

INNG (2015). Vibrant Response Q and A.

IRID, I. R. I. f. N. D. (2014). "Robots working inside the buildings at Fukushima Daiichi NPS Rosemary & Sakura." from http://irid.or.jp/en/research/rosemary_sakura/.

IRID, I. R. I. f. N. D. (2015). "Development and Utilization of Dry Ice Blast Decontamination Equipment for High Places ". from http://irid.or.jp/en/topics/%E9%AB%98%E6%89%80%E7%94%A8%E3%83%89%E3%83%A9%E3%82%A4%E3%82%A2%E3%82%A4%E3%82%B9%E3%83%96%E3%83%A9%E3%82%B9%E3%83%88%E9%99%A4%E6%9F%93%E8%A3%85%E7%BD%AE%E3%81%AE%E9%96%8B%E7%99%BA%E3%83%BB%E6%B4%BB/.

IRID, I. R. I. f. N. D. (2015). "Training on use of 'TEMBO' equipment to remove shielding blocks and iron plates now underway (Mitsubishi Heavy Industries)." from http://irid.or.jp/en/topics/%E9%81%AE%E8%94%BD%E3%83%96%E3%83%AD%E3%83%83%E3%82%AF%EF%BC%86%E9%89%84%E6%9D%BF%E5%8F%96%E3%82%8A%E5%A4%96%E3%81%97%E8%A3%85%E7%BD%AE%E3%80%8Ctembo%E3%80%8D%E3%81%AE%E4%BD%9C%E6%A5%AD%E3%83%88/.

JAXA, A. T. D. (2015). "Unmanned Airplane for Radiation Monitoring System (UARMS)." from http://www.aero.jaxa.jp/eng/research/star/uarms/.

Jiji (2015, April 13). "The Japan Times: News Report." from http://www.japantimes.co.jp/news/2015/04/13/national/radiation-measured-at-deadly-9-7-sieverts-in-fukushima-reactor/#article_history.

Johnson, R. T., et al. (2012). "Designed Experiments for the Defense Community." QUALITY ENGINEERING **24**(1): 60-79.

Johnson, T. (2006). The Battle of Chernobyl. Italy**:** 94 min.

Jones, B. and C. J. Nachtsheim (2009). "Split-Plot Designs: What, Why, and How." JOURNAL OF QUALITY TECHNOLOGY **41**(4): 340-361.

JTF-CS (2015). "JTFCS." Retrieved 10 September, 2015, from http://www.jtfcs.northcom.mil/JTFCS.aspx.

Kerigan-Kyro, D. (2012). NATO and Critical Infrastructure Resilience - Planning for the Unknown. NATO Advanced Research Workshop on Critical Infrastructure Protection, Ankara, Turkey, IOS Press BV.

Kyne, D. (2015). "Managing Nuclear Power Plant Induced Disasters." Journal of Emergency Management **13**(5): 417-430.

Labor, U. S. D. o. (2016). "Non-Ionizing Radiation." from https://www.osha.gov/SLTC/radiation_nonionizing/.

Langner, R. (2011). "Stuxnet: Dissecting a Cyberwarfare Weapon." IEEE Security & Privacy **9**(3): 49-51.

Lee, B. (2011). "How much radiation is too much? A handy guide." Need to Know on PBS. from http://www.pbs.org/wnet/need-to-know/the-daily-need/how-much-radiation-is-too-much-a-handy-guide/8124/.

Lewis, O. and L. Harash (2017). Mars astronaut radiation shield set for moon mission trial-developer Reuters, MSN News.

Limer, E. (2016). Fukushima's Radiation Is So Bad It's Even Killing Robots. Popular Mechanics, Popular Mechanics.

Löchner, S. (2011). "Radiation Damages to Electronic Components." Retrieved September 15th, , 2019, from https://wiki.gsi.de/foswiki/pub/EE/GRISU/SD_05052011.pdf.

Lyon, J. (2014). "Helping to Prepare for Dangerous Incidents." from http://www.simudyne.com/2014/01/08/helping-to-prepare-for-dangerous-incidents/.

Maki, T. (2011). "Faculty Column: Underwater witness." from http://www.u-tokyo.ac.jp/en/about/publications/tansei/10/65-response-maki.html.

Makowski, D. (2006). THE IMPACT OF RADIATION ON ELECTRONIC DEVICES WITH THE SPECIAL CONSIDERATION OF NEUTRON AND GAMMA RADIATION MONITORING. Department of Microelectronics and Computer Science, Technical University of Łódź.

Management, U. S. D. o. H. a. H. S. R. E. M. (2016). "Differences between Contamination and Exposure." from https://www.remm.nlm.gov/diff_contam_exp.htm.

Marconi, L., et al. (2012). The SHERPA project: Smart collaboration between humans and ground-aerial robots for improving rescuing activities in alpine environments. Safety, Security, and Rescue Robotics (SSRR), 2012 IEEE International Symposium on.

Martin, L. (2015). "Fire Fighting to the K-Max." from http://www.abovetopsecret.com/forum/thread1089599/pg1.

Mase, K. (2013). Wide-area disaster surveillance using electric vehicles and helicopters. Personal Indoor and Mobile Radio Communications (PIMRC), 2013 IEEE 24th International Symposium on.

McGonigle, A. J. S., et al. (2008). "Unmanned aerial vehicle measurements of volcanic carbon dioxide fluxes." Geophysical Research Letters **35**(6): L06303.

MensHealth (2011). Radiation Its Everywhere. MensHealth.

Miller, C., Cubbage, A., Dorman, D., Grobe, J., Holahan, G., & Sanfilippo, N. (2011). Recommendations for Enhancing Reactor Safety in the 21st Century, Nuclear Regulatory Commission.

Ministry of Defense, J. (2011). Special Feature: Response to the Great East Japan Earthquake.

Mirion Technologies (2016). "How Does Radiation Affect Me?".

Mirion Technologies (2016). "Introduction to Radiation Safety." from https://www.mirion.com/introduction-to-radiation-safety/what-is-radiation/.

Mirion Technologies (2016). "Radiation vs Contamination." from https://www.mirion.com/introduction-to-radiation-safety/radiation-vs-contamination/.

Mirion Technologies (2016). "Types of Ionizing Radiation." from https://www.mirion.com/introduction-to-radiation-safety/types-of-ionizing-radiation/.

Montgomery, D. C. (2013). Design and Analysis of Experiments. Hoboken, NJ, John Wiley & Sons, Inc.

Morris, B. (2015). SFP Replenishment Times. M. D. Proctor, Oak Ridge National Laboratory, Modeling and Simulation Group.

Motors, Y. (2013). "Yamaha RMAX - History." from http://rmax.yamaha-motor.com.au/history.

NAAIC (2012). The Fukushima Nuclear Accident Independent Investigation Commission. The National Diet of Japan

NEI, N. E. I. (2016). "World Statistics." from http://www.nei.org/Knowledge-Center/Nuclear-Statistics/World-Statistics.

News, C. (2009). "Hurricane Bill washes away N.S. road." from http://www.cbc.ca/news/canada/nova-scotia/hurricane-bill-washes-away-n-s-road-1.783504.

News, W. N. (2013). "Tepco sends in the Raccoon." from http://www.world-nuclear-news.org/RS-Tepco-sends-in-the-Raccoon-2711131.html.

News, W. N. (2015). "Looking inside Fukushima Daiichi Unit 1." from http://www.world-nuclear-news.org/RS-Looking-inside-Fukushima-Daiichi-unit-1-1002154.html.

Newser (2017). "Robot Enters Fukushima Reactor, Doesn't Fare So Well ". from http://www.newser.com/story/238520/robot-headed-into-fukushima-reactor-never-came-out.html?utm_source=share&utm_medium=email&utm_campaign=def.

Nordion (2016). "Radiation Safety - Electromagnetic Spectrum." from http://www.nordion.com/social-responsibility/radiation-safety/.

Northrop Grumman (2015). MQ-8C Fire Scout Unmanned Air System. www.northropgrumman.com/firescout.

NRC (2010). Implications of Updated Probabilistic Seismic Hazard Estimates in Central and Eastern United States on Existing Plants, GI-199.

NRC (2011). "NRC frequently asked questions related to the March 11, 2011 Japanese Earthquake and Tsunami." from https://www.nrc.gov/japan/faqs-related-to-japan.pdf.

NRC (2012). Order Modifying Licenses with Regard to Reliable Spent Fuel Pool Instrumentation. EA-12-051. N. R. Commission.

NRC (2014). 2002 Davis-Besse Reactor Pressure Vessel Head Degradation Knowledge Management Digest, Nuclear Regulatory Commission: 24.

NRC (2014). "Backgrounder on Chernobyl Nuclear Power Plant Accident ". from https://www.nrc.gov/reading-rm/doc-collections/fact-sheets/chernobyl-bg.html.

NRC (2014). The Browns Ferry Nuclear Plant Fire of 1975 Knowledge Management Digest, Nuclear Regulatory Commission: 16.

NRC (2015). "Computer Codes." 2015, from http://www.nrc.gov/about-nrc/regulatory/research/safetycodes.html#sac.

NRC (2015, 18 Feb, 2015). "Operating Reactors." Retrieved 10 April, 2015, from http://www.nrc.gov/reactors/operating.html.

NRC (2016). "Radiation Basics." from http://www.nrc.gov/about-nrc/radiation/health-effects/radiation-basics.html#ionizing.

OFCM, O. o. t. F. C. f. M. (2003). "Atmospheric Transport and Dispersion Modeling Support for Homeland Security." from http://www.ofcm.gov/homeland/gmu2003/ofcm_session_at_gmu_proceedings_2003.pdf.

Office of the Assistant Secretary of Defense for Nuclear Chemical, a. B. D. P. N. M. (2016). "Specialized Radiological Monitoring and Hazard Assessment Capabilities."

Oikawa, K. (2015). Robot Technology for Nuclear Decommissioning of Fukushima Daiichi NPS, International Research Institute for Nuclear Decommissioning (IRID).

OPA (2013, May 2013). "Chernobyl Nuclear Power Plant Accident." Retrieved 4, from http://www.nrc.gov/reading-rm/doc-collections/fact-sheets/chernobyl-bg.html.

OPA (2013, February 2013). "Three Mile Island Accident." Retrieved 10 April, 2015, from http://www.nrc.gov/reading-rm/doc-collections/fact-sheets/3mile-isle.html.

OPEN-DIS (2016). "Distributed Interactive Simulation." from http://open-dis.sourceforge.net/DIS.html.

OSUMI, H. (2014). "Application of Robot Technologies to the Disaster Sites." Japan Society of Mechanical Engineers **Chapter 5**.

Palmer, B. (2011). Sievert, Gray, Rem, and Rad: Why are there so many different ways to measure radiation exposure? Slate.

Patrick, R. (1981). "Optimal Nuclear Radiation Criteria for Aeronautical Systems." Directorate of Aircraft Maintenance, Aircraft Engineering Division USAF **Engineering Report No. 2-110**.

PHYS (2013). "Dry ice vacuum cleaner robot bound for Fukushima." from http://phys.org/news/2013-02-ice-vacuum-cleaner-robot-bound.html.

Physics, F. I. o. N. P. a. P. (2016). "Radioactive iodine : A dangerous and short lived fission product." from http://www.radioactivity.eu.com/site/pages/Iodine_131.htm.

Pix4D (2016). "Large Scale Industrial Surveying via Drone Photogrammetry." from https://pix4d.com/large-scale-industrial-surveying-drone-photogrammetry/.

Power, N. (2016). "Delayed Neutrons." from http://www.nuclear-power.net/nuclear-power/fission/delayed-neutrons/.

Prasad, R., et al. (2011). Design-Basis Flood Estimation for Site Characterization at Nuclear Power Plants in the United States of America (NUREG/CR-7046), Nuclear Regulatory Commission.

Presagis (2015). CBRN Use Case: CBRN Event Response and Planning.

Presagis (2016). "Creator." from http://www.presagis.com/products_services/products/modeling-simulation/content_creation/creator/.

Presagis (2016). "FlightSim." from http://www.presagis.com/products_services/products/modeling-simulation/simulation/flightsim/.

Presagis (2016). "HeliSim." from http://www.presagis.com/products_services/products/modeling-simulation/simulation/helisim/.

Presagis (2016). "M&S Suite." Retrieved 2 July, 2016, from http://www.presagis.com/products_services/products/modeling-simulation/.

Presagis (2016). "STAGE." from http://www.presagis.com/products_services/products/modeling-simulation/simulation/stage/.

Presagis (2016). "Terra Vista." from http://www.presagis.com/products_services/products/modeling-simulation/content_creation/terra_vista/.

Presagis (2016). "Vega Prime." from http://www.presagis.com/products_services/products/modeling-simulation/visualization/vega_prime/.

Presagis (2017). "Ondulus IR." from http://www.presagis.com/products_services/products/modeling-simulation/simulation/ondulus_ir/.

Pripyat (2006). Chernobyl Disaster: Helicopter crash near Nuclear Power Plant.

Proctor, D. M., et al. (2015). "Considering Modeling and Simulation of DoD response to Accidental Nuclear Disaster." Journal of Defense Management.

Proctor, M. D. and G. Paulo (1996). "Modeling in support of operational testing." MATHEMATICAL AND COMPUTER MODELLING **23**(1-2): 9-14.

Proctor, M. D., et al. (2003). "Why the 'T' in SMART a constructive synergy." Acquisition Review Quarterly(3): 284.

Protection, F. D. o. E. (2004). HURRICANE FRANCES & HURRICANE JEANNE Post-storm Beach Conditions and Coastal Impact Report with Recommendations for Recovery and Modifications of Beach Management Strategies. D. o. W. R. M. Florida Department of Environmental Protection, Bureau of Beaches and Coastal Systems.

Rocchi, F., et al. (2014). Application of RASCAL 4.2 to estimate the Fukushima Accident Source Term. International Conference on Challenges Faced by Technical and Scientific Support Organizations (TSOs) in Enhancing Nuclear Safety and Security.

Saggiani, G. M. and B. Teodorani (2004). "Rotary wing UAV potential applications: an analytical study through a matrix method." Aircraft Engineering and Aerospace Technology **76**(1): 6-14.

Sanchez, R. (2016). Meltdown: Fallout from Chernobyl, 30 years later. MSNBC.

Sanders, R. and B. Panfil (2013). Integration of MELCOR Sever Accident Models, Areva / Corys Thunder Inc**:** 26.

Sawant, M. (2012). "Single Event Effects Complicate Military Avionics System Design." Journal of Military Electronics & Computing.

Scott, L. (2011). "The Relationship of Alpha, Beta and Power in Design of Experiments." ASQ Detroit(November - December 2011): 6 - 7.

Shageer, B. and M. D. Proctor (2020, IN REVIEW). "A simulation assessment of electronic survivability of UAVs responding to a NPP radiological emergency." Journal of Emergency Management, JEM.

Sharma, S., et al. (2014). ""Non-linear control algorithms for an unmanned surface vehicle." " PROCEEDINGS OF THE INSTITUTION OF MECHANICAL ENGINEERS PART M-JOURNAL OF ENGINEERING FOR THE MARITIME ENVIRONMENT **228**(2): 146-155.

Shea, D. (2004). Critical Infrastructure: Control Systems and the Terrorist Threat. L. o. Congress. Library of Congress, Congressional Research Service.

Sokolski, H. D. (2016). Underestimated: Our Not So Peaceful Nuclear Future. United States Army War College, Strategic Studies Institute.

Srour, J. and J. Mcgarrity (1988). "Radiation Effects on Microelectronics in Space." Proceedings of the IEEE **76**(11).

Staff, C. W. (2011). "China freezes nuclear plant approvals." from http://edition.cnn.com/2011/WORLD/asiapcf/03/16/china.nuclear/?hpt=T2.

Steinberg, D. M. and W. G. Hunter (1984). "Experimental Design: Review and Comment." Technometrics **26**(2): 71.

Sun, B. (2014). "Helicopters in Three Mile Island." from http://darkroom.baltimoresun.com/wp-content/uploads/2014/03/25-0017a.gif.

Svec, P., et al. (2014). "Target following with motion prediction for unmanned surface vehicle operating in cluttered environments." AUTONOMOUS ROBOTS **36**(4): 383-405.

Systems, B. C. (2016). "What radiation levels are considered safe?". from http://www.blackcatsystems.com/GM/safe_radiation.html.

Systems, S. T. (2019). "Fire Fighting." Retrieved October 14th,, 2019, from http://www.trainingfordisastermanagement.com/applications/fire-training-and-simulation/.

Technology, A. (2007). "Honeywell T-Hawk Micro Air Vehicle (MAV), United States of America." from http://www.army-technology.com/projects/honeywell-thawk-mav-us-army/.

TEPCO (2013). The Development of and Lessons from the Fukushima Daiichi Nuclear Accident, Tokyo Electric Power Company**:** 20.

TEPCO (2016). Robots being Applied Mainly Above the 1st Floor of the Reactor Building.

Thunder, C. (2014). "MELCOR Simulator Integration." from http://corysthunder.com/melcor.html.

Tokyo, A. P. i. (2011). Fukushima investigation reveals failings. The Guardian. Tokyo, Associated Press in Tokyo.

Tolk, A. (2012). "Terms and Application Domains, in Engineering principles of combat modeling and distributed simulation." Wiley: 55-78.

Training, P. D. O. o. G. a. (2007). Guide for the Selection of Chemical, Biological, Radiological, and Nuclear Decontamination Equipment for Emergency First Responders. H. Security.

Treacy, M. (2016). "Fukushima radiation has fried clean up robots." from http://www.treehugger.com/gadgets/fukushima-radiation-clean-up-robots.html.

UTM (2007). Palm Bay, FL, deploys unmanned air vehicles. The Urban Transportation Monitor, Lawley Publications. **21:** 1.

Van Niekerk, D., et al. (2015). Planning and Executing Scenario Based Simulation Exercises: Methodological Lessons. JOURNAL OF HOMELAND SECURITY AND EMERGENCY MANAGEMENT. **12:** 193.

Vanderbilt University, S. o. E. (2016). "Radiaton Effects on Electronics." from https://creme.isde.vanderbilt.edu/CREME-MC/help/radiation-effects-on-electronics.

Wang, D. A., et al. (2012). "Study Of Fukushima Daiichi Nuclear Power Station Unit 4 Spent-Fuel Pool." NUCLEAR TECHNOLOGY **180**(2): 205-215.

WeatherSpark (2017). "St. Lucie Wind Speed." from https://weatherspark.com/averages/30296/Fort-Pierce-Florida-United-States.

Wendle, J. (2016). "Chernobyl's Radioactive Ruins Get a New Tomb." from http://news.nationalgeographic.com/2016/04/042516-chernobyl-new-safe-confinement-contains-radiation/.

WIRE, B. (2012). "iRobot Warrior and PackBot Robots Support U.S. Nuclear Power Plant Operations." from http://investor.irobot.com/phoenix.zhtml?c=193096&p=irol-newsArticle&ID=1679059.

WNA (2012, Sep. 2012). "Fukushima: Background on Fuel Pools." 2015, from http://www.world-nuclear.org/information-library/safety-and-security/safety-of-plants/appendices/fukushima-fuel-ponds-background.aspx.

WNA (2016). "Nuclear Radiation and Health Effects." from http://www.world-nuclear.org/information-library/safety-and-security/radiation-and-health/nuclear-radiation-and-health-effects.aspx.

WNA (2016). "What is Radiation?". from http://www.world-nuclear.org/nuclear-basics/what-is-radiation.aspx.

WNA, W. N. A. (2019). "Nuclear Power in Saudi Arabia." from https://www.world-nuclear.org/information-library/country-profiles/countries-o-s/saudi-arabia.aspx.

WTHR, N. (2016). "Hurricane Matthew washes away segment of Florida highway ". from http://www.wthr.com/article/hurricane-matthew-strengthens-as-it-nears-florida.

Wunderground (2017). "Historical Weather." from https://www.wunderground.com/history/airport/KFPR/2011/3/11/CustomHistory.html

?dayend=18&monthend=3&yearend=2011&req_city=&req_state=&req_statename=&reqdb.zip=&reqdb.magic=&reqdb.wmo=.

ZeroHedge (2016). Durden, Tyler.

Zittel, R. C. (2001). "The Reality of Simulation-Based Acquisition -- And an Example of U.S. Military Implementation. (Tutorial)." Acquisition Review Quarterly(2): 121.